

AD-A081 305

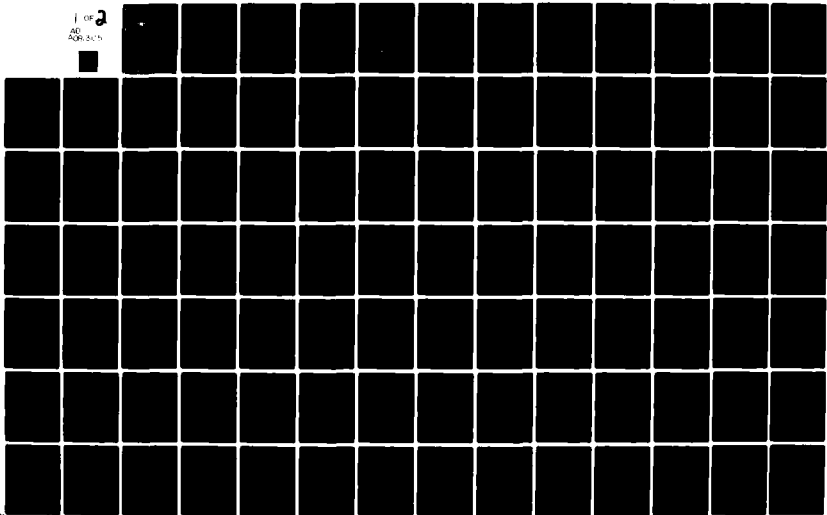
TEXAS A AND M UNIV COLLEGE STATION DEPT OF METEOROLOGY F/G 4/1
A STUDY OF THE VARIABILITY OF THUNDERSTORM ELECTRICAL EVENTS BA--EYC(U)
AUG 79 W B FREEMAN AFOSR-79-0003

UNCLASSIFIED

AFOSR-TR-80-0115

NL

1 of 2
AD
A081305



AFOSR-TR- 80-0115

2 JAN RECD

LEVEL

3

ADA081305



TEXAS A & M UNIVERSITY

DEPARTMENT OF METEOROLOGY

A STUDY OF THE VARIABILITY OF THUNDERSTORM ELECTRICAL
EVENTS BASED ON VERY-LOW-FREQUENCY
ELECTROMAGNETIC DATA



by

A

WILLIAM BURNS FREEMAN, JR.

AFOSR-79-0003

August 1979



80 3 3 018

Approved for public release;
distribution unlimited.

WILL HILL COPY

UNCLASSIFIED

SECURITY CLASSIFICATION OF THIS PAGE (When Data Entered)

REPORT DOCUMENTATION PAGE		READ INSTRUCTIONS BEFORE COMPLETING FORM	
1. REPORT NUMBER 18 AFOSR-TR-80-0115	2. GOVT ACCESSION NO.	3. RECIPIENT'S CATALOG NUMBER 9	
4. TITLE (and Subtitle) A Study of the Variability of Thunderstorm Electrical Events Based on Very-Low-Frequency Electromagnetic Data.		5. DATE OF REPORT & PERIOD COVERED Final r.p.f. 1 Oct 78 - 30 Sep 79,	
7. AUTHOR(s) William Burns/Freeman, Jr.		8. CONTRACT OR GRANT NUMBER(s) 15 AFOSR-79-0003	
9. PERFORMING ORGANIZATION NAME AND ADDRESS Texas A & M University Department of Meteorology College Station, Texas 77843		10. PROGRAM ELEMENT, PROJECT, TASK AREA & WORK UNIT NUMBERS 61102F 2310/A1 17 A1:1	
11. CONTROLLING OFFICE NAME AND ADDRESS AFOSR/NC Bldg. 410, Bolling AFB, DC 20332		12. REPORT DATE 11 August 1979	
14. MONITORING AGENCY NAME & ADDRESS (if different from Controlling Office)		13. NUMBER OF PAGES 82	
		15. SECURITY CLASS. (of this report) Unclassified	
		15a. DECLASSIFICATION/DOWNGRADING SCHEDULE	
16. DISTRIBUTION STATEMENT (of this Report) Approved for public release; distribution unlimited.			
17. DISTRIBUTION STATEMENT (of the abstract entered in Block 20, if different from Report)			
18. SUPPLEMENTARY NOTES			
19. KEY WORDS (Continue on reverse side if necessary and identify by block number) Sferics Cloud-to-Ground Freezing Level Lightning Discharge Discharge K Index Thunderstorm Lightning Lightning-Flash 1.3 TIMES TEN TO THE MINUS 5TH POWER / 50 KM/S			
20. ABSTRACT (Continue on reverse side if necessary and identify by block number) Sferics counts were used to estimate the incidence of lightning discharges; study the relationship of lightning-flash density to thunderstorm days; and explore the variability to cloud-to-ground discharges. Areal and global discharge incidence estimates were generated from sferics, yielding a global estimate of $1.3 \times 10^{-5} \text{ km}^{-2} \text{ s}^{-1}$. Gridded monthly values are given for much of the Eastern Hemisphere. The Southern Hemisphere tropics were found to have a higher average incidence of discharge than the Northern Hemisphere.			

400-161

Unclassified

306

UNCLASSIFIED

SECURITY CLASSIFICATION OF THIS PAGE (When Data Entered)

tropics. The linear regression relationship between flash density and thunder storm days indicated lower estimates of flash density when based on data stratifications compared to previous studies. Selected data from the Eastern Hemisphere were studied by linear regression techniques for causes of large-scale variability of cloud-to-ground discharges. In order of importance the regressors were the height of freezing level, the planetary geomagnetic index, a parameterization of the height of the freezing level, precipitable water in 1000-850 mb layer, the dew-point depression at 850 mb, the K index of stability, and the departure of the H-component of the magnetic force vector from its mean.

UNCLASSIFIED

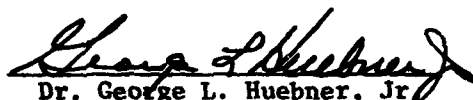
A STUDY OF THE VARIABILITY OF THUNDERSTORM ELECTRICAL
EVENTS BASED ON VERY-LOW-FREQUENCY
ELECTROMAGNETIC DATA

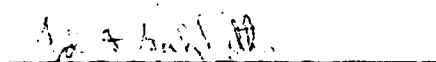
A Dissertation

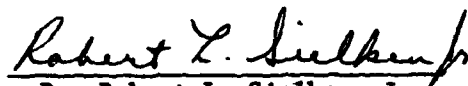
by

WILLIAM BURNS FREEMAN, JR.

Approved as to style and content by:

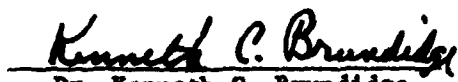

Dr. George L. Huebner, Jr.
(Chairman of Committee)


Prof. John F. Griffiths
(Member)


Dr. Robert L. Sielken, Jr.
(Member)


Dr. Vance E. Meyer
(Member)


Prof. Albert J. Druce
(Member)


Dr. Kenneth C. Brundidge
(Head of Department)

ABSTRACT

A Study of the Variability of Thunderstorm Electrical Events Based
on Very-Low-Frequency Electromagnetic Data. (August 1979)

William Burns Freeman, Jr., B.S., Middle Tennessee State College;
M.S., The George Washington University; M.S., Texas A&M University
Chairman of Advisory Committee: Dr. George L. Huebner, Jr.

The incidence of lightning discharge was estimated, the relationship of lightning-flash density to thunderstorm days was studied, and the causes of the variability in cloud-to-ground discharges were explored. The primary data were counts of sferics.

The estimates of the incidence of discharge include areal and global statistics. The global estimate was $1.3 \times 10^{-5} \text{ km}^{-2} \text{ s}^{-1}$. Also included are monthly values over a regularly-spaced grid that includes much of the Eastern Hemisphere. The Southern Hemisphere (S.H.) tropics (0° - 20° S) were higher in average incidence of discharge than the Northern Hemisphere (N.H.) tropics (0° - 20° N). The extra-tropical zone of the S.H. (20° S- 35° S) was dominant in incidence of discharge relative to other zones. Lightning occurred much less frequently in high vs. middle latitudes but the number of discharges per $\text{km}^{-2} \text{ s}^{-1}$ during stormy periods was similar in magnitude.

The relationship between flash density and thunderstorm days was studied for the months of January, April, August, and November

with a curvilinear regression analysis. Many useable regressions were produced. The relationship varied by season. The regressions for all the data produced estimates of flash density which were generally the same order of magnitude as that of previous studies. All estimates of flash density predicted by the regressions based on stratifications of the data were low in comparison to previous studies.

The large-scale causes of the variability of cloud-to-ground discharges (dependent variable) were studied. February and August data for a selected area of the Eastern Hemisphere were chosen for study. Multiple linear regression (11 regressors in February and 12 in August) was used with and without a logarithmic transformation of the dependent variable. The regressors were available on the National Meteorological Center (NMC) grid and were averaged in various ways to conform to the resolution of the dependent variable (10° -data blocks). The thrust was to explain the variability of cloud-to-ground discharges when significant lightning had occurred since this is the problem of physical and practical importance.

The models for February (R^2 of 0.3 to 0.6) were dramatically better than those for August (R^2 of 0.1 to 0.3). The backward selection technique produced model subsets that were very stable for February. All but one or two variables were eliminated for August. The coefficients of the February models made physical sense and all were statistically significant.

The regressors for February in order of importance were: the height of the freezing level (agl), the planetary geomagnetic

index (K_p linearized to ap), a parameterization of the height of the freezing level, precipitable water in the 1000-850 mb layer, the dew-point depression at 850 mb, the K index of stability, and the departure of the H-component of the magnetic force vector from its mean.

ACKNOWLEDGMENTS

The author's doctoral program was made possible by a scholarship from the Air Force Institute of Technology. The funds were provided by the Air Force Office of Scientific Research under contract No. 79-0003 and the Department of Meteorology.

My warmest regards go to Dr. George L. Huebner, Jr. for his mature judgement, generous donation of time and resources, and friendship. From the first suggestion to continue graduate work to the culmination of the research, Dr. Huebner provided the stimulus to persevere. Dr. Robert L. Sielken, Jr. is singled out for his considerable contribution of time and talent in the statistical aspects of the work. My thanks go to Professor John F. Griffiths, Dr. Vance E. Moyer, and Professor Albert J. Druce for their advice and assistance. Dr. Phanindramohan Das provided numerous bits of insight that became part of the study.

I wish to thank Dr. Ralph Markson of M.I.T. for his personal visit to discuss the work. His suggestions proved to be very helpful. Help with data reduction or computer programming were provided by Lenny Abreu, Peter Voges, Dianne Campbell, and Keith Knight. Joyce Landin provided excellent typing service.

Finally, I wish to thank my wife, Julie, and my sons, Will and Andrew, for the patience and encouragement extended during the brief periods of time that we crossed paths during the conduct of this research.

TABLE OF CONTENTS

	Page
ABSTRACT	iii
ACKNOWLEDGMENTS	vi
LIST OF TABLES	ix
LIST OF FIGURES	xii
I. INTRODUCTION	1
The Mystery of Lightning	1
Literature Review	4
The Need for This Investigation	18
Hypothesis and Contribution	19
II. DISCUSSION OF THE DATA	21
Introduction	21
Sferics Data	21
Thunderstorm-Day Data	28
Synoptic Data	31
Geographic Data	33
Geomagnetic and Sunspot Data	33
Summary of the Data	36
III. INCIDENCE OF LIGHTNING DISCHARGE	38
Introduction	38
The Physical Model	38
The Statistical Distributions	41

	Page
The Incidence of Lightning Discharge	43
IV. RELATIONSHIP BETWEEN LIGHTNING-FLASH DENSITY AND THUNDERSTORM DAYS	77
Introduction	77
Lightning-Flash Density	78
Thunderstorm Days	79
The Regression of Lightning-Flash Density onto Thunderstorm Days	80
Discussion of Results	87
V. ANALYSIS OF THE LARGE-SCALE CAUSES OF THE VARIABILITY OF ELECTRICAL ACTIVITY	94
Purpose and Approach	94
The Regressors	96
Linear Model and Assumptions	103
February Results	107
August Results	118
Physical Significance	118
VI. SUMMARY AND CONCLUSIONS	126
VII. RECOMMENDATIONS	132
REFERENCES	134
APPENDIX A	141
APPENDIX B	155
APPENDIX C	162
VITA	167

LIST OF TABLES

	<u>Page</u>
1 Conversion of K_p to a_p	34
2 Geomagnetic Observatories for H Data.	34
3 Summary of the Data	37
4 Definition of the Statistical Distributions Used in This Study	42
5 Areas on Earth Bounded by Any Two Meridians 10° Apart and the Two Indicated Parallels	48
6 Estimate of the Average Incidence of Lightning Discharge by Latitude Zone for January.	62
7 Estimate of the Average Incidence of Lightning Discharge by Latitude Zone for February	63
8 Estimate of the Average Incidence of Lightning Discharge by Latitude Zone for March.	64
9 Estimate of the Average Incidence of Lightning Discharge by Latitude Zone for April.	65
10 Estimate of the Average Incidence of Lightning Discharge by Latitude Zone for May.	66
11 Estimate of the Average Incidence of Lightning Discharge by Latitude Zone for June	67
12 Estimate of the Average Incidence of Lightning Discharge by Latitude Zone for July	68
13 Estimate of the Average Incidence of Lightning Discharge by Latitude Zone for August	69
14 Estimate of the Average Incidence of Lightning Discharge by Latitude Zone for September.	70
15 Estimate of the Average Incidence of Lightning Discharge by Latitude Zone for October.	71

	<u>Page</u>
16 Estimate of the Average Incidence of Lightning Discharge by Latitude Zone for November.	72
17 Estimate of the Average Incidence of Lightning Discharge by Latitude Zone for December.	73
18 Sensitivity of Regression to Addition of Arbitrary Constant to Values of Dependent Variable, σ , in a Logarithmic Transformation of Data	82
19 Summary of the Regression of Lightning-Flash Density (Units of $\text{km}^{-2} \text{ month}^{-1}$) and Monthly Thunderstorm Days (W.M.O. and Sferics (AF) Data).	86
20 Results for January of Regression of Lightning-Flash Density, σ , onto Thunderstorm Days, T, (W.M.O. and AF (Sferics) Data) with the Assumed Model, $\sigma = aT^b$	88
21 Results for April of Regression of Lightning-Flash Density, σ , onto Thunderstorm Days, T, (W.M.O. and AF (Sferics) Data) with the Assumed Model, $\sigma = aT^b$	89
22 Results for August of Regression of Lightning-Flash Density, σ , onto Thunderstorm Days, T, (W.M.O. and AF (Sferics) Data) with the Assumed Model, $\sigma = aT^b$	90
23 Results for November of Regression of Lightning-Flash Density, σ , onto Thunderstorm Days, T, (W.M.O. and AF (Sferics) Data) with the Assumed Model, $\sigma = aT^b$	91
24 Lightning-Flash Density ($\text{km}^{-2} \text{ month}^{-1}$) for Selected Monthly Thunderstorm Days (W.M.O.).	92
25 The February Models with an Asterisk Denoting the Significant Coefficients at the 10% Level for Various Stratifications of the Number of Cloud-to-Ground Discharges, D_G	108
26 The February Coefficients (Part A), Level of Significance (Part B), and Other Useful Statistics (Part C) for the Models of Table 25	109

LIST OF FIGURES

	<u>Page</u>
1 The time and half-cycle criteria a) for a spheric waveform to be recorded and b) examples of intense waveforms recorded at Chicopee (1) and Bedford (2), Massachusetts, from the same source thunderstorms.	23
2 Grid of the area of data coverage in the Eastern Hemisphere	26
3 Thunderstorm-day chart of the W.M.O. for January (all years of record) for the world.	29
4 Thunderstorm-day chart of the M.S. thesis for January, 1972 for the Eastern Hemisphere	29
5 The number of W.M.O. stations in the Eastern Hemisphere (as of 1953) by 10° latitude- longitude blocks	30
6 The magnetic force, \vec{F} , and the elements of the earth's magnetic field	35
7 Model of the thundercloud with electrical charge distribution and types of discharge.	39
8 Log normal curves of relative likelihood	45
9 Distribution of the average incidence of lightning discharge ($\text{km}^{-2} \text{s}^{-1}$) for January	50
10 Distribution of the average incidence of lightning discharge ($\text{km}^{-2} \text{s}^{-1}$) for February.	51
11 Distribution of the average incidence of lightning discharge ($\text{km}^{-2} \text{s}^{-1}$) for March	52
12 Distribution of the average incidence of lightning discharge ($\text{km}^{-2} \text{s}^{-1}$) for April	53
13 Distribution of the average incidence of lightning discharge ($\text{km}^{-2} \text{s}^{-1}$) for May	54

	<u>Page</u>
14	Distribution of the average incidence of lightning discharge ($\text{km}^{-2} \text{s}^{-1}$) for June. 55
15	Distribution of the average incidence of lightning discharge ($\text{km}^{-2} \text{s}^{-1}$) for July. 56
16	Distribution of the average incidence of lightning discharge ($\text{km}^{-2} \text{s}^{-1}$) for August. 57
17	Distribution of the average incidence of lightning discharge ($\text{km}^{-2} \text{s}^{-1}$) for September 58
18	Distribution of the average incidence of lightning discharge ($\text{km}^{-2} \text{s}^{-1}$) for October 59
19	Distribution of the average incidence of lightning discharge ($\text{km}^{-2} \text{s}^{-1}$) for November. 60
20	Distribution of the average incidence of lightning discharge ($\text{km}^{-2} \text{s}^{-1}$) for December. 61
21	Illustration of the sensitivity of logarithmic models to the addition of an arbitrary constant (α) to values of the dependent variable (lightning-flash density) 83
22	The portion of the NMC grid used in this study 95
23	Illustration of values used in (31) to estimate the average terrain height at X_5 , the center grid point of a 10° latitude-longitude block 103
24	Scatter diagrams and their associated correlation coefficients, r 114
25	Signal monitor operation 142
26	Fix geometry 144
27	Example of a threshold array for part of the Eastern Hemisphere 148
28	Illustration of the procedure used to develop the threshold arrays 149

	<u>Page</u>
29	Illustration of the method used to determine a single threshold-array value (61.4 dB) by the use of a four station fix. 152
30	Flow chart of model calculations used to determine the threshold arrays 154
31	Comparison of the distributions of lightning discharge for August for standard deviations of received sferics of a) 6 dB, b) 7 dB, and c) 8 dB. . . 157
32	Comparison of the distribution of lightning discharge for August for estimates of the variation with latitude of the ratio of cloud to cloud-to-ground discharges by a) Pierce and b) Prentice and MacKerras. 161

CHAPTER I

INTRODUCTION

The Mystery of Lightning

Brief historical perspective. The lightning discharge is perhaps the most dramatic electrical event in nature and one of the most misunderstood [Viemeister, 1961]. The history of scholarly interest in lightning is traceable to the ancient natural philosophers. Frisinger [1977] gives an account of the theories of lightning and thunder from the period of the Greek philosophers to 1800. This perspective is taken from Frisinger's work.

Anaximenes (ca. 585-528 B.C.) and Anaximander (ca. 611-547 B.C.) held that lightning and thunder were caused by air smashing against clouds. Anaxagoras (ca. 499-427 B.C.) maintained that an "aether" or fire in the upper atmosphere descended into the lower atmosphere and flashed through clouds as lightning. Empedocles (ca. 492-430 B.C.) believed that lightning was due to the trapping of the sun's rays by the clouds. The last natural philosopher of the pre-Aristoteleian period to offer an explicit theory of the cause of lightning was Democritus (ca. 460-370 B.C.). He explained that lightning and thunder were caused by the unequal mixture of "atoms" in clouds and the concomitant violent collisions of these atoms. He surmised that lightning and thunder occurred

The citations on the following pages follow the style of the Journal of Geophysical Research.

together but were sensed separately because sight was "quicker" than hearing.

Aristotle (384-322 B.C.) summarized the earlier theories in Meteorologica and gave his interpretation of the cause of thunder and lightning. He thought both were due to the "dry exhalation" in the atmosphere. Aristotle believed that this exhalation was ejected from clouds and caused thunder upon striking nearby clouds. Lightning was due to the exhalation itself, which Aristotle thought to be a fiery "wind." He believed that lightning followed thunder.

The Romans replaced the Greeks in the first century B.C. as the dominant force in the Mediterranean. Except for applications, the Romans virtually ignored the study of natural science. One notable investigator, Posidonius (135-50 B.C.) emerged during this period. He thought that thunder was caused by the bursting of the Aristotelean dry exhalation. Seneca (3 B.C.-65 A.D.) believed that science and theology were entwined. He attributed atmospheric phenomena, such as lightning, to fate.

Aristotle's ideas dominated meteorological thought until the seventeenth century. In 1637, René Descartes published his classic work, Discours de la Méthode. Although his notion that clouds were composed of water and ice particles was advanced for his time, his explanation of lightning and thunder showed once again the influence of Aristotle. Lightning was explained as due

to fiery exhalations between two clouds and thunder was due to the collisions between clouds.

Proof of the electrification of thunderclouds and the knowledge that the lightning discharge is a form of spark discharge was first given by Benjamin Franklin and d'Alibard in 1752. Schonland [1950] gives an excellent account of early experiments. Franklin correctly theorized that the sparks that he produced by friction were similar to lightning. The first experiment to test this notion was conducted in France. In May 1752, Coiffer, working under the scientist, d'Alibard, obtained a stream of sparks between a 40-ft rod and a grounded wire under the influence of a thundercloud. Franklin conducted his famous kite experiment approximately one month later.

Present uncertainties. One should not be critical of early theories that may appear absurd by modern criteria. We need only reflect that scientists have yet to explain many of the mysteries of lightning. There is no general agreement on how charges are generated and separated in thunderclouds. The direction of flow of charge in thunderclouds in given synoptic situations is a moot point. The precise mechanism that causes the tortured path of lightning is disputed. Whether there exists a direct, solar influence on disturbed-weather atmospheric electricity is unknown and the distribution of the occurrence of thunderstorms and lightning is poorly understood.

Literature Review

Introduction. The literature is voluminous on the various aspects of lightning. This review was abridged to include only work on the physical aspects of lightning that were important to this study. The papers cited are representative of the field, but not necessarily exclusively important.

Statistics of thunderstorms and lightning discharges. A thunderstorm day is defined as a day on which thunder is heard at a weather station. The observation of lightning without the sonic noise that it produces (thunder) is not a sufficient criterion for a thunderstorm day to be recorded [W.M.O., 1953]. The thunderstorm day is the only planetary-scale estimate of thunderstorm occurrence that is available. Although a useful statistic, it has obvious deficiencies. Thunderstorm-day data provide no estimate of diurnal variation, duration, or electrical intensity of thunderstorms. A thunderstorm day is recorded at a station whether there occurred a single isolated thunderstorm or several thunderstorms during the day. Moreover, the efficacy of thunderstorm-day statistics is based on the obviously false premise that thunder always is heard no matter where it occurs.

Personnel of the World Meteorological Organization (W.M.O.) compiled the thunderstorm-day statistics from raw material submitted by the meteorological services of the member countries. The following quote is taken from Part 2 of the data presentation

[W.M.O., 1956]: "It should be made clear that this project is not a detailed climatological study of thunderstorm activity over the world . . . The maps cannot be considered to be in any way final; they are subject to revision in light of new data."

Brooks [1925], in a classic paper, pointed out that thunderstorm-day records may be inaccurate. He said:

Thunderstorms which pass directly over the station may be noted, but those which occur at a distance of several miles are often ignored; this is especially the case in tropical stations where thunderstorms are severe but extremely local - at certain times of the day in the rainy season distant thunder is so common that it simply does not occur to the observer to enter it in the register - in fact, he may not be consciously aware of its occurrence . . .

In the same paper, Brooks [1925] estimated from a review of station reports that there are approximately 1800 thunderstorms in existence on earth at any one time and that roughly 100 discharges occur per second. Heydt and Volland [1964] used a heterodyne receiver to study the amplitude spectra of received atmospherics. They estimated, based on counts of signals at frequencies of 5 kHz, 10 kHz, and 40 kHz, that approximately 120 discharges occur per second. This result is in close agreement with that of Brooks, especially when one considers the disparate methods of analysis.

The lightning discharge. Lightning, in general, is the visible discharge produced by thunderstorms. The lightning discharge is a series of electrical processes by which charge is transferred

between centers of opposite polarity [Huschke, 1959].

One of the most interesting and controversial areas in cloud physics is the problem of separation of charge in thunderclouds. The controversy has centered on whether the primary particles that are charged are hydrometeors in clouds or the cloud particles themselves. In the case of hydrometeors, differential fall velocities is posited as the mechanism by which the particles of opposite charge are separated. The theorists that favor cloud particles as the carriers of charge argue that separation occurs through differential convection (updrafts and downdrafts) in clouds [Quart. J. Roy. Meteorol. Soc., 1976].

These separate views on charging mechanisms in thunderclouds were summarized by Mason [1972] in the Bakerian Lecture of 1971 (hydrometeor mechanisms) and Moore [1974] (cloud-particle electrification). Mason [1972] believes that two mechanisms are candidates to explain the acquisition of charge by hydrometeors. One mechanism is the collision of ice crystals with polarized hail pellets that leaves the ice crystals positively charged and the pellets negatively charged. The other is the collision of cloud droplets and hail pellets. The pellets become negatively charged and the rebounding droplets (splash effect) are positively charged. Moore [1974] finds unacceptable any theory that relies on the necessity for the presence of frozen hydrometeors. He has observed lightning in clouds everywhere warmer than the melting

temperature (0°C). Others have reported similar findings [e.g., Rossby, 1966; Hiser, 1973]. Mason [1976] and Moore [1976] have exchanged views on their respective summaries of theories. Mason impeaches the validity of Moore's observations and Moore offers a detailed criticism of the hydrometeor theories.

Lightning discharges almost always are accompanied by thunder. In April 1855, five "brilliant flashes" of lightning were seen to strike the Washington Monument without any observation of thunder. However, observations of this nature are extremely rare [Viemeister, 1961]. The types of discharge which are within the scope of this study include cloud-to-ground and cloud discharges. Other types of discharge (e.g., cloud-to-air, and cloud-to-cloud) occur very rarely [Ishikawa, 1960; Viemeister, 1961].

The cloud-to-ground discharge is a composite and complicated event. It may be studied conveniently in three stages. The initial stage of the step leaders forms the conductive path to earth and ends at the first return stroke; the intermediate stage includes all return strokes; and the final stage comprises the residual variations in electric field after the last return stroke [Pierce et al., 1962].

The leaders follow a stepped tortuous trajectory from the cloud to the ground and ionize a conductive path which typically connects the negative center of charge in the cloud to an induced positive center on the ground. The return stroke gives off light

as it moves upward from ground to cloud. The visual combination of leader and return stroke is popularly termed "lightning." The return-stroke current actually moves downward, typically carrying negative charges from cloud-to-ground [Chalmers, 1967]. Takeuti et al. [1973] observed cloud-to-ground discharges during winter in Japan and found that the return stroke neutralized positive charge in the thunderclouds. They found that return strokes neutralized negative charge in clouds in summer.

There are multiple return strokes in most cloud-to-ground discharges. The number of return strokes may vary from one to as many as 20 [Pierce, 1955; Workman et al., 1960; Takeuti, 1965; MacKerras, 1968]. Pierce [1970] developed empirical rules for the variation with latitude of the average number of return strokes per cloud-to-ground discharge and the proportion of all discharges that go to ground. He found that the proportion of the discharges-to-ground increases and the number of return strokes per discharge decreases with geographic latitude. Prentice and MacKerras [1977] reviewed the literature on the ratio of cloud to cloud-to-ground discharges and developed an empirical expression for the variation with latitude of this ratio. The ratio decreases with latitude in reasonably close agreement with Pierce's results (see Appendix B).

The nature of the cloud discharge is not clearly understood. Smith [1957] observed that most (56 per cent) cloud discharges transfer negative charge upward from a negative center of charge

near cloud base to a positive center above. Ogawa and Brook [1964] observed that the direction of propagation of charge was predominantly (75 per cent of cases studied) from the positive center of charge downward to the negative center of charge. Moyer [1974] observed from aloft a storm in which about 75 per cent of the discharges appeared to parallel the bases of single clouds with the stroke typically emerging from one extremity and reentering an opposite extremity. This observation was made on 8 November 1974 at a location south of Dallas, Texas.

It is important in this study to understand the orientation of the discharge channel in cloud discharges and cloud-to-ground discharges. The remote sensor that was used to collect incident sferics was designed to consider only the vertically polarized component of the field-strength intensity ($V m^{-1}$). Investigators have shown that the cloud discharge and the cloud portion of the cloud-to-ground discharge are oriented dominantly in the horizontal [Ogawa and Brook, 1969; Few, 1970; Teer, 1973; Teer and Few, 1974; Brantley, Tiller, and Uman, 1975; Nakano, 1976; Taylor, 1978]. The portion of the cloud-to-ground discharge from cloud base to the ground is usually vertical or quasi-vertical.

The incidence of lightning discharge. The incidence of lightning discharge is the number of discharges that occur during stormy periods per square kilometer per second.

Aiya [1968] used lightning flash counters to estimate that a

local thunderstorm in India lasts 3 h on the average and produces about one discharge per km^2 . This corresponds to an incidence of discharge of approximately $9 \times 10^{-5} \text{ km}^{-2} \text{ s}^{-1}$. Horner [1965] reviewed data based on various sources (e.g., lightning flash counters, strikes to power lines, and radio noise) and estimated that the incidence for the "main thunderstorm areas" of the world is $10^{-5} \text{ km}^{-2} \text{ s}^{-1}$. He also estimated that the incidence for the world as a whole is of the order $10^{-6} \text{ km}^{-2} \text{ s}^{-1}$. Neither Aiya nor Horner indicated over what period the respective estimates of incidence were averaged. By assuming that on the average one thunderstorm occurs per thunderstorm day, one may infer from Brooks' work [1925] that the incidence of discharge is of the order of $10^{-4} \text{ km}^{-2} \text{ s}^{-1}$ for the world as a whole.

Investigators have used photometer data from satellites to depict a "snapshot" of world lightning activity. The photometers used thus far have been restricted remote sensors. Vorpahl, Sparrow, and Ney [1970] and Sparrow and Ney [1971] used photometers (0.35-0.50 μm and 0.60-0.80 μm) on board the OGO-2 and OGO-5 satellites to sense night-time lightning. As these investigators point out, the satellite data represent lightning from thundery regions as opposed to individual thunderstorms. Turman and Edgar [1978] used data of the Defense Meteorological Satellite Program (DMSP) to depict a snapshot at dawn and dusk of global lightning activity. DMSP photometers were thresholded to collect only an

estimated 8 per cent of incident flashes. The authors estimated that the incidence of discharge for the globe was about $2 \times 10^{-8} \text{ km}^{-2} \text{ s}^{-1}$. This is considerably lower than previous estimates.

Freeman [1974] used sferics data (defined below) to estimate the number of lightning discharges that occurred per month in 1972. This estimate was valid over a regularly-spaced grid that covered much of the Eastern Hemisphere. One could assume an effective area over which lightning-flash counters collect sferics and an average duration of thunderstorms (tropical and extratropical) to estimate the incidence of lightning discharge from sferics data. This is the topic of Chapter III.

Lightning-flash density vs. thunderstorm-days. Lightning-flash density, as used in this study, is defined as the number of lightning flashes that occur during stormy periods per square kilometer per month. Only two groups of investigators have completed thorough studies of this important relationship [Pierce, 1968; Maxwell et al., 1970; Cianos and Pierce, 1972]. Both groups used local lightning-flash-counter data and thunderstorm-day data. The data of this study provide an opportunity to give perhaps the best estimate to date of this relationship [Pierce, 1973]. The results of the studies referenced will be presented in Chapter IV along with those of this study.

Atmospherics. Atmospherics are electromagnetic signals which emanate from lightning discharges [Chalmers, 1967]. The term

"atmospherics" is frequently shortened to "sferics." Popov [1896], working at the Pavlovsk Magnetic and Meteorological Observatory, was the first investigator to study sferics with the use of a detector. Recent advances in sferics work have been largely refinements and extensions of pioneer work accomplished before 1940. According to Horner [1964], the principal early workers were Appleton and Watson-Watt in the United Kingdom, Schonland in South Africa, Bureau in France, Lugeon in Switzerland, Austin in the United States, and Norinder in Sweden.

A common method used to study sferics is to examine the amplitude frequency spectrum of the received sferic waveform. A broad-band receiver may be used to record incident sferic waveforms for analysis. By using electromagnetic propagation laws for very-low-frequency (VLF), one may make inferences concerning the amplitude spectrum of the source from a study of the received spectrum [Pierce et al., 1962].

Leushin [1964] studied the geographic correspondence of centers of sferic activity and thunderstorms in the Soviet Union and concluded that there is a one-to-one correspondence between them. Barkalova [1964] found that there was a good correlation (ranging from 0.73 to 0.97) between the number of thunderstorms and the count of sferics signals (recorded above a threshold) at two stations in the Soviet Union. Hiser [1973] found good association between sferics activity and radar-measured precipitation in

thunderclouds. It should be mentioned that sferics may originate in the sun or the other stars as well as in lightning [Chalmers, 1967].

Sferics in the form of discrete pulses. Lightning discharges produce energy at various frequencies. Cloud-to-ground discharges, or more precisely, the associated return strokes, produce intense energy in the very-low-frequency portion of the spectrum. The noise thus produced is of the form of intermittent pulses superimposed on the continuous background noise [Horner, 1958; Malan, 1958; Kitagawa and Brook, 1960, Takagi, 1961]. Horner and Bradley [1964] report that the transition from essentially discrete pulses to continuous waveforms occurs between 40 kHz and 550 kHz.

The return stroke of the cloud-to-ground discharge also generates significant sferics (K pulses) at very-low-frequency that are perhaps one-tenth the magnitude of the largest pulses [Ishikawa, 1960]. Recoil streamers, which occur when a propagating streamer meets a center of charge opposite in sign to the streamer, produce relatively small K pulses. The leader also generates K pulses, but these are very small in magnitude [Pierce et al., 1962]. Although the various types of K pulses are much less intense than the large, discrete, very-low-frequency pulses, they are more numerous and must be considered when analyzing received sferics [Pierce, 1973].

The cloud discharge generates quasi-discrete K pulses at

very-low-frequency that are remarkably similar to those of the cloud-to-ground discharge. The recoil streamer process is thought to cause these pulses [Pierce et al., 1962]. It is clear that the dominant energy at very-low-frequency in cloud discharges is due to K pulses [Malan, 1958; Horner, 1960]. In rare instances, cloud discharges generate energy of "superbolt" intensity. Superbolts have optical power in the range of 10^{11} - 10^{13} W. Turman [1977] estimates that only five flashes in 10^7 exceed an optical power of 3×10^{12} W.

In summary, both cloud-to-ground and cloud discharges generate significant sferics at very-low-frequency in the form of quasi-discrete pulses. The largest pulses are associated with cloud-to-ground discharges and are due to the initial and subsequent return strokes. Both the return stroke (cloud-to-ground discharge) and recoil streamer (cloud-to-ground and cloud discharges) produce quasi-discrete K pulses, which are less intense but more numerous than the "main" very-low-frequency pulses. The leader stage of a discharge produces sferic pulses at very-low-frequency, but these are very weak in magnitude.

The possibility of direct solar influence on the occurrence of lightning. All of the energy that drives the heat engine of the atmosphere is received from the sun [Griffiths, 1976]. Therefore, the sun is the ultimate cause of earth's weather. However, all the features of the mechanisms by which electromagnetic radiation, both in the form of waves and corpuscles, causes the

intricate patterns that we observe are not known. Meteorologists are skeptical of claims that a direct solar influence produces changes in composite meteorological variables (e.g., vorticity index) which are, in turn, based on the fundamental meteorological variables (i.e., pressure, temperature, density, moisture, and wind velocity). By direct is meant an isomorphic correspondence of fluctuations of solar events (e.g., flares) with meteorological variables. The primary reason for the skepticism is the lack of physical theory, based on arguments of energetics, to explain the results of solar-terrestrial studies. Both the solar and the meteorological variables represent the integrated effects of the fundamental variables and for this reason the underlying physics is masked.

Markson [1971, 1978b] has pointed out that perhaps a definitive "sun-weather effect" will emerge first in the area of atmospheric electricity. In this area, we have a direct physical linkage. Galactic cosmic ray decreases and solar photon enhancements decrease ionization in the atmosphere; the percentage of decrease in ionization increases with altitude and geomagnetic latitude [Ney, 1959]. Ney [1959] and Herman and Goldberg [1978] have offered theories that relate the decrease in ionization to an increase in thunderclouds because of the associated decrease in conductivity and increase in the intensity of the electric field. The solar influence is seen as a modulating effect or enhancement of the occurrence of thunderclouds. For reasons of energetics

it is clear that synoptic and mesometeorological conditions for the occurrence of thunderstorms must be present. Also of interest is the observation that the time constant for all atmospheric electrical changes is less than 1 h [Dolezalek, 1978].

Brooks [1934] studied the association of the annual frequency of occurrence of thunderstorms and the relative sunspot number in selected countries and regions. The correlation coefficient (r) was greatest for Siberia (0.88) and the tropical Pacific (0.49). Mid-latitude areas showed poor correlations. It would seem that Brooks showed interesting evidence only of a high latitude effect. The coefficient of determination (r^2) was 0.77 for Siberia and 0.24 for the tropical Pacific. Therefore, the amount of variance unexplained in the occurrence of thunderstorms by a knowledge of sunspot numbers was 0.23 and 0.76, respectively.

Sparrow and Ney [1971] found no useful relationship between the occurrence of lightning and the variation in the K_p index of geomagnetic activity. Photometer data from the OGO-5 satellite was used to estimate the occurrence of lightning. The data extended north and south of the equator by 35° . Markson [1978a] recommended that data should be stratified into low-, middle-, and high-latitude increments in solar-terrestrial studies since geomagnetic latitude is an important factor in the influx of corpuscular radiation.

Markson [1971; 1974; 1975; 1976] has studied the "thunderstorm

generator" of the atmospheric-electrical global circuit. His work mainly involved a study of the correspondence of thunderstorm activity to solar sector passages and the variability of the potential of the ionosphere relative to the surface of the earth. His data indicated that the occurrence of thunderstorms maximizes at the beginning of a solar sector change from positive to negative.

Dolezalek [1972] stated that the classic picture of a global circuit has never been proven to exist, although it is probably a reasonable general model. The sum of all thunderstorms in existence at any given time is the d.c. generator of the global circuit. The ionosphere and the ground are outer shells in a spherical capacitor. The atmosphere is a leaky dielectric that separates the shells of the capacitor. Isotropic cosmic rays are the main cause of ionization and conductivity in the classic global circuit.

A new theory has been proposed that atmospheric electrical variations in conductivity and the flow of current may be explained by changes in stratospheric ionization [Markson, 1978b]. Most of the resistance in the global circuit is posited to be located in the small area of current flow between the tops of thunderstorms and the ionosphere. The control of this "resistor" by variations in stratospheric ionizations due to the influx of cosmic rays modulates the flow of current in the global circuit. The resistance in the area below thunderclouds is smaller than that above thunder-

clouds due to the effect of corona-discharge ions at low level and the associated increase in conductivity.

The Need for This Investigation

There is a need to understand better all aspects of the lightning discharge, including its climatology. In a classic, survey paper dedicated to Hans Israëel, Dolezalek [1972] stated:

It is obvious that the assessment of the global thunderstorm activity is the weakest point in our attempt to understand global electricity. Reports on thunder and lightning from local stations are bound to give wrong results, even if we average over many years. The network of stations is not dense enough, and at some regions of high thunderstorm activity there are no stations at all.

Horner [1964] stated that there is a need in radio science for a better understanding of the temporal and spatial distribution of the areal density of lightning discharge. Horner [1964] stated:

If a more complete knowledge existed of the densities of lightning discharges in different parts of the world, it could be coupled with a knowledge of the energy radiated by an average discharge to give the world distribution of radiated power. Hitherto this distribution has been assumed to follow the distribution of thunderstorm days, for want of a better index.

Martin and Hildebrand [1965] have expressed the need for a climatology of thunderstorm and lightning parameters. They stated:

Many scientific and engineering disciplines have an interest in the geographic distribution of thunderstorm activity . . . In much of this work there is need for information regarding the expected thunderstorm activity at various geographic locations around the world to enable assessment

of its contribution to the total atmospheric noise level at any other geographic location. On a worldwide basis, knowledge concerning the number and location of lightning discharges, which create large amounts of radio frequency energy, is still very meager and based to a large extent upon studies made in 1925.

Extensive and biased data are available on some aspects of the spatial and temporal occurrence of thunderstorms; there is a relative paucity of data on the occurrence of lightning.

Hypothesis and Contribution

The goal of this study is to contribute information on some aspects of the distribution of the lightning discharge and to study possible meteorological causes of this distribution. The hypothesis that underlies this research is that an estimate of the distribution of lightning discharge may be derived from sferics data. Further, the variation in these data may be studied both physically and statistically by the use of a model. The model includes synoptic, geomagnetic, and solar variables.

The subject of Chapter II is a description of the sferics and other data used in this study. In Chapter III, an estimate is presented of the incidence of lightning discharge over a regularly-spaced grid that covers much of the Eastern Hemisphere. This area of earth was chosen due to the availability of data. The relationship between lightning-flash density and thunderstorm days is the topic of Chapter IV. In Chapter V, the variation in disturbed-weather electrical activity is studied in an attempt

to understand better the variables important to the occurrence of lightning. A summary of the study and conclusions comprise Chapter VI, and recommendations for future work are given in Chapter VII.

CHAPTER II

DISCUSSION OF THE DATA

Introduction

The hypothesis stated in Chapter I was presented in outline form in the author's M.S. thesis [Freeman, 1974] as part of the recommendations for further study. The original data sets of this study were acquired in view of the hypothesis to be tested and on the basis of plausible physical importance. The original data sets are discussed. The procedures used to convert the data to the final variables are explained in Chapters III, IV, and V.

Sferics Data

Definition and source. The sferics data are counts in 6-h intervals of electromagnetic signals (above a threshold intensity) which emanate from lightning discharges. Personnel of the Air Force Technical Applications Center (AFTAC) collected these data in 1972 from a network of sensors capable of recording incident sferics on a global basis. The data were used to depict the noise environment at VLF in a system designed to detect thermonuclear explosions in the atmosphere. A detailed explanation of the remote sensing technique is presented in Appendix A. It is clear [Pierce, 1973; Heydt and Frisius, 1974] that sferics at VLF may be collected and located (fixed) at long range (i.e., thousands

of kilometers).

The sferics recorders. Although sophisticated electronically, the recorders are essentially direction finders of the type introduced by Watson-Watt in the United Kingdom more than 40 years ago. The recorders, called signal monitors, are passive remote sensors that detect, classify, and record the vertically polarized component of incident sferics. The location on earth of a sferic is determined by the use of three or more stations. The time of arrival at each station is recorded; then the difference in time of arrival between stations is converted to distance by the use of the estimated propagation rate at VLF. Finally, the location or "fix" of the sferic is determined by a straightforward application of spherical trigonometry. Sferics incident upon the antennae are recorded on a selective basis. The criteria for recording a signal are the azimuth of arrival (sectoring), the waveform cycle characteristics, and the relative intensity of the waveform (thresholding). All incident sferics that are recorded have peak energies in the broadband frequency range of 250 Hz to 60 kHz [Bailey, 1972]. Most of the energy from VLF sferics is concentrated near 6 kHz [Horner, 1964].

All sferic waveforms recorded by the signal monitors satisfied the time and half-cycle criteria illustrated in Figure 1. Also in Figure 1 are examples of actual large-source-strength sferic waveforms taken from a paper by Kalakowsky and Lewis [1966]. The

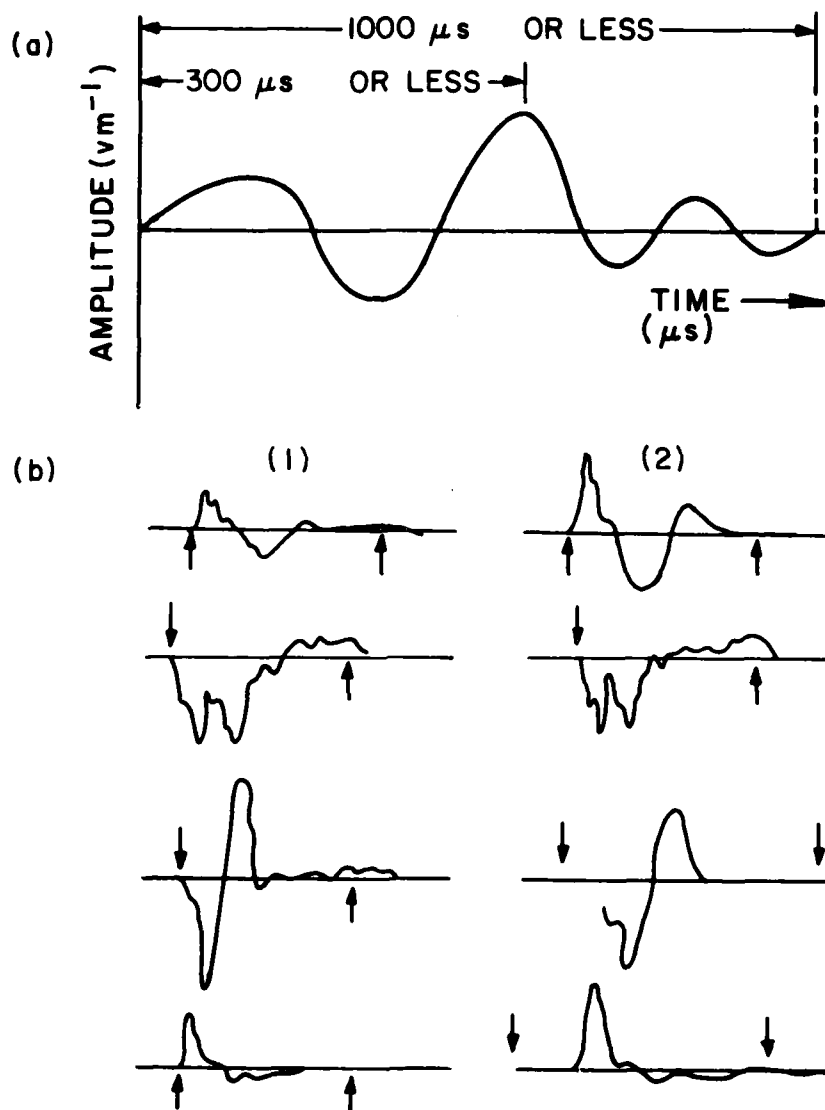


Fig. 1. The time and half-cycle criteria a) for a spheric waveform to be recorded and b) examples of intense waveforms recorded at Chicopee (1) and Bedford (2), Massachusetts, from the same source thunderstorms. Arrows in b) are $3000 \mu\text{s}$ apart and the vertical scale is in V m^{-1} . (After Kalakowsky and Lewis, 1966).

waveforms of VLF sferics (at distances greater than about 60 km) are of the form of sinusoidal waves that build to a peak and then decay to zero. The criteria for recording a waveform are that the half-cycle of maximum amplitude must occur within the first 300 μ s of the waveform and that the total waveform trace must be no greater than 1000 μ s in duration. The actual waveforms shown in Figure 1 were recorded simultaneously at Chicopee and Bedford, Massachusetts, which are 110.4 km apart. These sferics occurred as single events associated, usually, with cold fronts and squall lines, in close proximity to the monitored area. Since these sferics were very large in peak field strength (20 V m^{-1} at 9.3 km minimum), it is not surprising that all of them meet the criteria shown in Figure 1.

The threshold intensity (dB) is a mean estimate of the minimum field-strength intensity below which no signal may be recorded. Virtually all sferics sensors operate above a threshold limit, including the original instrument designed and used by Popov in 1896. The threshold values used in this study were determined by personnel of the U. S. Air Force from a computer-based model. The model inputs were the geographic location of the sensors, propagation laws at VLF, and the individual sensor thresholds (20 dB minimum above a 1 mV m^{-1} reference). The model output was two system threshold values for the periods January to July and August to December of 1972. Two arrays were necessary

because the number of sensors changed in August (see Appendix A).

Area of data coverage. Various areal stratifications of the sferics data were used in Chapter III for the estimates of the incidence of discharge. The total area of coverage is given in Figure 2. It should be noted that the areal resolution was by 10° latitude and longitude blocks centered about the grid points shown. This gross areal resolution affected greatly the strategy for the development of the regressors in the model work of Chapter V.

Data were available for latitudes south of 35°S . However, threshold arrays were not available. A value of three standard deviations from the mean was chosen as the constant threshold value in this area in the thesis [Freeman, 1974]. Only data north of 35°S were included in this study in order to eliminate the uncertainty of the efficacy of the "three standard deviation" assumption.

Validity. How reliable were the sferics data? The answer is important in view of the ambiguous results that are known to accompany local sferics studies. The most serious problem is the reliability of the technique to locate the sferics source (i.e., the fix). The long-range location of incident sferics was accomplished unambiguously and correctly for these data. This was assured by the gross areal resolution of the data and the care exercised in the experimental design and the collection

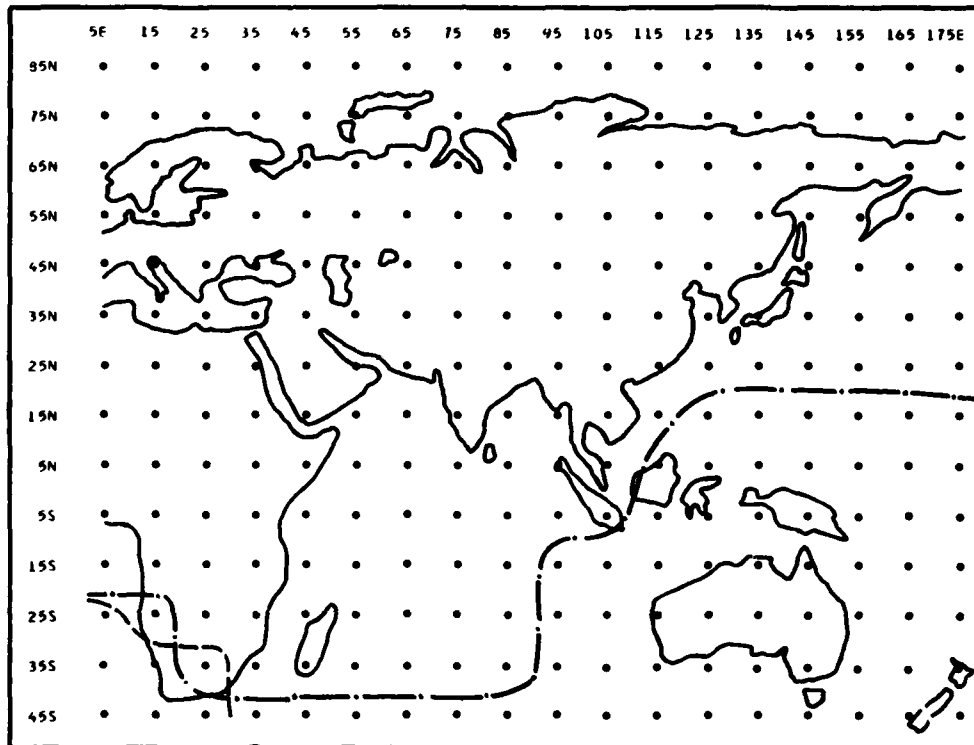


Fig. 2. Grid of the area of data coverage in the Eastern Hemisphere. Each grid point is centered within a data block bounded by parallels and meridians 10° apart. The area of coverage for the period January to July 1972 is north of the broken line. The area of data coverage for the period August to December 1972 is north of the dash-dot line.

of the data. There are sources of error associated with these data as there are with all sets of geophysical data. These errors are treated in Appendix B to the extent that they are known.

It should be pointed out that whistlers as well as sources of sferics other than lightning were excluded by the specific waveform recording criteria of the signal monitors. Whistlers are sferics that leak from the "waveguide" mode of propagation (i.e., between the ionosphere and the ground) into the ionosphere. Whistlers propagate between conjugate points along the geomagnetic lines of force.

Turman [1977] studied the occurrence of superbolt lightning flashes. Superbolts are those with optical power in the range 10^{11} - 10^{13} W. They occur an estimated five in 10^7 flashes (optical power in excess of 10^{12}). The counts of flashes were collected by optical sensors (photometers) on the Vela satellite. Turman used the same source of data as that of this study to correlate counts of sferics with counts of superbolts. He found perfect association in 40 cases collected over a two month period.

The answer to the question of validity is dependent on one's assessment of the accuracy of the data. Clearly, the data are imprecise due to the inherent complexities involved. The most severe logical judgement is that the data are useable relative numbers in some sense but that absolute values are not realized. It

is the author's view that the data represent rough yet valid absolute values as well.

Thunderstorm-Day Data

The widely used thunderstorm-day data of the W.M.O. were described in Chapter I. An example of an analyzed monthly thunderstorm-day chart for the world (January) is given in Figure 3. An estimate of the distribution of thunderstorm days for January derived from sferics data [Freeman, 1974] is given in Figure 4.

One aspect of the observational bias of the W.M.O. data was the uneven distribution of observing stations. The number of W.M.O. stations was counted within each of the 10° data blocks of this study. The results are shown in Figure 5. Obviously, thunderstorms frequently were not recorded because there were too few stations and observers.

A detailed comparison of W.M.O. thunderstorm days and sferics-derived thunderstorm days was presented in the M.S. thesis [Freeman, 1974]. The respective estimates of thunderstorm days differed considerably in each month studied. One possible cause of the differences was that the monthly charts based on sferics data (one year of record) could represent an anomaly from the mean pattern of the W.M.O. charts. Another cause of the difference that seems incontrovertible was that in the W.M.O. compilation of the data there were extensive areas on earth with a void of data

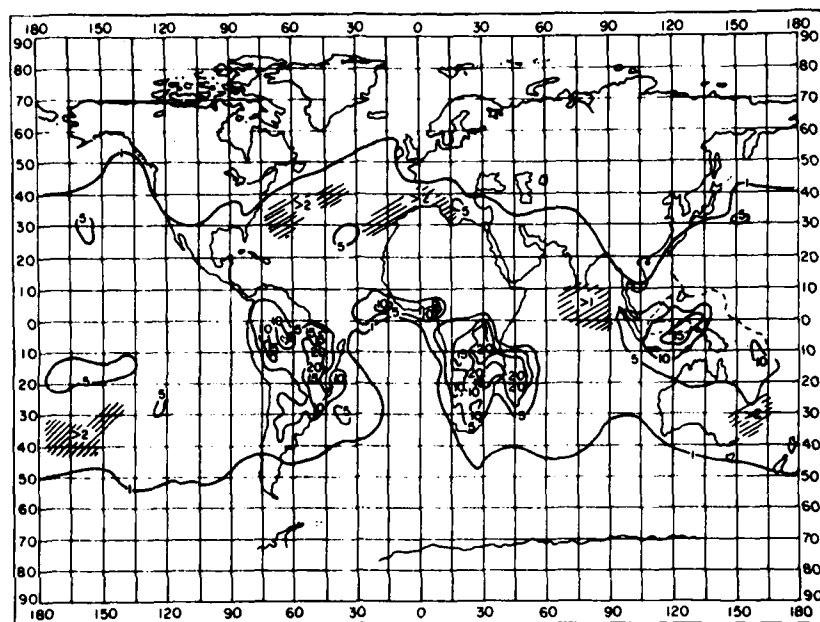


Fig. 3. Thunderstorm-day chart of the W.M.O. for January (all years of record) for the world. Isolines are in thunderstorm days. (After Valley, Ed., Handbook of Geophysics, 1960).

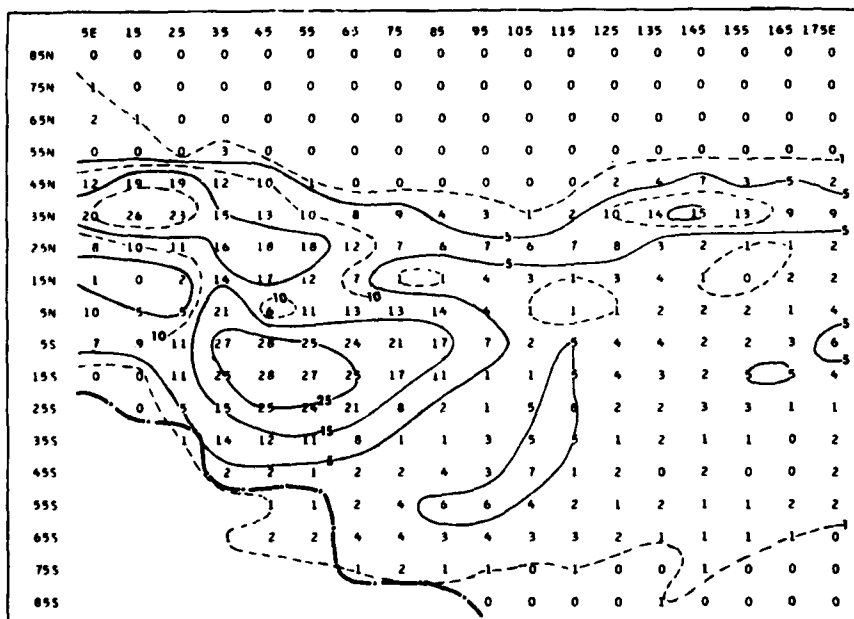


Fig. 4. Thunderstorm-day chart of the M.S. thesis for January, 1972 for the Eastern Hemisphere. Full isolines are in thunderstorm days. Broken lines are intermediate isolines. The dash-dot line is the threshold-sector line.

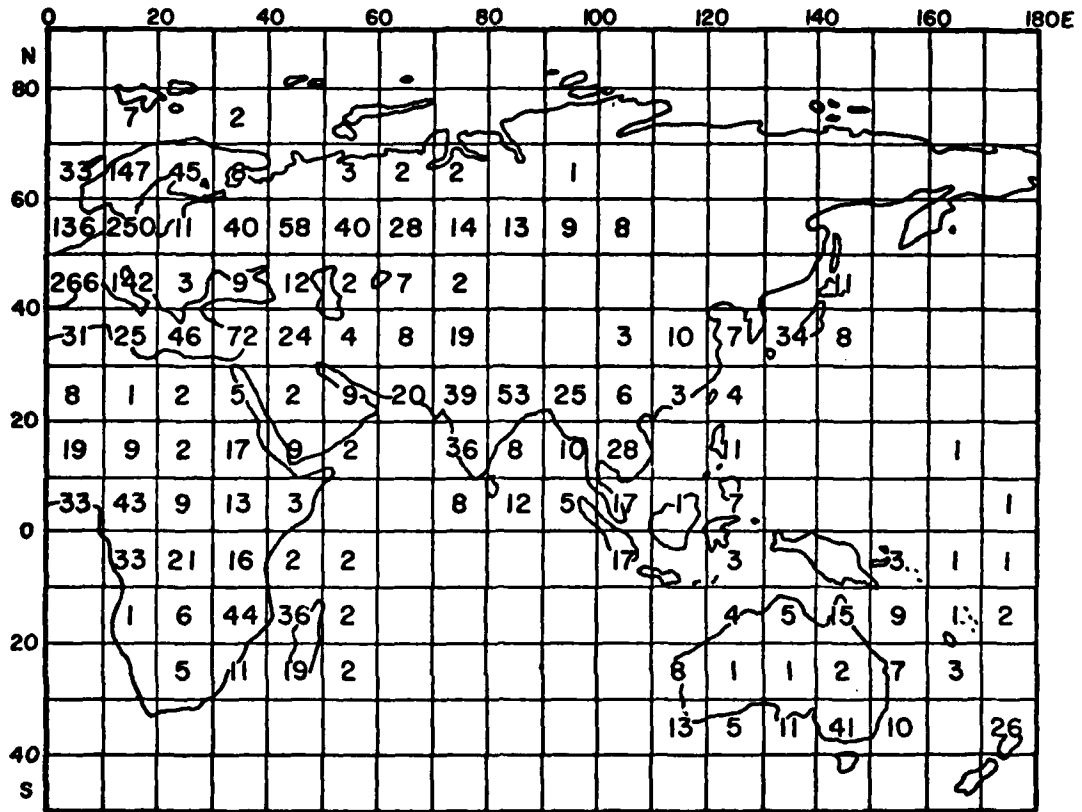


Fig. 5. The number of W.M.O. stations in the Eastern Hemisphere (as of 1953) by 10° latitude-longitude blocks.

coverage (e.g., the oceans).

Synoptic Data

Introduction. The synoptic data, as used in this study, refer to analyzed fields of data on the octagonal grid (47x51) of the National Meteorological Center (NMC). The projection of the NMC grid is polar stereographic and the grid spacing is 381 km at 60°N. The synoptic data were confined to February and August of 1972 due to the extensive effort required to obtain the data and prepare them for analysis. These winter and summer months were chosen for their seasonal representativeness and the fact that no sferics data were missing in these months.

The analyzed fields were obtained from the National Center for Atmospheric Research (NCAR) except for moisture grids which were obtained from the Fleet Numerical Weather Central (FNWC). The technique used to analyze "random" station data to grid points, as well as the grids, were the same regardless of agency. (The FNWC grid is an extension of the NMC octagon to include the area from the equator to 15°N.) The 12-h forecast from the previous forecast run was obtained and used as a "first guess" field for the upcoming analysis run. Then, observational data were fitted onto the first-guess field. In areas where there were no observations, or perhaps very sparse coverage, the first-guess data were used in lieu of observations. Finally, the observed data were interpolated in space and assigned to grid

points. The geostrophic approximation was used to obtain the first-guess fields for wind data.

The analyzed fields were available on CDC, binary-packed, magnetic tapes. It was necessary to write an assembly-language program to convert each tape from the 60-bit format (CDC) to the 32-bit format required for use on the available equipment (Amdahl 470 V/6).

Temperature-height-pressure. These fields were available at the mandatory pressure levels (1000, 850, 700, 500, 400, 300, 200, 150, and 100 mb). The temperature ($^{\circ}\text{C}$), geopotential height (cm), and pressure (mb) were available at each grid point for each level at 0000 UT and 1200 UT daily.

Layer relative humidity. Layer relative humidity (RH) data were available for August only on the NMC grid for the 1000-500 mb layer. The RH values were computed first for each 100 mb sub-layer. The values were then weighted by the pressure depth of the sub-layer, summed, and averaged by pressure over the 1000-500 mb layer.

Wind. The zonal (u) and meridional (v) components of the wind (knots) were available at the mandatory pressure levels for each grid point at 0000 UT and 1200 UT daily.

Low-level moisture. Low-level moisture data (FNWC) were available at each grid point for the surface, 850 mb, and 700 mb levels at 0000 UT and 1200 UT daily. These data included the vapor pressure (mb) at the surface and the temperature ($^{\circ}\text{C}$)

and dew-point depression ($^{\circ}\text{C}$) at 850 mb and 700 mb. The dew-point depression is the difference between the ambient and dew-point temperatures.

Geographic Data

Terrain data by 10'-latitude and -longitude blocks for the world were obtained from NCAR. The original source was the FNWC. The data included maximum and average elevation (m) for each square. The data were available on magnetic tape and were unpacked with an assembly-language program as explained previously.

A coarse grid of average terrain height (ft) at $5^{\circ}\times 5^{\circ}$ latitude-longitude intersections was available in the literature [Berkofsky and Bertoni, 1955].

Geomagnetic and Sunspot Data

These data included the K_p index of geomagnetic activity, magnetic hourly values (H-component of the magnetic vector), and sunspot numbers for the months of February and August 1972. The K_p values and sunspot numbers were available in the Journal of Geophysical Research (JGR). The H data were obtained from the National Geophysical and Solar-terrestrial Data Center (NGSDC).

The K_p index is a global measure of changes in the intensity of earth's magnetic field due to solar corpuscular radiation. The K_p values are 3-hourly quasi-logarithmic indices scaled from 0 (very quiet) to 9 (extremely disturbed) in thirds of a unit.

For example, 4_- is $3 \frac{2}{3}$, 4_0 is 4, and 4_+ is $4 \frac{1}{3}$.

The K_p index is intended for users outside the field of geophysics and a linear conversion is commonly used. The linear planetary index is a_p [King, 1971]. The conversion is given in Table 1.

TABLE 1. Conversion of K_p to a_p .

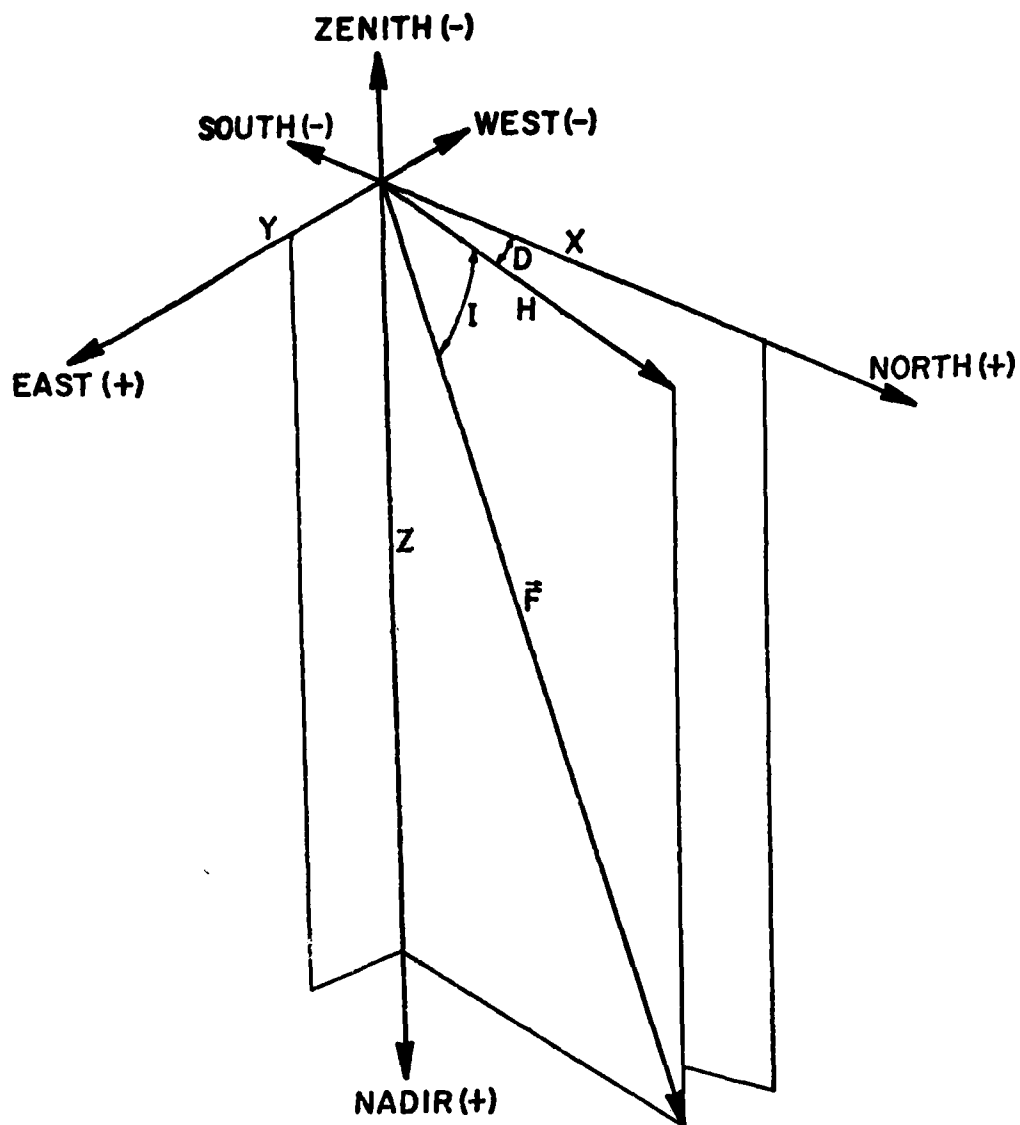
K_p :	0_0	0_+	1_-	1_0	1_+	2_-	2_0	2_+	3_-	3_0	3_+	4_-	4_0	4_+
a_p :	0	2	3	4	5	6	7	9	11	15	18	22	27	32

K_p :	5_-	5_0	5_+	6_-	6_0	6_+	7_-	7_0	7_+	8_-	8_0	8_+	9_-	9_0
a_p :	39	48	56	67	80	94	111	132	154	179	207	236	300	400

The magnetic force vector, \vec{F} , and the elements of earth's magnetic field are illustrated in Figure 6. The H-component data were obtained for the stations listed in Table 2. The data were on photostatic copies of the Russian station records. The specific stations were chosen due to their locations and because of the availability of data. The locations fit the experimental design of the model work in Chapter V.

TABLE 2. Geomagnetic Observatories for H Data.

Station Name	Geographic		Geomagnetic	
	Lat. (N)	Long. (E)	Lat. (N)	Long. (E)
Panagyurishte	42.5	24.2	40.8	103.8
Odessa	46.8	30.9	43.6	111.5
Tbilisi	42.1	44.7	36.6	122.5
Ashkhabad	37.9	58.1	30.5	133.5
Tashkent	41.3	69.6	32.3	144.4



D= Declination
H= Horizontal Intensity
I= Inclination or Dip
F= Total Intensity

X= North-South Component
Y= East-West Component
Z= Vertical Intensity

Fig. 6. The magnetic force, \vec{F} , and the elements of the earth's magnetic field.

Sunspots are optically dark regions of the photosphere that exhibit relatively low temperatures and high magnetic fields. Sunspot numbers have been the most common index of solar activity throughout the history of solar observation, which dates from the fourth century B.C. The most accepted form of this index is the Zürich sunspot number, R_Z . The Zürich relative sunspot number is defined as $R_Z = K (10 g + f)$, where K is an observatory-dependent factor that assures continuity with past observations, g is the number of spot groups observed, and f is the number of individual spots [King, 1971].

Summary of the Data

The basic sets of data are summarized in Table 3.

TABLE 3. Summary of the Data.

Data	Source	Observation Time or Interval (UT)	Maximum Percent Missing* %	Maximum Number of Observations*
Sferics	AFTAC	00-06, 06-12 12-18, 18-22	8	341,640
Thunderstorm-Day	W.M.O.	Monthly Average	N/A	N/A
Temperature-Height- Pressure	NCAR	00, 12	9	155,520
Layer Relative Humidity	NCAR	00, 12	15	80,352
Wind (u,v)	NCAR	00, 12	9	155,520
Low-Level Moisture	FNWC	00, 12	12	155,520
Geographic	FNWC	N/A	0	90,000
Geomagnetic and Sunspot	NGSDC			
K _p Index		3 Hourly	0	480
H ^p Data		Hourly	0	7,200
Sunspot		Daily	0	60

*Refers to the maximum number of observations used (assuming no missing data) and the maximum, missing percentage of observations in the analyses in subsequent chapters. The number of observations used in a given analysis varied with the stratification of the data chosen. The number of observations available always was considerably greater than that used.

CHAPTER III

INCIDENCE OF LIGHTNING DISCHARGE

Introduction

The incidence of lightning discharge, as defined in Chapter I, is the number of discharges that occur during stormy periods per square kilometer per second. An estimate was given in the author's M.S. thesis of the number of lightning discharges at grid points (see Figure 2) for each month and the incidence of lightning discharge for January and April [Freeman, 1974]. The purpose of this chapter is to present an estimate of the incidence of discharge for all months. The model that was developed in the thesis was used in this chapter with the exception of the method used to estimate the effective area under the influence of a thunderstorm within a 10° latitude-longitude block. Both methods will be explained.

Investigators recently have shown (see Chapter I) that horizontal discharges are dominant within clouds. This is important in the development of the physical model and the subsequent analyses of the sferics data.

The Physical Model

The physical model of the charged thundercloud, shown in Figure 7, differs from that in the M.S. thesis [Freeman, 1974]. Although

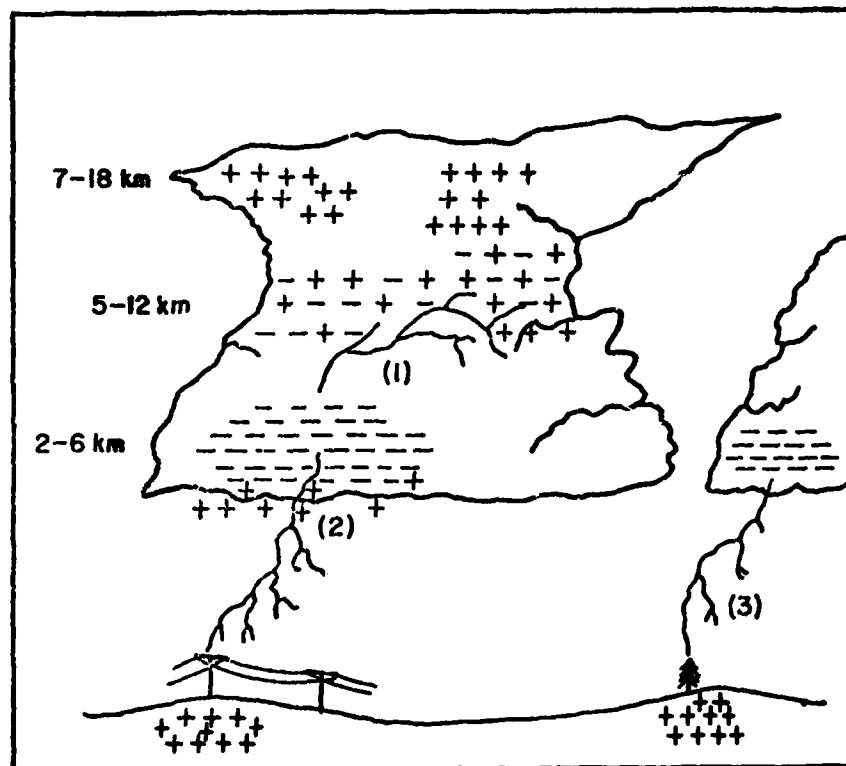


Fig. 7. Model of the thundercloud with electrical charge distribution and types of discharge. The latter include cloud discharges (1) and cloud-to-ground discharges (2) and (3).

it was suspected that many cloud discharges were horizontal in orientation, the thesis model showed quasi-vertical cloud discharges. An in-depth analysis was included in the thesis to demonstrate that few sferics due to cloud discharges were recorded. Essentially, the sferics from cloud discharges were too weak in field-strength intensity to be recorded. The only assumptions in the analysis were that the sample statistics given in Table 4 were close approximations to the state-of-nature, and the threshold values (explained in Appendix A) were reasonable estimates of system response in the mean.

We may now use the additional physical argument that few sferics from cloud discharges were recorded because most sferics from cloud discharges are horizontally polarized. The sferics recorders (signal monitors) were designed to collect only the vertically-polarized component of incident waveforms ($V\ m^{-1}$). The counts of sferics used in this study were assumed to be due to the return strokes of the cloud-to-ground discharge.

The classic cloud model, shown in Figure 7, includes a net positive center of charge in the upper portion of the thundercloud (7-18 km) and a net negative center of charge near the melting level (2-6 km). A weak positive center of charge is frequently observed near the cloud base [Chalmers, 1967]. Numerous workers have reported physical models of the distribution of charge in thunderclouds [e.g., Takagi, 1961; Horner, 1964; Huzita and Ogawa,

1976]. The various models differ mainly in the estimate of the height of centers of charge. The classic model of a charged thundercloud probably represents a reasonable composite depiction of the net effect of charges in thunderclouds by level within the cloud. It should be emphasized that atmospheric clouds are amazingly complex and intricate in all respects and no model (simple or complex) represents the variability in real clouds.

The most detailed study to date of a single lightning flash was conducted during the Thunderstorm International Program-1976 (TRIP-76) [Uman et al., 1978]. The negatively charged region in the cloud was located in a horizontally-stratified layer between heights of 6 and 8 km. The investigators concluded that the charge resided in a region of hail or graupel.

The Statistical Distributions

The efficacy of the estimation of the incidence of discharge based on sferics data (collected above a threshold) is dependent on knowledge of the statistical distributions of the quasi-discrete sferics. Specifically, the distributions of the field-strength intensity of sferics from first and subsequent return strokes are needed. Fortunately, the distributions of the peak field strength of sferics from return strokes has been studied extensively [e.g., Horner, 1964; Horner and Bradley, 1964; Pierce, 1969]. The weaker K-pulse sferics from cloud and cloud-to-ground discharges have not been studied sufficiently to define the

distribution of field-strength intensity of sferic waveforms to the same degree of certainty as that of the more intense sferics.

The estimates of the type and parameters of the distributions obtained from the literature and from personal contact with Pierce [1973] were covered in detail in the M.S. thesis [Freeman, 1974]. The statistical distributions used in this study are given in Table 4. The reader is referred to the thesis if further detail is of interest.

TABLE 4. Definition of the Statistical Distributions Used in This Study. Values are in dB. Standard Deviation is denoted by S.D.

Sferic Generator of Peak-Field Strength Intensity	Distribution	Mean	S.D.	+1S.D	+2S.D	+3S.D
First Return Stroke	log-normal	69.5	7	76.5	83.5	90.5
Subsequent Return Stroke	log-normal	63.5	7	70.5	77.5	84.5

The field-strength intensity ($V\ m^{-1}$) of source sferics were assumed to be log-normally distributed. The sferics were due to first and subsequent return strokes of cloud-to-ground discharges. The convention used in this study to convert field-strength intensity in volts per meter to decibels (dB) is

$$dB = 20 \log \frac{E}{E_r} \quad (1)$$

where E_p is the peak received field-strength intensity of the waveform above the reference field strength, E_r , of 1 mV m^{-1} .

The probability, Q_1 , of occurrence of an electrical event, such as a first return stroke, greater than or equal to a given threshold value, T_o (dB), of field strength, may be expressed according to the following probability law

$$Q_1 = P(R_1 \geq T_o) = \frac{1}{\sigma \sqrt{2\pi}} \int_{T_o}^{\infty} e^{-\frac{(x - \mu)^2}{2\sigma^2}} dx \quad (2)$$

where R_1 (dB) is the field strength intensity of the first return stroke; σ is the standard deviation (dB); μ is the mean of the intensity (dB) of first return strokes; and x is the variable of integration. The peak field strength of the first return stroke spheric, E_p (V m^{-1}), above a reference is log-normally distributed. (R_1 (dB) is normally distributed.)

The Incidence of Lightning Discharge

The system of sensors recorded counts of VLF sferics in a given 10° latitude-longitude block over 6-h intervals of time. We let

X = the number of sferics observed,

R_1 = the number of first return strokes that occurred,

R_s = the number of subsequent return strokes that occurred,

Q_1 = the probability of occurrence of a first return stroke,

Q_s = the probability of occurrence of a subsequent return stroke.

Therefore

$$X = Q_1 R_1 + Q_s R_s \quad (3)$$

and

$$X = Q_1 R_1 + q Q_s R_1 \quad (4)$$

where q is the number of subsequent return strokes per cloud-to-ground discharge (i.e., $R_1 : R_s = 1 : q$). This quantity, q , varies with latitude.

One may understand (4) better by the use of relative likelihood curves [Pierce, 1969]. Relative likelihood is defined as the likelihood of occurrence of a single event (R_1 or R_s) above a threshold intensity relative to the mean of the first return stroke distribution. The log-normal curves of relative likelihood for R_1 and R_s that are valid along the equator are shown in Figure 8. One must construct a different set of curves for each latitude. Pierce [1970] gave an estimate, based on empirical studies, of the variation with latitude, ϕ , of q

$$q = 5 - (\phi/20) \quad (5)$$

We may solve (4) for R_1 , which is equivalent to solving for the number of cloud-to-ground discharges, D_G , since there is one "first return stroke," R_1 , per D_G . Thus

$$D_G = \frac{X}{Q_1 + q Q_s} \quad (6)$$

Then we estimate the total number of discharges, D_T , which is comprised of cloud discharges, D_C , and cloud-to-ground discharges, D_G . Therefore:

$$D_T = D_G + D_C \quad (7)$$

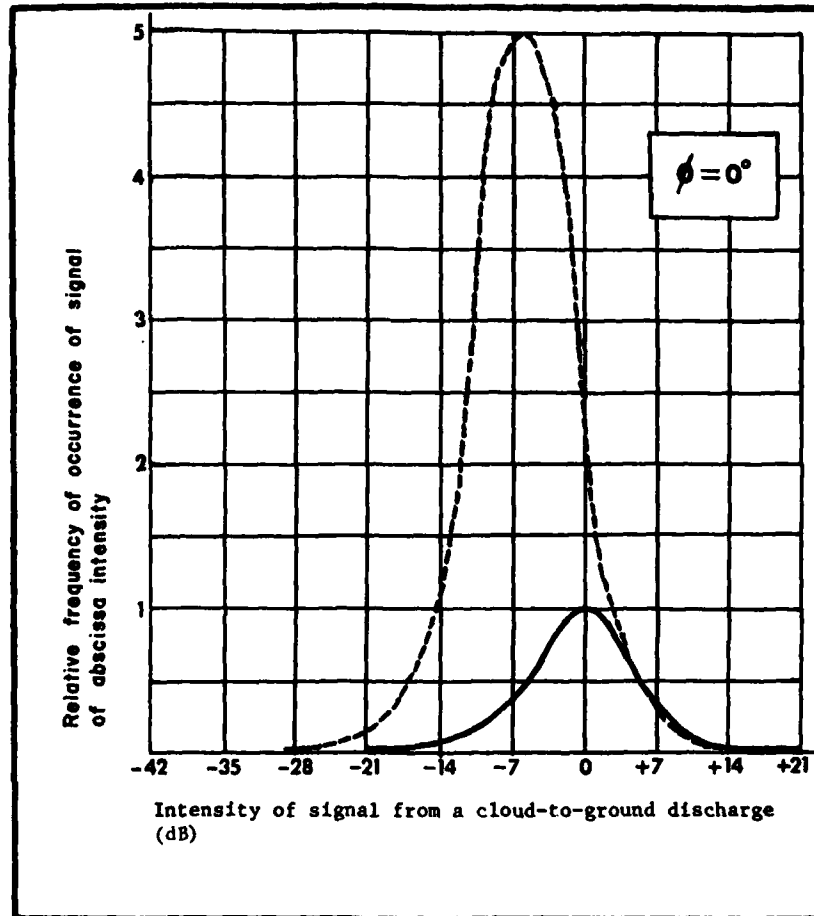


Fig. 8. Log normal curves of relative likelihood. Solid curve is the relative likelihood of the intensity of the first return stroke. Broken curve is the relative likelihood of the intensity of the subsequent return strokes multiplied by the average number of subsequent return strokes per first return stroke. Latitude is \emptyset .

$$D_T = D_G (1 + M) \quad (8)$$

where M is the ratio of D_C to D_G .

Pierce [1969] developed an empirical expression for M as a function of latitude, ϕ

$$M = \frac{9 - (\phi/30)^2}{1 + (\phi/30)^2} \quad (9)$$

Prentice and MacKerras [1977] developed equivalent empirical rules for the variation with latitude of the ratio of cloud to cloud-to-ground discharges, M'

$$M' = 4.16 + 2.16 \cos 3\phi \quad (10)$$

There is not sufficient difference, in view of other sources of error, in (9) and (10) to make the choice of rules critical. The expression by Pierce, (9), was used in this study. The effect of the use of (10) in place of (9) is covered in the analysis of error in Appendix B.

The equation for the estimated number of lightning discharges, D_T , at a given grid point, may be written in the following expanded form

$$D_T = \frac{X}{\frac{1}{\sigma\sqrt{2\pi}} \int_0^{\infty} T_0 e^{-\frac{(x-\mu)^2}{2\sigma^2}} dx + q \left\{ \frac{1}{\sigma'\sqrt{2\pi}} \int_0^{\infty} T_0' e^{-\frac{(x'-\mu')^2}{2\sigma'^2}} dx' \right\}} [1+M] \quad (11)$$

where the unprimed quantities refer to the distribution of the first return stroke and the primed quantities to that of the

subsequent return stroke, X is the number of sferics recorded, and the other quantities are defined with respect to (2), (5), and (9).

As mentioned in Chapter I, one may extend (11) to estimate the incidence of lightning discharge ($\text{km}^{-2} \text{s}^{-1}$) by the assumption of an effective area for lightning flash counters and a mean storm duration. The incidence of lightning discharge was estimated in the M.S. thesis for January and April over the grid in Figure 2 [Freeman, 1974]. It was assumed that a thunderstorm day represented an effective area of 1000 km^2 . The number of discharges per thunderstorm day (i.e., per 1000 km^2) was estimated. Then, an average storm duration of 3 h in the tropics (20°N - 20°S) [Aiya, 1968] and 1 h in extratropical latitudes [Horner, 1964] was assumed and the incidence of discharge ($\text{km}^{-2} \text{s}^{-1}$) calculated.

In the present work, the active storm area was the effective area of a lightning-flash counter. This areal value varies with type of counter. The value of 500 km^2 was chosen for this study because it perhaps affords the widest direct comparison with other work [Pierce, 1973]. The effective area under the influence of thunderstorms for a given 10° latitude-longitude block was then determined by dividing the area of the block by 500 km^2 . The areas of the blocks, given in Table 5, were determined by the use of spherical trigonometry. This method of determination of effective area allowed comparisons to be made of the estimates of incidence

based on sferics collected at long range (this study) with incidence determined in local areas with lightning-flash counters. Further, the effective area was not dependent on estimated thunderstorm days.

TABLE 5. Areas on Earth Bounded by Any Two Meridians 10° Apart and the Two Indicated Parallels

Parallel Bounds	Area (km ²)	Parallel Bounds	Area (km ²)
0 - 10	1,230,163	50 - 60	708,288
10 - 20	1,192,786	60 - 70	521,875
20 - 30	1,119,165	70 - 80	319,606
30 - 40	1,011,540	80 - 90	107,625
40 - 50	873,180		

The average incidence of lightning discharge was calculated by the use of (11) and the assumptions of effective area and storm duration. That is

$$\bar{D}_I = \frac{1}{N} \frac{D_1 + D_2 + \dots + D_N}{(A/500) \times t_1} \quad (12)$$

where \bar{D}_I is the average incidence of discharge (km⁻² s⁻¹) at a grid point (Figure 2) in a month; N is the number of 6-h synoptic intervals in a month with active storms (i.e., counts of sferics); D₁, D₂, etc. are the estimated number of discharges in each 6-h interval from (11); A is the area (km²) of the appropriate

10° block (Table 5); t_i is the average duration of the stormy period in a 6-h interval (i is 10,800 s in the tropics (20°N - 20°S) and 3,600 s elsewhere).

The average monthly value of incidence of discharge, \bar{D}_I , is displayed at grid points that cover much of the Eastern Hemisphere in Figures 9-20. One may multiply (12) by its denominator and divide by a new denominator that reflects different assumptions of effective area and storm duration to develop new sets of charts. The values in Figures 9-20 are negative ordinary logarithms of the incidence of discharge ($\text{km}^{-2} \text{s}^{-1}$). The characteristic for each value is one less than the appropriate negative power of 10. For example, in Figure 9 at 45°N , 25°E , one finds the value 5.5 and may immediately determine that the estimate of monthly average incidence for this data block is of the order of 10^{-6} lightning discharges per square kilometer per second. Estimates of the average incidence of lightning discharge were summarized by latitude zones and are given in Tables 6-17 for each month.

Aiya [1968] estimated that the incidence of discharge for India was $9 \times 10^{-5} \text{ km}^{-2} \text{ s}^{-1}$ based on lightning-flash counter data. The average of values for all months of this study for data blocks that include most of India (i.e., center points of 15°N , 75°E and 15°N , 85°E) is approximately $1.0 \times 10^{-5} \text{ km}^{-2} \text{ s}^{-1}$.

Horner [1965] estimated, on the basis of various sources of data (e.g., lightning flash counters and strikes to power lines), that

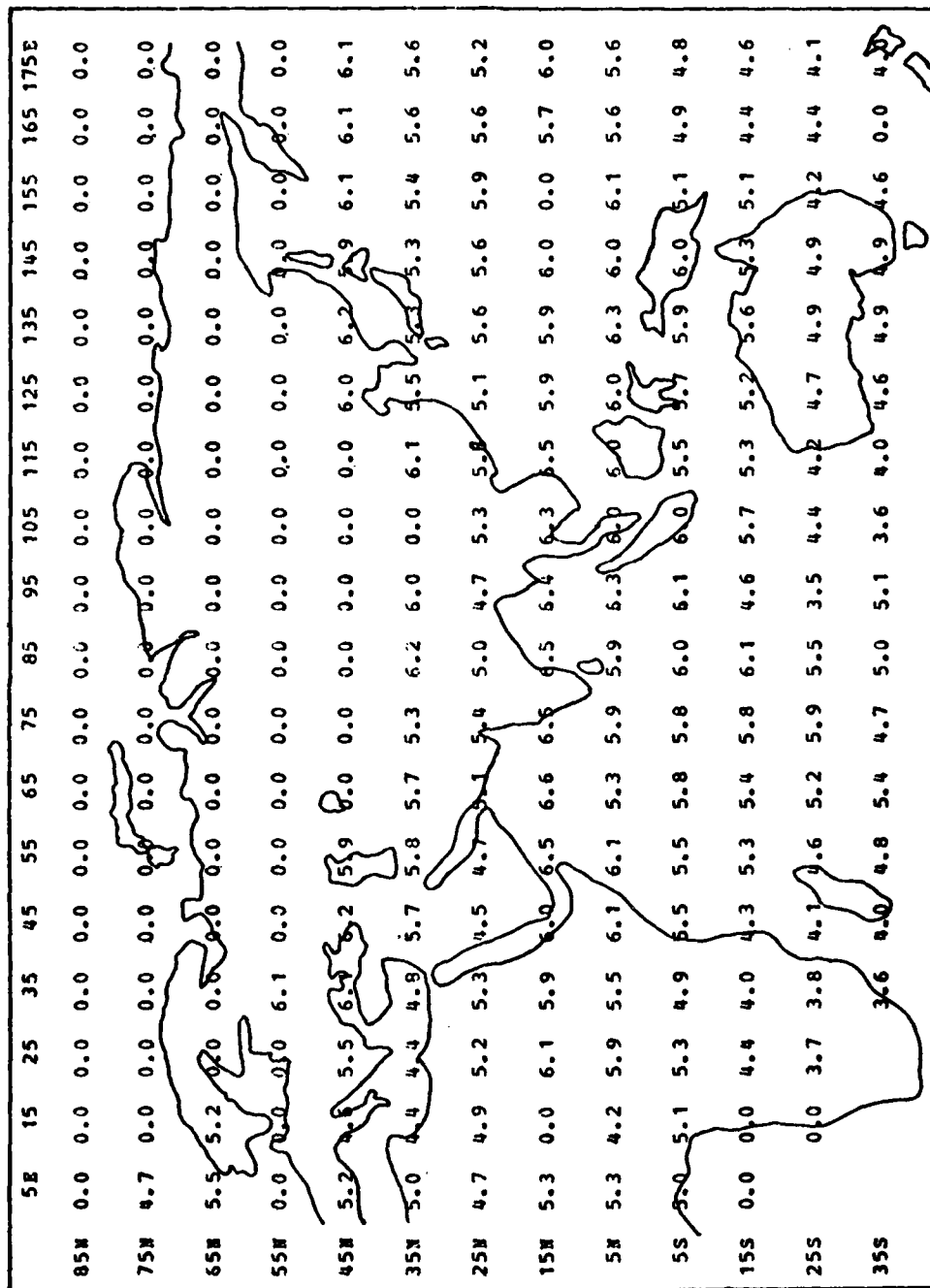


Fig. 9. Distribution of the average incidence of lightning discharge ($\text{km}^{-2} \text{s}^{-1}$) for January. Values are negative ordinary logarithms for 10° data blocks centered at the grid points shown.

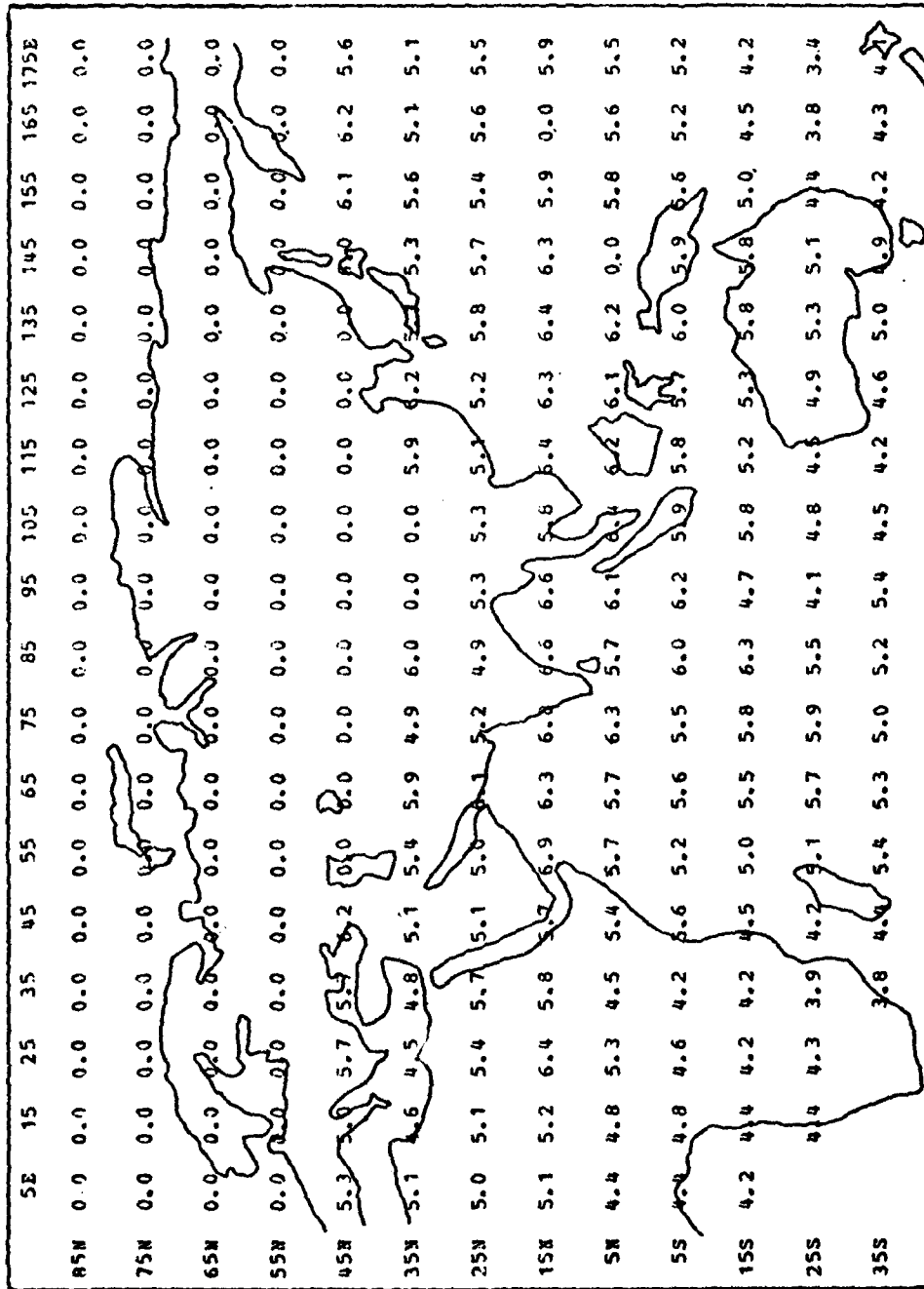


Fig. 10. Distribution of the average incidence of lightning discharge ($\text{km}^{-2} \text{s}^{-1}$) for February. Values are negative ordinary logarithms for 10° data blocks centered at the grid points shown.

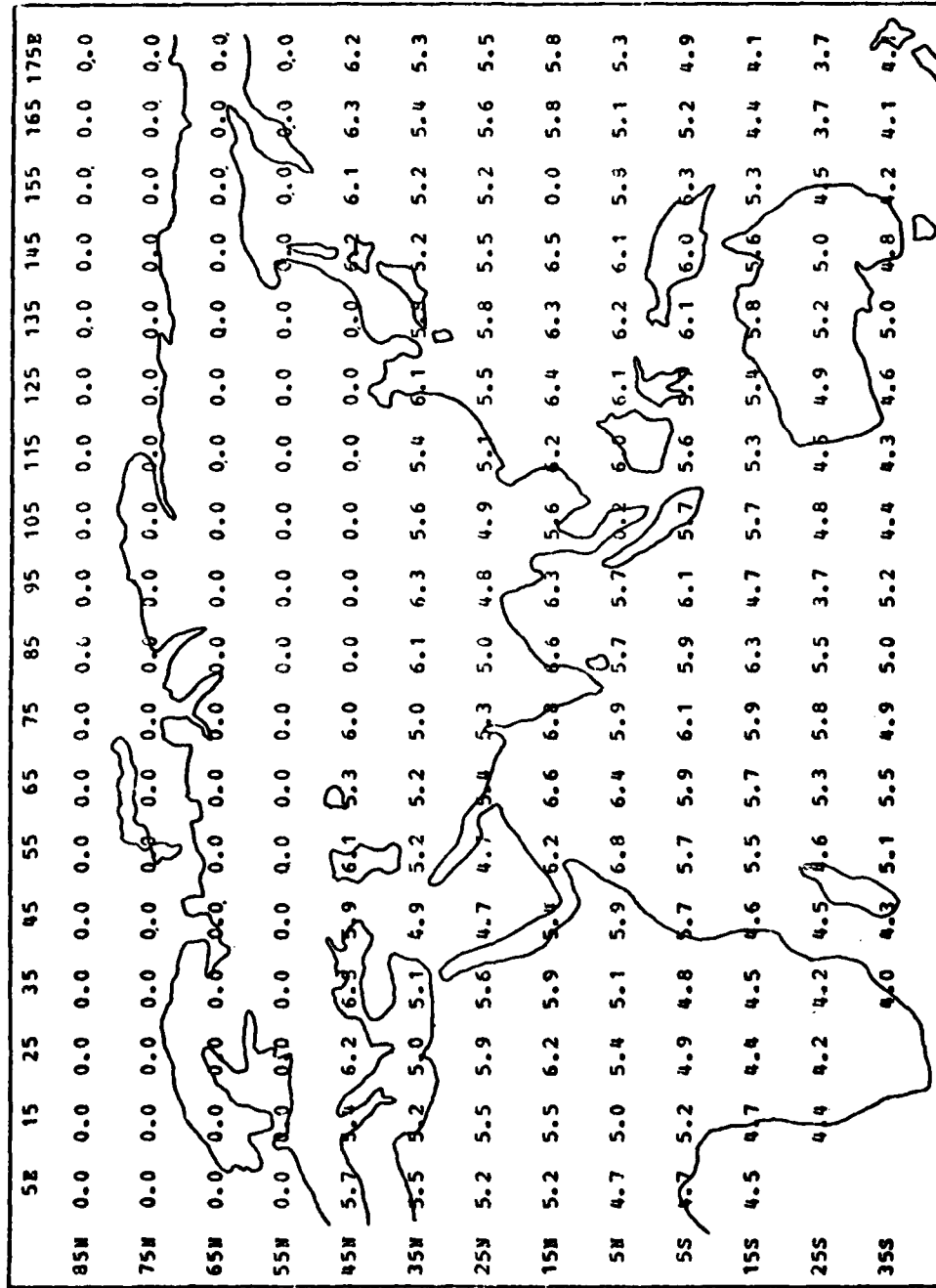


Fig. 11. Distribution of the average incidence of lightning discharge ($\text{km}^{-2} \text{s}^{-1}$) for March. Values are negative ordinary logarithms for 10° data blocks centered at the grid points shown.

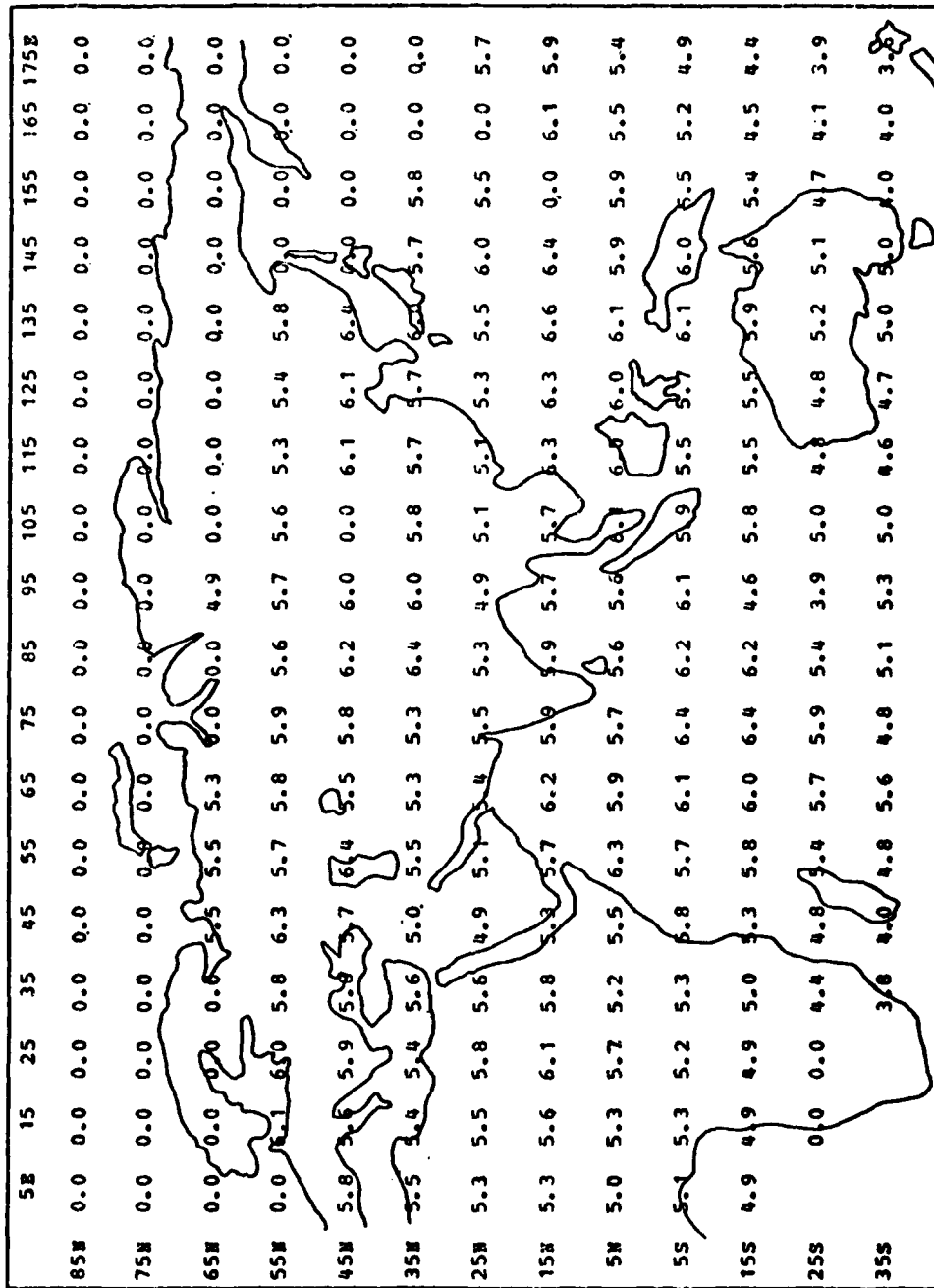


Fig. 12. Distribution of the average incidence of lightning discharge ($\text{km}^{-2} \text{s}^{-1}$) for April. Values are negative ordinary logarithms for 10° data blocks centered at the grid points shown.

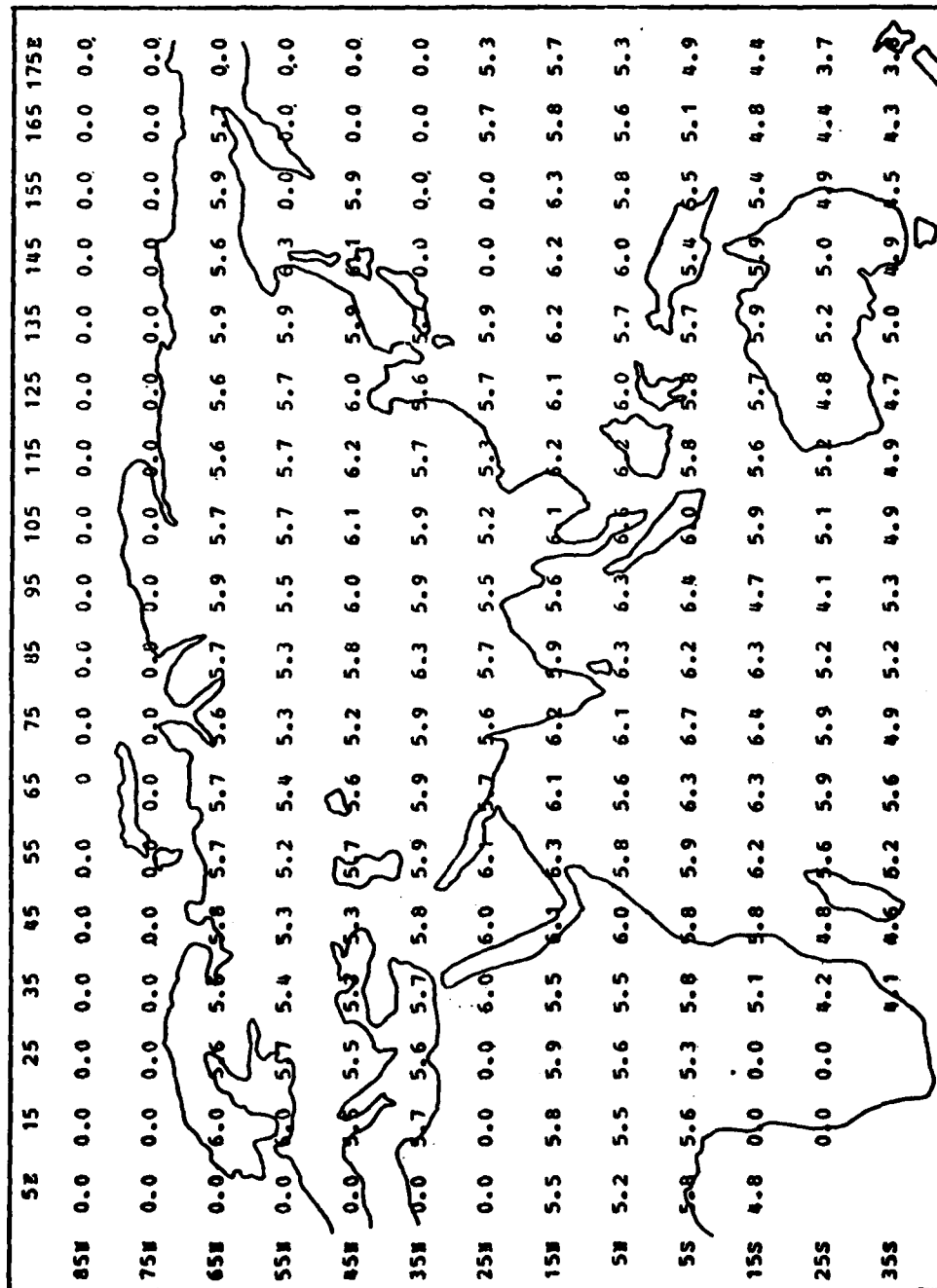


Fig. 14. Distribution of the average incidence of lightning discharge ($\text{km}^{-2} \text{s}^{-1}$) for June. Values are negative ordinary logarithms for 10° data blocks centered at the grid points shown.

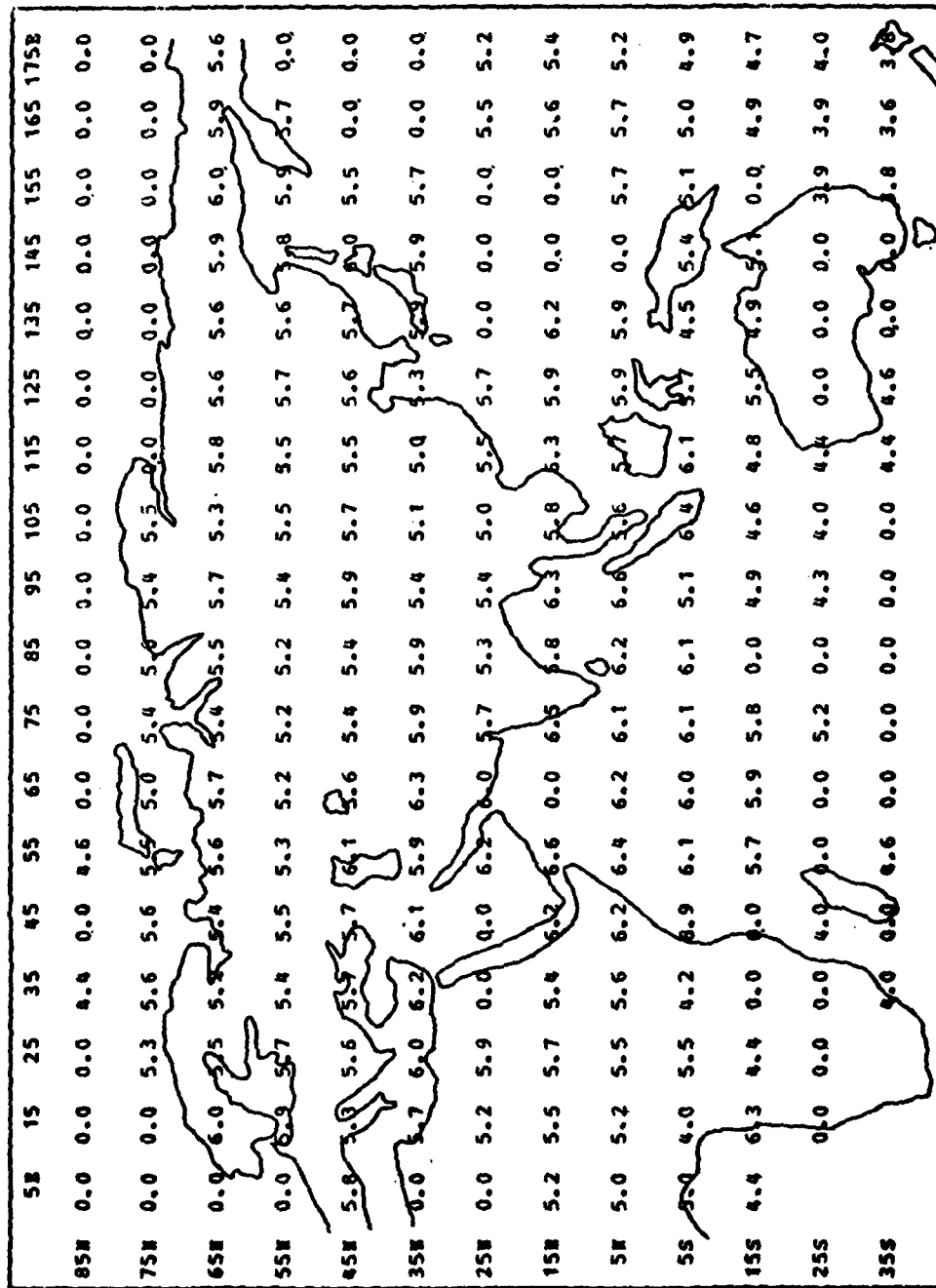


Fig. 15. Distribution of the average incidence of lightning discharge ($\text{km}^{-2} \text{s}^{-1}$) for July. Values are negative ordinary logarithms for 10° data blocks centered at the grid points shown.

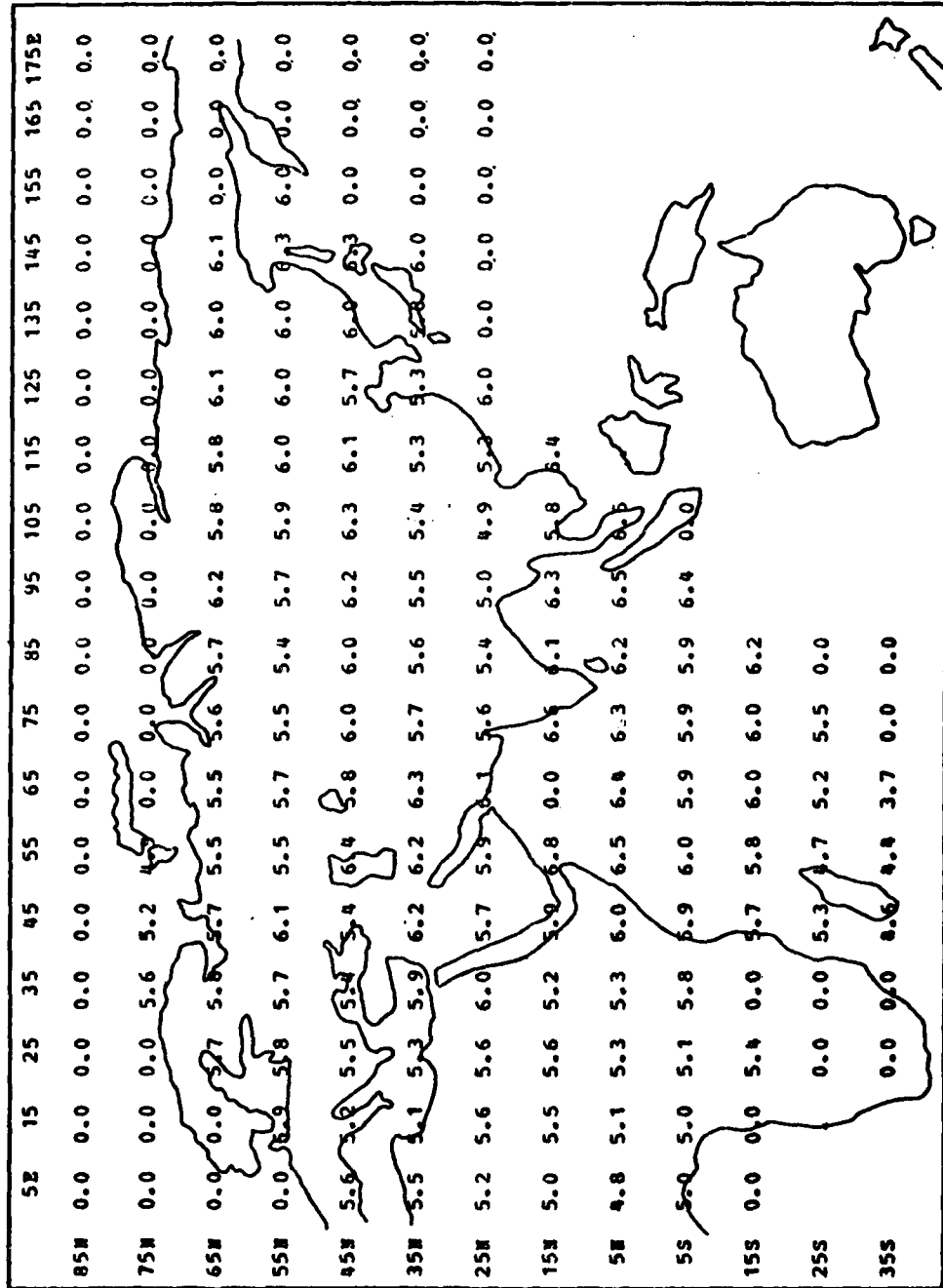


Fig. 16. Distribution of the average incidence of lightning discharge ($\text{km}^{-2} \text{s}^{-1}$) for August. Values are negative ordinary logarithms for 10° data blocks centered at the grid points shown.

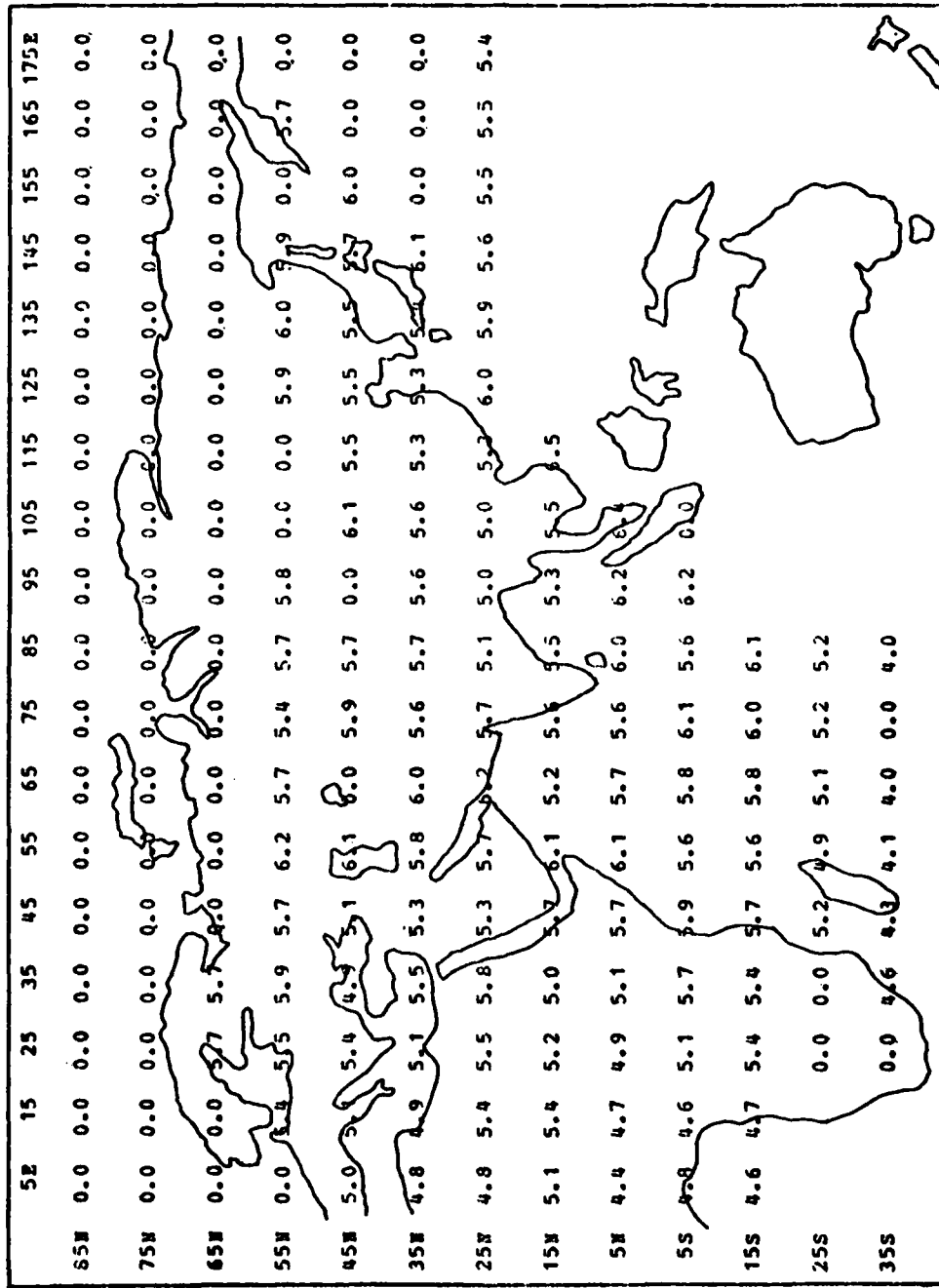


Fig. 17. Distribution of the average incidence of lightning discharge ($\text{km}^{-2} \text{s}^{-1}$) for September. Values are negative ordinary logarithms for 10° data blocks centered at the grid points shown.

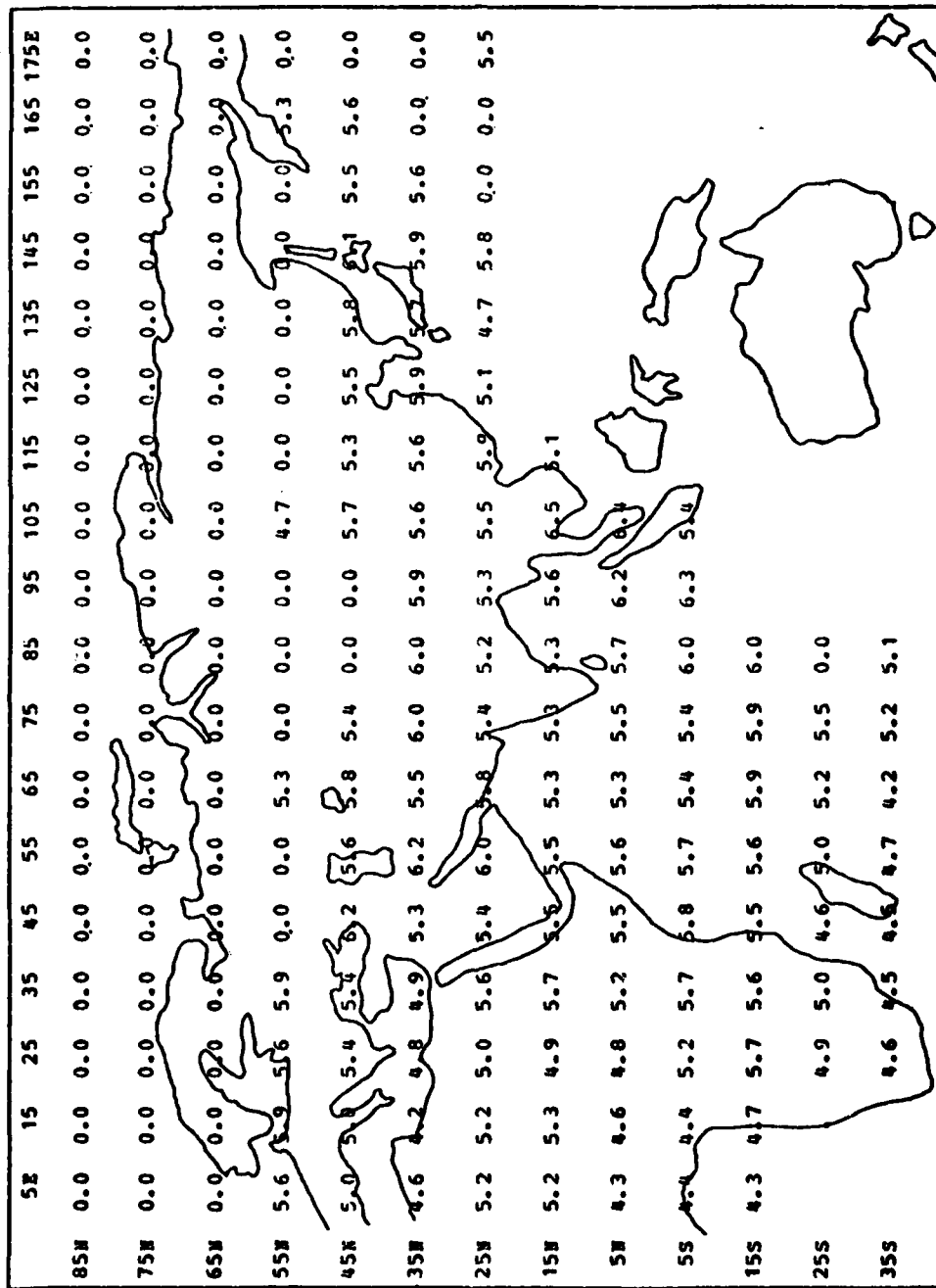


FIG. 18. Distribution of the average incidence of lightning discharge ($\text{km}^{-2} \text{s}^{-1}$) for October. Values are negative ordinary logarithms for 10° data blocks centered at the grid points shown.

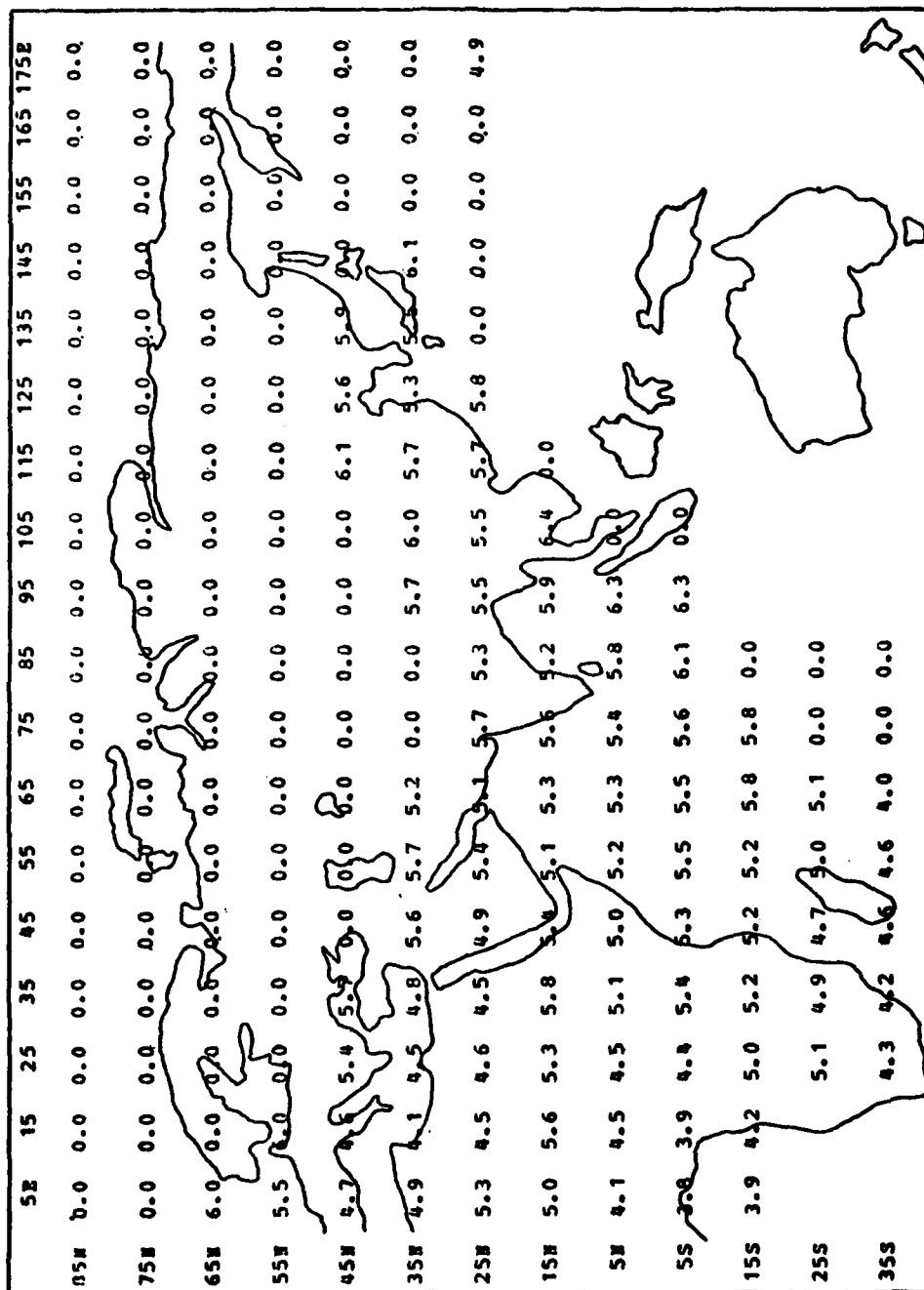


Fig. 19. Distribution of the average incidence of lightning discharge ($\text{km}^{-2} \text{s}^{-1}$) for November. Values are negative ordinary logarithms for 10° data blocks centered at the grid points shown.

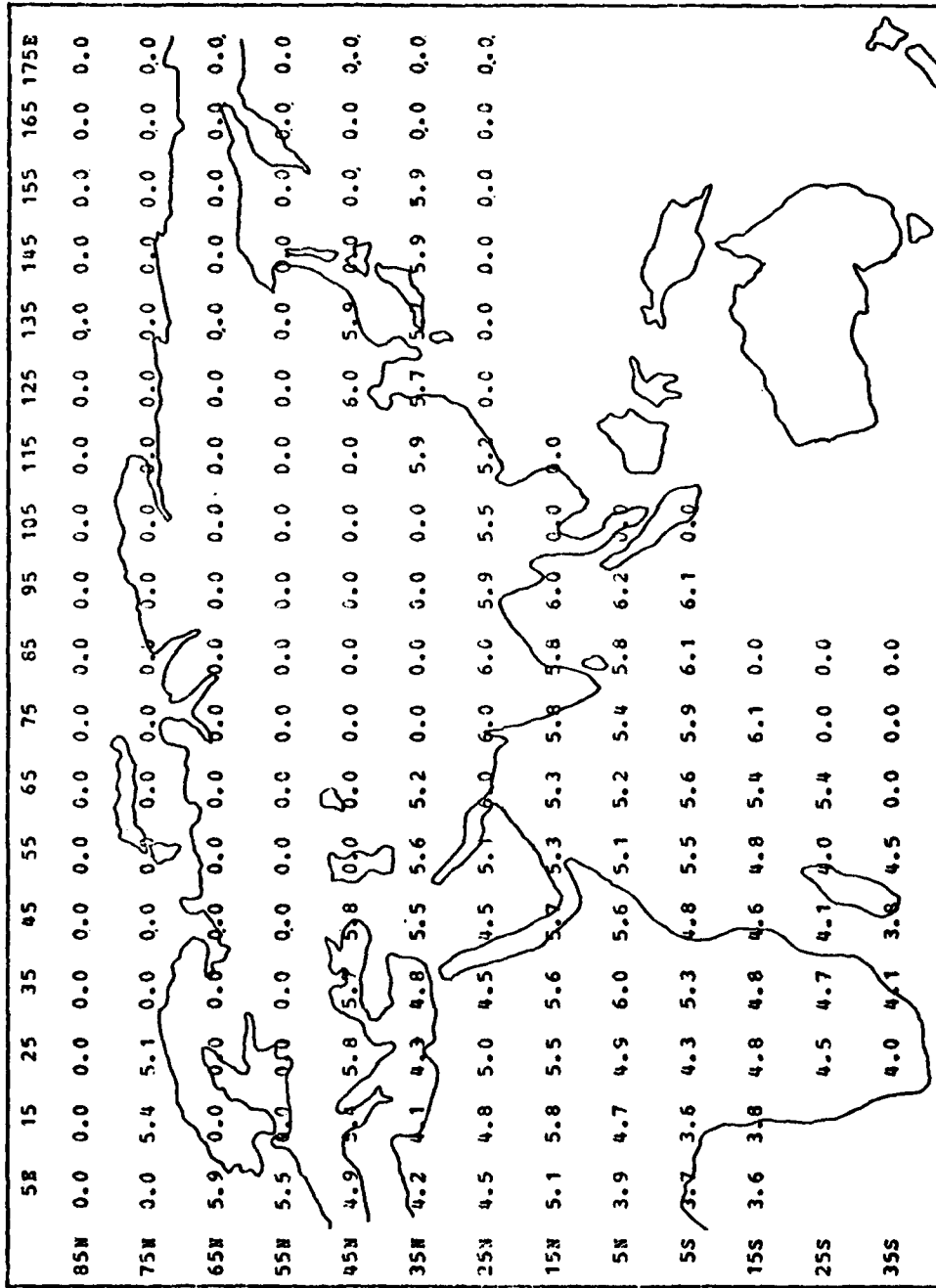


Fig. 20. Distribution of the average incidence of lightning discharge ($\text{km}^{-2} \text{s}^{-1}$) for December. Values are negative ordinary logarithms for 10° data blocks centered at the grid points shown.

TABLE 6. Estimate of the Average Incidence of Lightning Discharge by Latitude Zone for January. Units of $\text{km}^{-2} \text{s}^{-1}$.

Latitude Zone [No. of Values]	Minimum Value ($10^{-7} \text{ km}^{-2} \text{ s}^{-1}$)	Maximum Value ($10^{-5} \text{ km}^{-2} \text{ s}^{-1}$)	Average Value ($10^{-6} \text{ km}^{-2} \text{ s}^{-1}$)
High north latitudes (60°N-90°N) [3]	3.0	2.2	10.4
Middle latitudes (21°N-59°N) [48]	5.7	4.0	7.4
N. H. tropics* (0°-20°N) [34]	2.7	6.8	3.4
S. H. tropics* (0°-20°S) [34]	7.5	10.7	12.5
S. H. extratropical (21°S-35°S) [30]	13.1	31.0	69.5
N. Hemisphere portion of E. Hemisphere [85]	2.7	6.8	5.9
Eastern Hemisphere* tropics (20°N-20°S) [68]	2.7	6.8	7.9
All grid point estimates [149]	2.7	31.0	20.2

*The tropics were defined as 20°N-20°S due to the aggregation of the counts of sferics by 10° latitude-longitude blocks.

TABLE 7. Estimate of the Average Incidence of Lightning Discharge by Latitude Zone for February. Units of $\text{km}^{-2} \text{s}^{-1}$.

Latitude Zone [No. of Values]	Minimum Value ($10^{-7} \text{ km}^{-2} \text{ s}^{-1}$)	Maximum Value ($10^{-5} \text{ km}^{-2} \text{ s}^{-1}$)	Average Value ($10^{-6} \text{ km}^{-2} \text{ s}^{-1}$)
High north latitudes (60°N-90°N) [0]	0	0	0
Middle latitudes (21°N-59°N) [43]	5.7	3.2	6.0
N. H. tropics* (0°-20°N) [35]	1.2	4.1	3.9
S. H. tropics* (0°-20°S) [36]	5.6	6.7	16.8
S. H. extratropical (21°S-35°S) [32]	1.2	36.9	49.9
N. Hemisphere portion of E. Hemisphere [78]	1.2	4.1	5.1
Eastern Hemisphere* tropics (20°N-20°S) [71]	1.2	6.7	10.4
All grid point estimates [146]	1.2	36.9	17.8

*The tropics were defined as 20°N-20°S due to the aggregation of the counts of sferics by 10° latitude-longitude blocks.

TABLE 8. Estimate of the Average Incidence of Lightning Discharge by Latitude Zone for March. Units of $\text{km}^{-2} \text{s}^{-1}$.

Latitude Zone [No. of Values]	Minimum Value ($10^{-7} \text{ km}^{-2} \text{ s}^{-1}$)	Maximum Value ($10^{-5} \text{ km}^{-2} \text{ s}^{-1}$)	Average Value ($10^{-6} \text{ km}^{-2} \text{ s}^{-1}$)
High north latitudes (60°N-90°N) [0]	0	0	0
Middle latitudes (21°N-59°N) [48]	3.0	2.2	5.0
N. H. tropics* (0°-20°N) [35]	1.6	1.9	2.6
S. H. tropics* (0°-20°S) [36]	5.3	7.7	11.3
S. H. extratropical (21°S-35°S) [32]	16.9	19.2	46.2
N. Hemisphere portion of E. Hemisphere [83]	1.6	2.2	4.0
Eastern Hemisphere* tropics (20°N-20°S) [71]	1.6	7.7	7.0
All grid point estimates [151]	1.6	19.2	14.7

*The tropics were defined as 20°N-20°S due to the aggregation of the counts of sferics by 10° latitude-longitude blocks.

TABLE 9. Estimate of the Average Incidence of Lightning Discharge by Latitude Zone for April. Units of $\text{km}^{-2} \text{s}^{-1}$.

Latitude Zone [No. of Values]	Minimum Value ($10^{-7} \text{ km}^{-2} \text{ s}^{-1}$)	Maximum Value ($10^{-5} \text{ km}^{-2} \text{ s}^{-1}$)	Average Value ($10^{-6} \text{ km}^{-2} \text{ s}^{-1}$)
High north latitudes (60°N-90°N) [3]	29.6	1.3	8.2
Middle latitudes (21°N-59°N) [59]	3.6	1.4	3.0
N. H. tropics* (0°-20°N) [35]	2.8	0.9	2.2
S. H. tropics* (0°-20°S) [36]	4.1	4.1	6.4
S. H. extratropical (21°S-35°S) [30]	13.4	24.4	43.1
N. Hemisphere portion of E. Hemisphere [97]	2.8	1.4	3.0
Eastern Hemisphere tropics (20°N-20°S) [71]	2.8	4.1	4.3
All grid point estimates [163]	2.8	24.4	11.1

* The tropics were defined as 20°N-20°S due to the aggregation of the counts of sferics by 10° latitude-longitude blocks.

TABLE 10. Estimate of the Average Incidence of Lightning Discharge by

Latitude Zone for May. Units of $\text{km}^{-2} \text{s}^{-1}$.

Latitude Zone [No. of Values]	Minimum Value ($10^{-7} \text{ km}^{-2} \text{ s}^{-1}$)	Maximum Value ($10^{-5} \text{ km}^{-2} \text{ s}^{-1}$)	Average Value ($10^{-6} \text{ km}^{-2} \text{ s}^{-1}$)
High north latitudes (60°N-90°N) [8]	7.8	9.8	14.1
Middle latitudes (21°N-59°N) [47]	5.2	1.0	2.5
N. H. tropics* (0°-20°N) [34]	2.7	0.6	1.7
S. H. tropics* (0°-20°S) [36]	2.4	2.7	4.1
S. H. extratropical (21°S-35°S) [29]	6.9	14.1	28.4
N. Hemisphere portion of E. Hemisphere [89]	2.7	9.8	3.2
Eastern Hemisphere* tropics (20°N-20°S) [70]	2.4	2.7	2.9
All grid point estimates [154]	2.4	9.8	8.2

*The tropics were defined as 20°N-20°S due to the aggregation of the counts of sferics by 10° latitude-longitude blocks.

TABLE 11. Estimate of the Average Incidence of Lightning Discharge by Latitude Zone for June. Units of $\text{km}^{-2} \text{s}^{-1}$.

Latitude Zone [No. of Values]	Minimum Value ($10^{-7} \text{ km}^{-2} \text{ s}^{-1}$)	Maximum Value ($10^{-5} \text{ km}^{-2} \text{ s}^{-1}$)	Average Value ($10^{-6} \text{ km}^{-2} \text{ s}^{-1}$)
High north latitudes (60°N-90°N) [16]	11.1	0.3	2.0
Middle latitudes (21°N-59°N) [55]	4.6	0.6	2.4
N. H. tropics* (0°-20°N) [36]	2.6	0.6	1.6
S. H. tropics* (0°-20°S) [34]	2.1	3.6	4.7
S. H. extratropical (21°S-35°S) [30]	93.1	21.1	31.3
N. Hemisphere portion of E. Hemisphere [107]	2.6	0.6	2.1
Eastern Hemisphere* tropics (20°N-20°S) [70]	2.1	3.6	3.1
All grid point estimates [171]	2.1	21.1	7.7

*The tropics were defined as 20°N-20°S due to the aggregation of the counts of sferics by 10° latitude-longitude blocks.

TABLE 12. Estimate of the Average Incidence of Lightning Discharge by Latitude Zone for July. Units of $\text{km}^{-2} \text{s}^{-1}$.

Latitude Zone [No. of Values]	Minimum Value ($10^{-7} \text{ km}^{-2} \text{ s}^{-1}$)	Maximum Value ($10^{-5} \text{ km}^{-2} \text{ s}^{-1}$)	Average Value ($10^{-6} \text{ km}^{-2} \text{ s}^{-1}$)
High north latitudes (60°N-90°N) [28]	9.5	4.3	5.7
Middle latitudes (21°N-59°N) [59]	9.6	9.9	3.0
N. H. tropics* (0°-20°N) [32]	2.7	1.0	2.3
S. H. tropics* (0°-20°S) [32]	1.3	9.2	14.1
S. H. extratropical (21°S-35°S) [15]	62.1	25.4	98.3
N. Hemisphere portion of E. Hemisphere [119]	2.7	9.9	3.5
Eastern Hemisphere* tropics (20°N-20°S) [64]	1.3	9.2	8.2
All grid point estimates [166]	1.3	25.4	14.1

*The tropics were defined as 20°N-20°S due to the aggregation of the counts of sferics by 10° latitude-longitude blocks.

TABLE 13. Estimate of the Average Incidence of Lightning Discharge by Latitude Zone for August. Units of $\text{km}^{-2} \text{s}^{-1}$.

Latitude Zone [No. of Values]	Minimum Value ($10^{-7} \text{ km}^{-2} \text{ s}^{-1}$)	Maximum Value ($10^{-5} \text{ km}^{-2} \text{ s}^{-1}$)	Average Value ($10^{-6} \text{ km}^{-2} \text{ s}^{-1}$)
High north latitudes (60°N-90°N) [16]	9.5	1.2	2.8
Middle latitudes (21°N-59°N) [58]	4.5	1.0	2.6
N. H. tropics* (0°-20°N) [22]	1.5	1.5	2.9
S. H. tropics* (0°-20°S) [16]	4.2	1.0	2.8
S. H. extratropical (21°S-35°S) [37]	31.0	19.2	41.4
N. Hemisphere portion of E. Hemisphere [96]	1.5	1.5	2.7
Eastern Hemisphere* tropics (20°N-20°S) [38]	1.5	1.5	2.8
All grid point estimates [119]	1.5	19.2	5.0

*The tropics were defined as 20°N-20°S due to the aggregation of the counts of sferics by 10° latitude-longitude blocks.

TABLE 14. Estimate of the Average Incidence of Lightning Discharge by

Latitude Zone for September. Units of $\text{km}^{-2} \text{s}^{-1}$.

Latitude Zone [No. of Values]	Minimum Value ($10^{-7} \text{ km}^{-2} \text{ s}^{-1}$)	Maximum Value ($10^{-5} \text{ km}^{-2} \text{ s}^{-1}$)	Average Value ($10^{-6} \text{ km}^{-2} \text{ s}^{-1}$)
High north latitudes (60°N-90°N) [2]	19.0	0.2	2.1
Middle latitudes (21°N-59°N) [60]	6.5	1.7	4.0
N. H. tropics* (0°-20°N) [23]	3.4	4.1	6.3
S. H. tropics* (0°-20°S) [19]	4.2	2.7	6.4
S. H. extratropical (21°S-35°S) [10]	62.1	9.6	37.8
N. Hemisphere portion of E. Hemisphere [85]	3.4	4.1	4.6
Eastern Hemisphere* tropics (20°N-20°S) [42]	3.4	4.1	6.4
All grid point estimates [114]	3.4	9.6	7.8

*The tropics were defined as 20°N-20°S due to the aggregation of the counts of sferics by 10° latitude-longitude blocks.

TABLE 15. Estimate of the Average Incidence of Lightning Discharge by Latitude Zone for October. Units of $\text{km}^{-2} \text{s}^{-1}$.

Latitude Zone [No. of Values]	Minimum Value ($10^{-7} \text{ km}^{-2} \text{ s}^{-1}$)	Maximum Value ($10^{-5} \text{ km}^{-2} \text{ s}^{-1}$)	Average Value ($10^{-6} \text{ km}^{-2} \text{ s}^{-1}$)
High north latitudes (60°N-90°N) [0]	0	0	0
Middle latitudes (21°N-59°N) [54]	5.7	5.7	5.7
N. H. tropics* (0°-20°N) [23]	4.2	5.4	7.6
S. H. tropics* (0°-20°S) [20]	5.4	5.2	9.8
S. H. extratropical (21°S-35°S) [13]	31.0	6.9	20.5
N. Hemisphere portion of E. Hemisphere [77]	4.2	5.7	6.3
Eastern Hemisphere* tropics (20°N-20°S) [43]	4.2	5.4	8.6
All grid point estimates [110]	4.2	6.9	8.6

*The tropics were defined as 20°N-20°S due to the aggregation of the counts of sferics by 10° latitude-longitude blocks.

TABLE 16. Estimate of the Average Incidence of Lightning Discharge by Latitude Zone for November. Units of $\text{km}^{-2} \text{s}^{-1}$.

Latitude Zone [No. of Values]	Minimum Value ($10^{-7} \text{ km}^{-2} \text{ s}^{-1}$)	Maximum Value ($10^{-5} \text{ km}^{-2} \text{ s}^{-1}$)	Average Value ($10^{-6} \text{ km}^{-2} \text{ s}^{-1}$)
High north latitudes (60°N-90°N) [1]	10.2	0.1	1.0
Middle latitudes (21°N-59°N) [37]	7.2	8.3	10.1
N. H. tropics* (0°-20°N) [21]	4.2	8.1	10.7
S. H. tropics* (0°-20°S) [18]	5.4	14.4	30.8
S. H. extratropical (21°S-35°S) [10]	16.4	96.1	31.6
N. Hemisphere portion of E. Hemisphere [59]	4.2	8.3	10.2
Eastern Hemisphere* tropics (20°N-20°S) [39]	4.2	14.4	20.0
All grid point estimates [87]	4.2	14.4	16.9

*The tropics were defined as 20°N-20°S due to the aggregation of the counts of sferics by 10° latitude-longitude blocks.

TABLE 17. Estimate of the Average Incidence of Lightning Discharge by Latitude Zone for December. Units of $\text{km}^{-2} \text{s}^{-1}$.

Latitude Zone [No. of Values]	Minimum Value ($10^{-7} \text{ km}^{-2} \text{ s}^{-1}$)	Maximum Value ($10^{-5} \text{ km}^{-2} \text{ s}^{-1}$)	Average Value ($10^{-6} \text{ km}^{-2} \text{ s}^{-1}$)
High north latitudes (60°N-90°N) [3]	11.6	0.7	4.0
Middle latitudes (21°N-59°N) [32]	9.2	7.6	12.3
N. H. tropics* (0°-20°N) [20]	7.0	11.6	10.2
S. H. tropics* (0°-20°S) [18]	7.5	25.0	58.4
S. H. extratropical (21°S-35°S) [9]	41.4	16.0	66.9
N. Hemisphere portion of E. Hemisphere [55]	7.0	11.6	11.1
Eastern Hemisphere* tropics (20°N-20°S) [38]	7.0	25.0	33.1
All grid point estimates [82]	7.0	25.0	27.6

*The tropics were defined as 20°N-20°S due to the aggregation of the counts of aeric by 10° latitude-longitude blocks.

the order of magnitude of the incidence of discharge for the main thunderstorm areas of the world is $10^{-5} \text{ km}^{-2} \text{ s}^{-1}$. The main thunderstorm areas include the Americas, Africa, and Southeast Asia. The African focus of thunderstorm activity is the greatest. A focus corresponds to a geographic area with 100 or more thunderstorm days per year. A roughly comparable estimate is that of this study for the tropics of the Eastern Hemisphere (20°N - 20°S) shown in Tables 6-17. The average of all months is $1 \times 10^{-5} \text{ km}^{-2} \text{ s}^{-1}$.

Horner [1965] also gave a range of estimates for the global incidence of discharge. The range is from $6 \times 10^{-6} \text{ km}^{-2} \text{ s}^{-1}$ to $1.6 \times 10^{-5} \text{ km}^{-2} \text{ s}^{-1}$. One may infer from Brooks' work [1925], as mentioned in Chapter I, that the incidence of discharge for the world is of the order of $10^{-4} \text{ km}^{-2} \text{ s}^{-1}$. Turman and Edgar [1978] have estimated, from a short record of satellite data with measurements at dawn and dusk, that the global incidence of discharge is $2 \times 10^{-8} \text{ km}^{-2} \text{ s}^{-1}$. The photometer of the satellite collected approximately 8% of the flashes and estimates were made based on this sample. The mean estimate for all grid points and months of this study is $1.3 \times 10^{-5} \text{ km}^{-2} \text{ s}^{-1}$ in close agreement with Horner's maximum estimate. The minimum monthly average value is $5.0 \times 10^{-6} \text{ km}^{-2} \text{ s}^{-1}$ for August and the maximum is $2.8 \times 10^{-5} \text{ km}^{-2} \text{ s}^{-1}$ for December.

It should be pointed out that the estimates of this study include not only the important areal and global estimates of the incidence of discharge but also monthly values over a regularly-

spaced grid that covers a large portion of the earth. Further, the estimates are based on a single set of data that is internally consistent.

A study of Figures 9-20 and Tables 6-17 reveals the following observations:

1) The Southern Hemisphere tropics (0° - 20° S) are higher in average incidence of discharge than the Northern Hemisphere tropics (0° - 20° N) except for the months of August and September which show similar values. The contribution of the northern part of the South African focus and that of the tropical Pacific islands is evident.

2) The extratropical zone of the Southern Hemisphere (21° S- 35° S) is clearly dominant in average incidence of discharge relative to other zones. One could argue that this region is largely "tropical," and it is admitted that the selection of the tropics as 20° N- 20° S is arbitrary and based on convenience due to the fact that the sferics data were collected in 10° blocks. The high values in this zone reflect the force of the southern part of the South African focus and the lesser contribution of thunderstorms in Australia. Turman and Edgar [1978] showed the dominance of the South African focus, especially in the southern part, and also the center of activity in Australia. Their analysis represents a global "snapshot" of intense lightning activity.

3) The average incidence of discharge in high northern latitudes

(60°N-90°N) is based, for most months, on a few values that vary from zero in February to 28 in July. However, it is of interest that the average incidence of discharge in high latitudes is generally of the same magnitude as that of middle latitudes (21°N-59°N). That is, lightning occurred much less frequently in high than in middle latitudes but the number of discharges per square kilometer per second during stormy periods was of similar magnitude.

CHAPTER IV
RELATIONSHIP BETWEEN LIGHTNING-FLASH DENSITY
AND THUNDERSTORM DAYS

Introduction

The relationship between monthly lightning-flash density and monthly mean thunderstorm days was studied due to the recommendation of Pierce [1973]. Monthly lightning-flash density, as defined in Chapter I, is the number of lightning flashes that occur during stormy periods per square kilometer per month.

The effective area was that within range of a lightning-flash counter, assumed to be 500 km^2 in this study (see Chapter III). The total effective area under the influence of a thunderstorm in a given 10° latitude-longitude block was determined by dividing the area of the block (see Table 5) by 500 km^2 . An immediate, practical application of this work is in the estimation of radio noise interference due to lightning and in the design of power lines [Pierce, 1968].

Meteorologists do not expect an isomorphic relationship between these variables. The occurrence of thunderstorms is highly variable and there is variability in the occurrence of lightning within and among thunderstorms. Livingston and Krider [1978] showed that the number of discharges due to individual storms in Florida ranged from 8 to 1987. The thunderstorm-day statistics, as pointed out in Chapter I, have serious shortfalls

as indicators of the occurrence of thunderstorms. Therefore, a rough relationship was expected between these variables.

Only two thorough studies of this relationship have been completed [Cianos and Pierce, 1972]. Pierce [1968] based his study on lightning-flash counter data obtained in England, Thailand, and Singapore, and estimated that the data fit the equation

$$\sigma^2 = a T + a^2 T^4 \quad (13)$$

where σ is the monthly lightning-flash density ($\text{km}^{-2} \text{ month}^{-1}$) and T is the mean number of thunderstorm days per month (W.M.O.). The value of the constant, a , is 0.03.

Maxwell et al. [1970] based their work on lightning-flash counter data from 12 locations on earth and obtained the equation

$$\sigma = 0.06 T^{1.5} \quad (14)$$

The variables are the same as in (13).

An estimate of the goodness-of-fit was not provided for either (13) or (14). However, a scatter diagram was provided for (14) and the fit appeared to be useful although certainly very rough.

A month in each season was chosen for study. The months selected were January, April, August, and November due to the fact that no data were missing in these months except for January (10% missing data).

Lightning-Flash Density

The dependent variable was lightning-flash density, σ , in

flashes per square kilometer per month. This was estimated for each chosen month over the regularly-spaced grid of Figure 2. First, the total number of discharges per month at grid points was estimated by the use of (11). The result was divided by the total effective area in each block as defined in the previous section.

Thunderstorm Days

Two estimates of monthly thunderstorm days were used. The first was based on W.M.O. thunderstorm day data (Figure 3). It was necessary to develop smoothed monthly estimates of thunderstorm days valid for the areal resolution of the lightning-flash density estimates (i.e., 10° latitude-longitude blocks). This was accomplished by the use of both analyzed W.M.O. charts (e.g., Figure 3) and the basic W.M.O. data [W.M.O., 1953; 1956]. The formula used to estimate the thunderstorm days for a 10° block was

$$T = 0.5a_0 + 3a_1 + 7.5a_2 + 12.5a_3 + 17.5a_4 + 22.5a_5 + 27.5a_6 \quad (15)$$

where T is the smoothed mean value of thunderstorm days for a 10° block. Each a_i (i.e., a_0 to a_6) is the proportion of area in a 10° data block represented by the respective group of mean thunderstorm days. The a_i 's sum to unity. The respective groups are: 0 = 0-1, 1 = 1-5, 2 = 5-10, 3 = 10-15, 4 = 15-20, 5 = 20-25, 6 = 25-30. The constant coefficients are center values in the respective groups of mean thunderstorm days.

The second estimate of thunderstorm days was simply a count by month of days in each 10° data block on which counts of sferics other than zero occurred (Figure 4). A detailed analysis of the difference in the W.M.O. estimate of thunderstorm days and that derived from sferics data was presented in the M.S. thesis [Freeman, 1974]. The respective monthly charts differed significantly over the oceans, North Africa, Arabia, the Mediterranean Sea, and Southeast China.

The sferics data were relatively unbiased whereas the thunderstorm-day data were very biased. However, the thunderstorm-day data included varying periods of record (1-81 years) and the sferics data covered only 1972. The spatial distribution was represented better by the use of the sferics data, at least for 1972, whereas the W.M.O. data represented on average a much longer period of record, typically 10 years or more.

The Regression of Lightning-Flash Density onto Thunderstorm Days

Log transformation sensitivity analysis. The work by Pierce [1968] and Maxwell et al. [1970] showed a power-law relationship between monthly lightning-flash density, σ , and thunderstorm days, T , as given in (13) and (14), respectively. Maxwell et al. used the most extensive set of data (σ from 12 locations). Initially, a logarithmic model was assumed in this analysis in order to estimate the coefficients and power of (14) when fitted to the sferics data

for January; that is,

$$\sigma = a T^b + \epsilon \quad (16)$$

or equivalently,

$$\ln \sigma = \ln a + b \ln T + \epsilon' \quad (17)$$

where a and b are the coefficient and power, respectively, of the power law; σ and T refer to values at the grid points of Figure 2, ϵ and ϵ' are the error in the respective equations.

An arbitrary constant, α , was added to all values of lightning flash density (flashes $\text{km}^{-2} \text{month}^{-1}$) due to the presence of zeroes in the data. This was necessary since the logarithm of zero is undefined. That is

$$\ln (\sigma + \alpha) = \ln a + b \ln T + \epsilon' \quad (18)$$

The January estimates of σ were transformed with an α of 1.0. The sferics data were used to estimate T for January (Figure 4). Then, linear least squares estimation was used to obtain the coefficient, a , and the power, b , in (18) with the result

$$\sigma = 0.90 T^{0.64} \quad (19)$$

It was considered prudent to determine the effect of the arbitrary choice of α . Additional regressions were accomplished with values of α of 0.01, 0.50, and 2.00. The results obtained with the various arbitrary choices of α are given in Table 18 and Figure 21.

TABLE 18. Sensitivity of Regression to Addition of Arbitrary Constant to Values of Dependent Variable, σ , in a Logarithmic Transformation of Data. Model is (16). Logarithmic transformation is (18). Lightning-flash density is σ . Thunderstorm days (AF data) is T.

Constant Added to Values of σ	Regression Equation	Coefficient of Determination (R^2)
0.01	$\sigma = 0.31 T^{0.78}$	0.80
0.50	$\sigma = 0.69 T^{0.66}$	0.56
1.00	$\sigma = 0.90 T^{0.64}$	0.50
2.00	$\sigma = 1.19 T^{0.63}$	0.47

The fit to the data (R^2 in Table 18) and the respective estimates of σ for a given T (Figure 21) vary considerably with choice of α . This analysis pointed out that one must be aware of the possible sensitivity of logarithmic models to the arbitrary choice of the constant that is added to values of a variable due to the presence of zeroes in the data. It was decided to use a curvilinear regression approach to avoid an arbitrary choice of α .

Curvilinear Regression. A least-squares approach with an assumed model of the form, (16), was used. The quantity to be minimized was

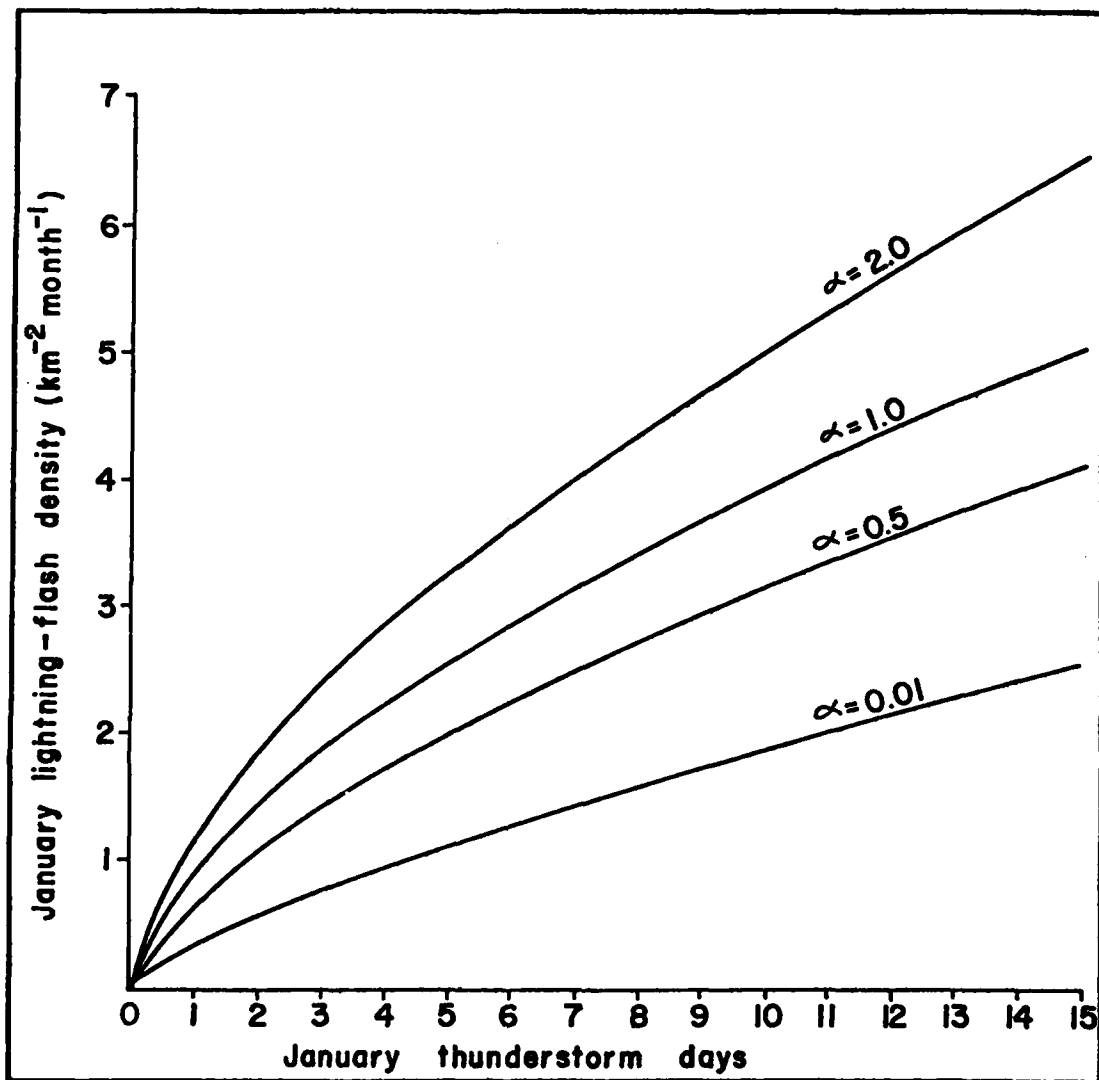


Fig. 21. Illustration of the sensitivity of logarithmic models to the addition of an arbitrary constant (α) to values of the dependent variable (lightning-flash density). Curves are regression equations that correspond to values of α .

$$SSE = \sum_{ij} (\sigma_{ij} - a T_{ij}^b)^2 \quad (20)$$

where SSE is the error "sum of squares"; σ_{ij} and T_{ij} are values at grid points (ij) (Figure 2) of monthly, lightning-flash density ($\text{km}^{-2} \text{ month}^{-1}$) and monthly thunderstorm days respectively. The minimum of SSE occurs when both $\frac{\partial(SSE)}{\partial a} = 0$ and $\frac{\partial(SSE)}{\partial b} = 0$. The condition $\frac{\partial(SSE)}{\partial a} = 0$ is equivalent to

$$\sum 2 (\sigma_{ij} - a T_{ij}^b) (-T_{ij}^b) = 0 \quad (21)$$

or

$$-\sum \sigma_{ij} T_{ij}^b + a \sum T_{ij}^{2b} = 0 \quad (22)$$

The condition $\frac{\partial(SSE)}{\partial b} = 0$ is equivalent to

$$\sum 2 (\sigma_{ij} - a T_{ij}^b) (-a T_{ij}^b \ln T_{ij}) = 0 \quad (23)$$

From (22) we obtain

$$a = \frac{\sum \sigma_{ij} T_{ij}^b}{\sum T_{ij}^{2b}} \quad (24)$$

Therefore, for each b, the value of the coefficient, a, which minimizes SSE is given by (24). The estimate of (a, b) was consequently found by enumerating SSE for b = 0.01, 0.02, ..., 4.0 and choosing that pair (a, b) which minimized SSE.

A measure of goodness-of-fit was defined as

$$\text{Fit} \equiv \frac{SST - SSE}{SST} \quad (25)$$

where SST is the "total sums of squares" (i.e., $\sum(\sigma_{ij} - \bar{\sigma})^2$ where $\bar{\sigma}$ is the average of the σ_{ij}).

Regressions corresponding to various stratifications of the data (e.g., land, sea, etc.) for each of the four months were analyzed. Both W.M.O. and sferics data were used to estimate the thunderstorm-day variable.

A summary of regressions is given in Table 19 for January, April, August, and November in terms of data set, sample size, and goodness-of-fit. The respective sample sizes are different for January and April than for August and November (see Figure 2). Only regressions with associated fits to the data greater than or equal to 0.25 were considered useable. All of the fits of this study less than 0.25 were very much less, typically 0.01 or less. Linear regressions of the form $\sigma = \theta_0 + \theta_1 T + \epsilon$ also were attempted by the stratifications of data listed in Table 19. The power-law model (16) always was fit considerably better than the linear model.

A non-trivial effort was expended to improve the regressions reported in Table 19 without success. Regressions which involved the number of W.M.O. stations in a data block (Figure 5) were attempted. Six classes of number of stations were used. Regressions involving the number of thunderstorm days (W.M.O. and AF data) were also attempted. Six classes were used. Various areal stratifications of the data were attempted in combination with the above schemes. The W.M.O. thunderstorm-day data were weighted by a scheme designed to improve the observational bias. The

TABLE 19. Summary of the Regression of Lightning-Flash Density (Units of $\text{km}^{-2} \text{ month}^{-1}$) and Monthly Thunderstorm Days (W.M.O. and Sferics (AF) Data). The goodness-of-fit for useable

regressions ($\text{Fit} \geq 0.25$) is given. A dash means a poor fit.

Data	Sample Size Jan and Apr	Sample Size Aug and Nov	JAN		APR		AUG		NOV	
			WMO	AF	WMO	AF	WMO	AF	WMO	AF
All	234	183	0.30	0.29	--	--	0.32	0.34	--	0.28
Land	145	122	0.32	0.53	--	0.26	0.30	0.36	0.29	--
Sea	89	61	--	--	--	--	--	--	--	0.43
N. Hemisphere	162	149	--	0.77	0.29	0.73	--	0.36	0.67	--
N.H. Land	114	111	--	0.76	0.30	0.67	--	--	0.62	--
N.H. Sea	48	38	--	--	0.73	0.81	--	--	--	0.97
N.H., 0°-90°E	81	81	--	0.45	--	0.51	--	--	0.76	--
N.H., 90°-180°E	81	68	--	0.78	--	0.73	--	0.45	--	0.43
S. Hemisphere	72	34	--	--	--	--	--	0.25	--	0.56
S.H. Land	31	*	0.25	0.62	--	--	*	--	--	*
S.H. Sea	41	*	--	--	--	--	*	--	--	*
S.H., 0°-90°E	36	*	--	--	--	--	*	--	--	*
S.H., 90°-180°E	36	*	0.32	--	--	--	*	--	--	*

*Regressions were not performed on stratifications of Southern Hemisphere data for August and November due to insufficient sample size.

modified thunderstorm days, T' , were given by

$$T' = \frac{T}{[(400 \text{ km}^2 \times N)/A]} \quad (26)$$

where T is the recorded W.M.O. thunderstorm days; the constant, 400 km^2 , is an assumed area of coverage per W.M.O. station (based on the ability of an observer to hear thunder); N is the number of W.M.O. stations per data block (Figure 5); and A is the area of a 10° -data block (Table 5).

The details of the regressions summarized in Table 19 are given by months in Tables 20-23 for the useable regressions ($\text{Fit} \geq 0.25$).

Discussion of Results

This analysis provided many useable regressions valid for the months of January, April, August, and November. A cursory examination of Tables 20-23 leads one to the conclusion that the relationship of lightning-flash density to thunderstorm days varies by month. Estimates of lightning-flash density for selected values of thunderstorm days are shown in Table 24 for the single empirical equations given by Pierce [1968] and Maxwell et al. [1970] and the equations of this study (the regression equations corresponding to all available data). The results of this study for August and the results of Maxwell et al. agree remarkably well. The estimated lightning-flash density of the previous studies and of this study

TABLE 20. Results for January of Regression of Lightning-Flash Density, σ , onto Thunderstorm Days, T, (W.M.O. and AF (Sferics) Data) with the Assumed Model, $\sigma = aT^b$. Fits ≥ 0.25 given. Dash means poor fit.

Data*	Sample Size	Thunderstorm Days (WMO)		Thunderstorm Days (AF)			
		a	b	Fit	Fit		
All	234	1.3×10^{-3}	3.6	0.30	1.6×10^{-3}	2.9	0.29
Land	145	4.9×10^{-3}	2.0	0.32	2.3×10^{-5}	3.4	0.53
N.H. All	162	--	--	--	3.1×10^{-7}	3.5	0.77
N.H. Land	114	--	--	--	9.9×10^{-9}	3.7	0.76
N.H., 0°-90°E	81	--	--	--	1.8×10^{-9}	3.3	0.45
N.H., 90°-180°E	81	--	--	--	2.1×10^{-7}	1.2	0.78
S.H. Land	31	1.2×10^{-5}	1.9	0.25	5.1×10^{-5}	1.3	0.62
S.H., 90°-180°E	36	6.8×10^{-6}	1.0	0.32	--	--	--

*Regressions for all stratifications of the data in Table 19 were attempted.

TABLE 21. Results for April of Regression of Lightning-Flash Density, σ , onto Thunderstorm Days, T, (W.M.O. and AF (Sferics) Data) with the Assumed Model, $\sigma = aT^b$. Fits ≥ 0.25 given. Dash means poor fit.

Data*	Sample Size	Thunderstorm Days (WMO)			Thunderstorm Days (AF)		
		a	b	Fit	a	b	Fit
Land	145	--	--	--	1.4×10^{-2}	0.6	0.26
N.H. All	162	6.3×10^{-4}	1.0	0.29	1.7×10^{-7}	3.1	0.73
N.H. Land	114	4.7×10^{-5}	0.7	0.30	1.0×10^{-6}	2.4	0.67
N.H. Sea	48	2.1×10^{-7}	3.8	0.73	3.2×10^{-7}	1.9	0.81
N.H., 0° - 90° E	81	--	--	--	4.0×10^{-7}	1.0	0.51
N.H., 90° - 180° E	81	--	--	--	4.2×10^{-9}	2.4	0.73

*Regressions for all stratifications of the data in Table 19 were attempted.

TABLE 22. Results for August of Regression of Lightning-Flash Density, σ , onto Thunderstorm Days, T, (W.M.O. and AF (Sferics) Data) with the Assumed Model, $\sigma = aT^b$. Fits > 0.25 given. Dash means poor fit.

Data*	Sample Size	Thunderstorm Days (WMO)			Thunderstorm Days (AF)		
		a	b	Fit	a	b	Fit
All	183	7.0×10^{-2}	1.5	0.32	1.2×10^{-2}	1.5	0.34
Land	122	7.4×10^{-2}	1.1	0.30	1.2×10^{-3}	1.3	0.36
N.H. All	149	--	--	--	3.6×10^{-4}	0.7	0.36
N.H., 90° - 180° E	68	--	--	--	1.2×10^{-6}	0.6	0.45
S.H. All	34	--	--	--	5.5×10^{-4}	0.6	0.25

*Regressions for all stratifications of the data in Table 19 were attempted except that the stratifications of Southern Hemisphere data for August and November were not attempted due to insufficient sample size.

TABLE 23. Results for November of Regression of Lightning-Flash Density, σ , onto Thunderstorm Days, T, (W.M.O. and AF (Sferics) Data) with the Assumed Model, $\sigma = aT^b$. Fits > 0.25 given. Dash means poor fit.

Data*	Sample Size	Thunderstorm Days (WMO)			Thunderstorm Days (AF)		
		a	b	Fit	a	b	Fit
All	183	--	--	--	4.7×10^{-5}	4.0	0.28
Land	122	3.6×10^{-2}	1.5	0.29	--	--	--
Sea	61	--	--	--	3.3×10^{-6}	4.0	0.43
N.H. All	149	2.2×10^{-4}	2.6	0.67	--	--	--
N.H. Land	111	1.6×10^{-5}	2.3	0.62	--	--	--
N.H. Sea	38	--	--	--	1.9×10^{-7}	2.3	0.97
N.H., 0° - 90° E	81	1.9×10^{-6}	1.9	0.76	--	--	--
N.H., 90° - 180° E	68	--	--	--	4.1×10^{-7}	0.5	0.43
S.H. All	34	2.0×10^{-6}	4.0	0.56	2.0×10^{-6}	4.0	0.56

*Regressions for all subdivisions of the data in Table 19 were attempted except that the stratifications of Southern Hemisphere data for August and November were not attempted due to insufficient sample size.

for January and August are close for the value of 5 thunderstorm days. However, there are notable differences among the three studies in all other cases.

TABLE 24. Lightning-Flash Density ($\text{km}^{-2} \text{ month}^{-1}$) for Selected Monthly Thunderstorm Days (W.M.O.). Parenthesis refer to sferics-derived thunderstorm days. Dash means poor fit.

Investigator(s)	Thunderstorm days		
	5	10	20
Pierce	0.6	3.0	12.0
Maxwell <u>et al.</u>	0.7	1.9	12.0
Freeman			
Jan	0.5 (0.2)	5.6 (1.2)	68.2 (8.3)
Apr	-- (--)	-- (--)	-- (--)
Aug	0.8 (0.1)	2.1 (0.4)	5.9 (1.1)
Nov	-- (0.03)	-- (0.5)	-- (7.6)

An interesting feature of the results of this study was that the useable regressions for "all available data" produced estimates of lightning flash density generally the same order of magnitude as that of the previous studies. However, it is worth noting that the regressions for all of the stratifications of the data (Tables

20-23) produced lower estimates of the lightning-flash density than the regressions based on all the data. This was true whether W.M.O. or AF (sferics) data were used to estimate thunderstorm days. It is not known whether the variability in the occurrence of lightning, which is great, necessitated a large sample size (i.e., all the data) for efficacy of these regressions or whether the low densities predicted by the regressions based on stratifications of the data are real.

It was interesting, and somewhat surprising, that the goodness-of-fit (all data) was very close (Table 19) whether the smoothed W.M.O. data (all periods of record) or the sferics data (1972) were used to estimate thunderstorm days. The sferics data provided a good estimate of the distribution of thunderstorm days for the months of 1972. This may mean that the rough fits (W.M.O. data) reported here, and undoubtedly achieved by the other investigators, represented the best relationships that were possible due to the inherent problems in relating these disparate variables.

It should be noted that the extremely good fit (0.97), shown in Table 23 for "Northern Hemisphere Sea" in November, was due to the fact that the lightning-flash density was zero over the sea in 34 of 38 available datum points. The commensurate values of thunderstorm days also were low, typically 0-1. This empirical equation, and that for all stratifications by "sea," therefore, were of interest only in that the data on which they were based showed that the occurrence of thunderstorms and lightning over water is low compared to that over land.

CHAPTER V
ANALYSIS OF THE LARGE-SCALE CAUSES OF THE VARIABILITY
OF ELECTRICAL ACTIVITY

Purpose and Approach

The purpose of this chapter is to study the possible causes of the variation in disturbed-weather electrical activity. The dependent variable was the estimated number of cloud-to-ground discharges, D_G , from (6). A regression approach was used. Regressors were chosen based on their potential as contributors to the reduction in variation of the dependent variable. The criteria for the selection of regressors were plausible physical importance and the availability of data.

The source of data and the data reduction were explained in chapter II. The specific treatment of each regressor is explained in this chapter. The months of February and August of 1972 were selected for study. The area of study is given in Figure 22. This area was chosen because no sferics data and a minimum of meteorological data were missing.

An important problem in the data phase of this study was to represent the values of the regressors, which were available on the NMC grid (Figure 22), on the coarser grid of the sferics data (Figure 2). A weighted average was attempted with weights that were the areas of 2° -latitude bands within a 10° -data block. Since

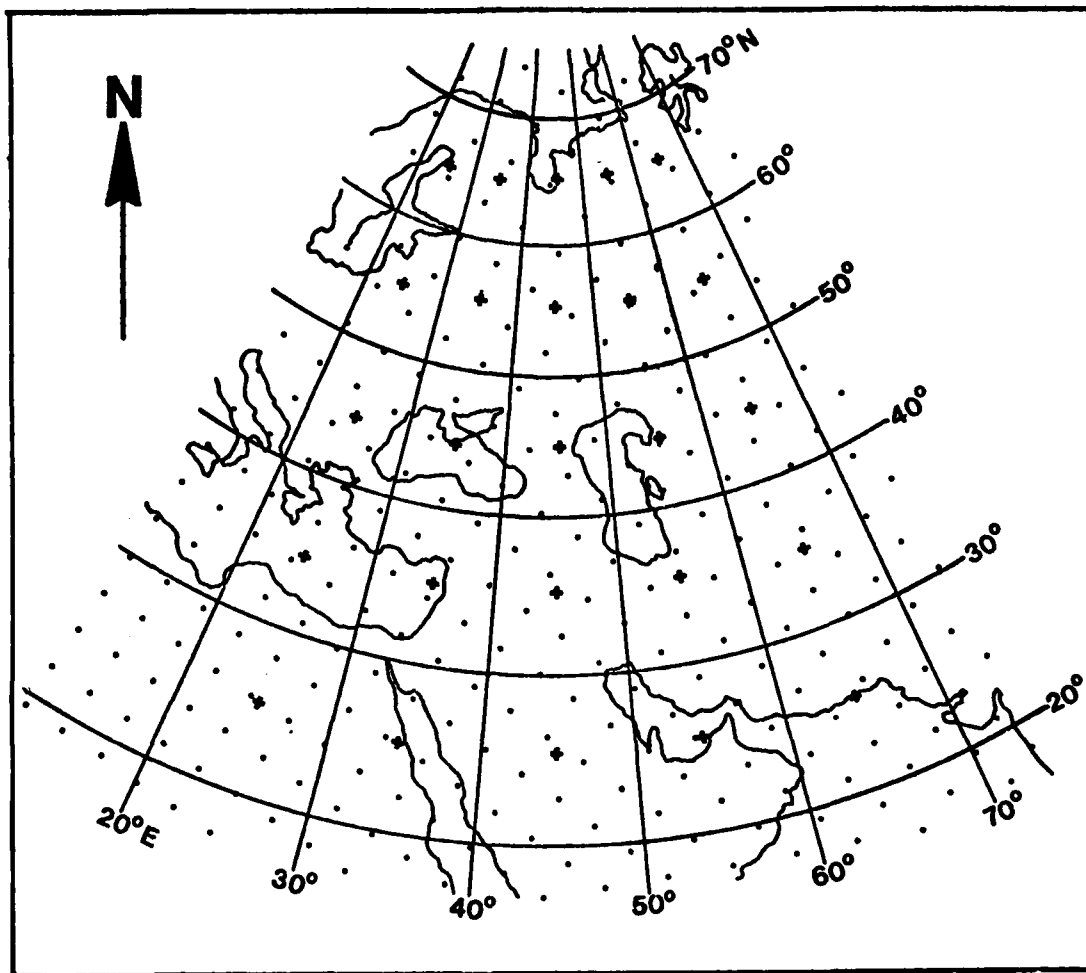


Fig. 22. The portion of the NMC grid used in this study. Grid points are dots. The center grid points (♣) in the 10° -data blocks (5×5 grid) correspond to the resolution of the spherical data in Figure 2.

this was about the same as a simple arithmetic average within 10°-data blocks, the latter was used. Regressors were thresholded (i.e., values set to zero under specified conditions) if information was available to allow a logical choice of threshold. This was considered a reasonable approach since lightning is an impulsive phenomenon and the regressors have associated smooth fields of data.

Several regressors (e.g., relative humidity and precipitable water) are sometimes used to represent the same physical effect (e.g., moisture). This is because the best method of representing the particular physical effect is not known.

The Regressors

Introduction. It is widely held that the important synoptic-scale conditions necessary for the occurrence of thunderstorms are low-level moisture, potential instability, and a trigger mechanism. In addition, Miller [1972] stated that bands of strong winds from, say, 850 to 500 mb are an indicator of thunderstorms, especially severe storms. These synoptic conditions should also be important for the occurrence of lightning.

The regressors of this study represent the synoptic-scale conditions, except for the trigger mechanism, that are important to the occurrence of thunderstorms and lightning. The trigger mechanism is usually vertical motion that causes the potential instability of the air to be released. Reliable vertical motion data were not available. Zak [1977] attempted to predict thunder-

storm occurrence with a regression approach. He represented vertical motion indirectly by estimating fields of divergence from the wind fields. This regressor explained only a very small part of the variability in the occurrence of thunderstorms.

The height of the "freezing level" is included as a regressor. This is the melting level in the strict sense, but we will use the common term. As explained by Pierce [1970], the basic physics of spark breakdown implies that the smaller the distance from ground to the negative center of charge near the freezing level, the greater the probability of a cloud-to-ground discharge. However, Bosart et al. [1974] conducted an experiment in Switzerland and found no significant correlation between the height of the freezing level above instrumented towers and the number of discharges to the towers.

It is common knowledge that lightning "prefers" tall objects in cloud-to-ground discharges. Again, the basic physics would lead us to expect more strikes on the average to high than to low terrain. For this reason, the mean terrain height at grid points was a regressor.

Geomagnetic (K_p and H-component) data and sunspot numbers were included as regressors to determine if these factors support the notion that there is a direct solar influence on the occurrence of lightning.

Moisture. Layer relative humidity (1000-500 mb), the dew-point depression (850 mb), and precipitable water (1000-850 mb)

were the measures of low-level moisture used in this study.

Layer relative humidity, RH (%), was available at the NMC grid points (Figure 22) for August only. The values of RH were averaged within 10°-data blocks to obtain the same resolution as the sferics data. Layer relative humidity has been shown to correlate well ($r = 0.78$) with a satellite classification of cloud cover [Thompson and West, 1967]. Clouds were classified on a scale from 1 to 8. The lowest classification referred to clear skies and the highest to clouds associated with a frontal zone and with thunderstorms.

The dew-point depression, DD (°C), at 850 mb is a useful operational tool to determine if sufficient low-level moisture is available for thunderstorms. A DD of 13°C or more means that thunderstorms are very unlikely. The DD at 850 mb was available on magnetic tape. It was averaged within 10°-data blocks to obtain the final grid values.

Precipitable water, PW (cm), was estimated at NMC grid points for the 1000-850 mb layer. Precipitable water is defined as: "The total atmospheric water vapor content in a vertical column of unit cross-sectional area extending between any two specified levels, commonly expressed in terms of the height to which that water substance would stand if completely condensed and collected in a vessel of the same unit cross-section." [Huschke, 1959]. Following Byers [1974], a useful equation for this quantity is

$$PW = \frac{0.622}{g} \int_{p}^{P_0} \frac{e}{p} d(\ln p) \quad (27)$$

where PW is precipitable water (cm), g is the acceleration due to gravity (cm s^{-2}), p is pressure (mb), P_0 is the pressure (mb) of the lowest level, and e is vapor pressure (mb).

The estimation of PW at each grid point was accomplished by vertical integration. Simpson's rule was used to evaluate the integrand of (27). The computer was programmed to use the following calculation formula for PW

$$PW = 0.052 (e_{1000} + e_{850}) \quad (28)$$

where the constant is the aggregate value of constants in (27) and includes those due to the conversion of units, and e_{1000} and e_{850} are vapor pressures at the respective levels.

The vapor pressure at 1000 mb was available on magnetic tape. The vapor pressure at 850 mb was calculated from

$$e_{850} = C_0 + C_1 T_d + C_2 T_d^2 + C_3 T_d^3 + C_4 T_d^4 + C_5 T_d^5 \quad (29)$$

where T_d is the dew-point temperature at 850 mb and the constants are: $C_0 = 6.0689226$, $C_1 = 4.4358312 \times 10^{-1}$, $C_2 = 1.4590816 \times 10^{-2}$, $C_3 = 2.7619554 \times 10^{-4}$, $C_4 = 2.9952590 \times 10^{-6}$, $C_5 = 1.4398885 \times 10^{-8}$. This formula was given by Rasmussen [1978] for saturation vapor pressure as a function of temperature. It may be used at a constant pressure level for the calculation of vapor pressure as a function of dew-point temperature. This formula is valid for the temperature

range -50°C to $+50^{\circ}\text{C}$.

The final values of precipitable water were the averages within 10° -data blocks of the vertically integrated values from the NMC grid.

Stability. The K index of stability was chosen for this study based on work by Scoggins and Wilson [1976]. They found that the K index correlated better with convective activity than the total totals or lifted indices. The K index was used in the following form [George, 1960]:

$$K = (T_{850} - T_{500}) + \frac{(T_{d,1000} + T_{d,850})}{2} - (T - T_d)_{700} \quad (30)$$

where T and T_d are the ambient and dew-point temperatures at the indicated pressure levels (subscripts).

The K index is a measure of thunderstorm potential based on the vertical temperature lapse rate, the moisture content of the lower atmosphere, and the vertical extent of the moist layer as represented by the three terms in (30).

Before the values of K were averaged within 10° -data blocks, all values less than 24 were set to zero (thresholded). An index value of 24 or greater indicates significant convection.

Wind speed. The wind speed, $W1$ (knots), was calculated from the 500 mb components (u , v) at NMC grid points and averaged within 10° -data blocks. The standard deviation of the wind speed, $W2$ (knots) was also determined. A property of the mean is that

it is affected by extreme values, such as wind speed in a jet. Also, a relatively homogeneous wind field with an embedded jet would have a higher standard deviation than if no jet were present.

Freezing level. Two methods were used to represent the effect of the freezing level. In both cases, the height (m) of the freezing level above mean sea level (msl) was estimated from the temperature-height data. The environmental lapse rate of 6.5°C per km was used. The height at which the temperature decreased to 0°C was selected as the freezing level.

In the first method, the height of the terrain at NMC grid points (actually, within 15 km of grid points) was subtracted from the height of the freezing level (msl) to obtain the height of the freezing level above ground level (agl). The heights of the freezing level (agl) within a given 10° -data block on the NMC grid were averaged to obtain a value, Z_1 (m), at the resolution of the sferics data. The number of cloud-to-ground discharges was expected to vary indirectly with Z_1 .

The second method of representing the effect of the freezing level was a vertical distance, Z_2 (m), from a reference level, 7000 m (msl), in the cloud to the freezing level (msl). Most cloud-to-ground discharges are believed to emanate from negative centers of charge near the freezing level and lower than 7000 m (msl) [Kitagawa and Brook, 1960]. In the case of a freezing level higher than 7000 m, Z_2 was set to zero (thresholded). Also, Z_2 was set to zero when the

temperature at 1000 mb was less than or equal to -5°C . These thresholds were used to assign zero values to Z2 when the probability of occurrence of cloud-to-ground lightning was considered low. That is, when the freezing level was very high in low latitudes and when the surface temperature was low in middle and high latitudes in February. Values of Z2 within a 10° -data block of the NMC grid were averaged to obtain the resolution of the sferics data. The number of cloud-to-ground discharges within a data block was considered likely to vary directly with Z2.

Terrain. A weighted average of terrain height, TH (m), was obtained for each 10° -data block in this manner

$$\text{TH} = 1/16 [X_1 + 2X_2 + X_3 + 2X_4 + 4X_5 + 2X_6 + X_7 + 2X_8 + X_9] \quad (31)$$

where TH is the weighted average of terrain height (m), X_1 to X_9 are values of average terrain height at 5° latitude-longitude intersections with center value at X_5 (see figure 23).

Geomagnetic regressors. Values of K_p were converted to a_p (i.e., linearized) as explained in chapter II. Values were available at 3-h intervals and were averaged to 6-h intervals to conform to the time resolution of the sferics data. K_p is a global measure of geomagnetic activity.

H-component data, H (γ), were available in hourly values at five stations roughly along 45°N (see Table 2). (H is the scalar intensity of the horizontal component of the field in gamma (γ)). The five stations each represent a respective center longitude in the area of

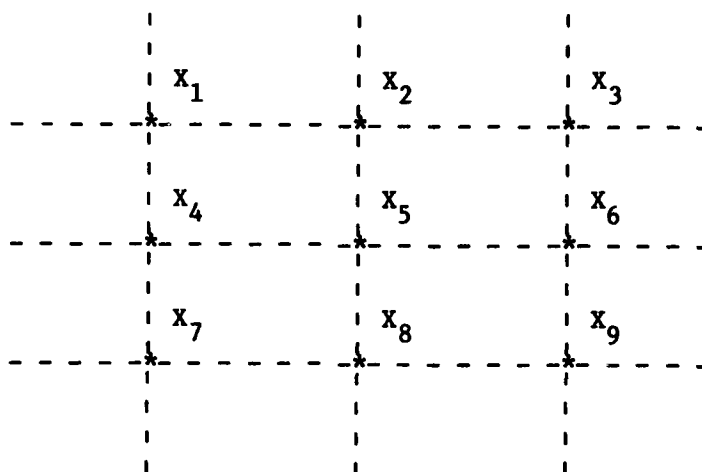


Fig. 23. Illustration of values used in (31) to estimate the average terrain height at X_5 , the center grid point of a 10° latitude-longitude block. Values of average terrain height at 5° intersections are X_1 to X_9 .

study (i.e., 25, 35, 45, 55, and 65°E). The H-component variable was selected as a regressor in addition to K_p since it varied in space.

Sunspots. The Zürich sunspot number, S , for each day of February and August of 1972 was used as a regressor to attempt to link activity on the sun to electrical events on earth. Despite its frequent use in solar-terrestrial studies, it would appear that a spurious relationship is quite possible with this regressor.

Linear Model and Assumptions

Multiple linear regression is the analysis method used in this chapter. The model is

$$\begin{aligned}
 D_G = & \beta_0 + \beta_1 * RH + \beta_2 * DD + \beta_3 * PW + \beta_4 * K + \beta_5 * W1 + \\
 & \beta_6 * W2 + \beta_7 * Z1 + \beta_8 * Z2 + \beta_9 * TH + \beta_{10} * ap + \\
 & \beta_{11} * H + \beta_{12} * S + \epsilon
 \end{aligned}
 \tag{32}$$

where D_G is the number of cloud-to-ground discharges, the coefficients, β 's, are unknown constants to be estimated, and the regressors are as explained previously. Specifically,

RH = layer relative humidity in % (August only),

DD = 850-mb dew-point depression in °C,

PW = precipitable water (1000-850 mb) in cm,

K = K index of stability,

W1 = wind speed in knots,

W2 = standard deviation of wind speed in knots,

Z1 = height of the freezing level (agl) in m,

Z2 = the distance from a reference level, 7000 m (msl), to
the freezing level (msl) in m,

TH = height of the terrain in hundreds of m,

ap = linear planetary index of geomagnetic activity,

H = horizontal component of magnetic field vector in γ ,

S = Zürich sunspot number,

ϵ = the error; that is, the variability in D_G unexplained by
the rest of the model.

In this chapter, the dependent variable, D_G , refers to the

synoptic time intervals of 0000-0600 UT and 1200-1800 UT. The regressors refer to the synoptic observation times of 0000 UT and 1200 UT. All variables were made to conform to the regularly-spaced grid of the sferics data (Figure 2).

The model, (32), is actually an assumption. It is assumed that the dependent variable is related linearly to the regressors. The exact relationship is unknown. The coefficients, β 's, are estimated from the data by the method of least squares which minimizes the sum of squared differences between actual and estimated values of the dependent variable. The quantity to be minimized is

$$SSE = \Sigma (D_G - \hat{\beta}_0 - \hat{\beta}_1 * RH - \hat{\beta}_2 * DD - \dots - \hat{\beta}_{12} * S)^2 \quad (33)$$

where SSE is the sum of squares of the errors and the estimates of the β 's are denoted by $\hat{\beta}$'s. The values of the $\hat{\beta}$'s are found by taking the partial derivatives of SSE with respect to $\hat{\beta}_0, \hat{\beta}_1, \dots$, setting each equation to zero, and solving the resulting linear system of equations.

The assumptions that underlie regression and least squares analysis are:

1. The β 's in (32) are constants.
2. The regressors in (32) are not random variables. After measurement, they are constants known without error.
3. The values of ϵ in (32) are independent, identically distributed, random variables with a mean of zero and common variance. The distribution of the ϵ 's should be normal if standard t and F tests are to be used.

The first assumption presented no problem in the present study. Clearly, the second assumption was violated. Meteorological measurements always have an associated error (see Appendix B). However, measurement error was one of the least significant problems in this study because it was almost certainly small compared to the variability in the regressors. Also, we were dealing with rough estimates of complex processes so that relatively small measurement errors were not important.

The third assumption is always a problem in meteorology in that the observations are functions of time and space. The violation of the assumption that the ϵ 's are independent is due to specification error. This error arises because we do not know the correct model. Specification error can cause SSE to be inflated and the $\hat{\beta}$'s to be biased.

A high degree of linear relationship among regressors is called multicollinearity. Severe multicollinearity is common in meteorological studies [e.g., Zak, 1977] since the regressors are linked by physical laws (e.g., the first law of thermodynamics and the equation of state) provided that there are no sources or sinks. Also, the use of several regressors to represent a single effect may contribute to multicollinearity. The existence of multicollinearity does not invalidate a regression analysis since the lack of multicollinearity is not a basic assumption. However, intercorrelation complicates the interpretation of results and the inferences that are possible concerning the β 's.

February Results

Analysis technique. The results for February are summarized in Tables 25 and 26. The backward selection technique was used to obtain the models. First, the regression was obtained with all 11 regressors entered. Then, regressors were eliminated in successive steps. The regressor eliminated in each step was that with the least significant coefficient. The process was continued until a regression was obtained with all coefficients significant at the 10% level.

The "best" regression model will not necessarily be found by any variable selection technique. Therefore, after reasonable models were found by backward selection, all 2^{11} possible regressions were considered. The best three (i.e., with maximum R^2) in each subset were analyzed. In every case, this analysis pointed to the selection of the same variables and models chosen by the use of backward selection.

The data were stratified by the estimated number of cloud-to-ground discharges. The stratifications corresponding to values greater than or equal to five and values greater than or equal to ten were chosen because it is important to estimate and study the cause of the occurrence of significant lightning. It is this quantity that greatly affects the VLF noise environment. The sample size for each stratification is given in Table 26.

TABLE 25. The February Models with an Asterisk Denoting the Significant Coefficients at the 10% Level for Various Stratifications of the Number of Cloud-to-Ground Discharges, D_G .

Regressor	Full Grid [†]				2-Box Data [§]			
	LOG [¶]		LOG [¶]		LOG [¶]		LOG [¶]	
	>5	>5	>10	>10	>5	>5	>10	>10
Z1	*	*	*	*	*	*	*	*
ap	*			*	*	*	*	*
Z2	*	*	*	*		*		
PW	*	*	*	*	*			
DD	*	*		*	*		*	
K	*	*		*	*		*	
H					*	*	*	*
TH					*	*	*	*
W2			*					
S								*
W1								

†Full grid refers to the 5 x 5 grid of Figure 22.

§2-box data refers to the 10° latitude-longitude blocks of Figure 22 with center grid points of 35°N, 25°E and 35°N, 35°E.

¶LOG is Napierian logarithm.

TABLE 26. Continued

Part C - Other Useful Statistics									
Full Grid [†]					2-Box Data [‡]				
Statistic	>5	LOG [¶] >5	>10	LOG [¶] >10	>5	LOG [¶] >5	>10	LOG [¶] >10	LOG [¶] >10
Intercept	39.0	3.1	190.2	4.0	-74,552.0	-1,025.4	-67,172.1	-820.9	
N	79	79	52	52	36	36	30	30	30
R ²	0.38	0.45	0.31	0.43	0.56	0.56	0.50	0.53	
$\hat{\sigma}_\epsilon$	43.9	0.9	49.5	0.7	47.8	0.8	51.2	0.6	

Sample size is N, coefficient of determination is R², and the estimated standard deviation of the error is $\hat{\sigma}_\epsilon$.

[†]Full grid refers to the 5 x 5 grid of Figure 22.

[‡]2-box data refers to the 10° latitude-longitude blocks of Figure 22 with center grid points of 35°N, 25°E and 35°N, 35°E.

[¶]LOG is Napierian logarithm.

There were many (75%) zero values of D_G in February. All attempts to fit a model to the data with zeroes and small values present failed. A typical R^2 was 0.08. It is clear that models that include all the data were influenced by the low values which entered as substantial noise.

For each stratification of the data, models were obtained with a logarithmic transformation of the dependent variable, D_G . In the ordinary model, we study the change in the dependent variable due to a unit change in each regressor, all other regressors held constant. In the logarithmic transformation of the dependent variable, we study the proportional change in the dependent variable due to a unit change in each regressor. In other words, we are searching for a multiplicative effect as opposed to an additive affect. A multiplicative effect was considered possible because there were many small values of the dependent variable, a few values of moderate magnitude, and even fewer of large magnitude.

The data also were stratified by frequency of occurrence of significant lightning. The two most active 10° blocks were clearly those with center grid points at $35^\circ\text{N}, 25^\circ\text{E}$ and $35^\circ\text{N}, 35^\circ\text{E}$ (see Figure 22). This is the "2-box data" of Tables 25 and 26. These boxes are in the Eastern Mediterranean where cyclones and associated fronts are frequently observed in winter. There were 25 boxes (5×5 grid) available in the area of study.

In a regression analysis, the significance of coefficients

should be tested. The hypothesis that a regressor does not affect the dependent variable in an additive fashion is equivalent to the hypothesis that the coefficient is zero. A test statistic is constructed whose distribution is known when the hypothesis that the coefficient is zero is true. Since the distribution is known, a critical region is selected such that the probability that the test statistic is included within the region is a prescribed significance level. The test statistics used follow t distributions and the critical region corresponds to large absolute values of the test statistic. The significance level used throughout is 10%.

The coefficient of determination, R^2 , in Table 26 expresses the linear fit of the model to the data. Specifically, it is the proportion of the error that is explained by extending the model beyond the mean to include all regressors. It is important to realize the difference between R^2 and the correlation coefficient, R . The latter is a measure of association between two variables. A R^2 of 0.5 corresponds to a R of 0.7. A sense of the meaning of correlation may be obtained by studying Figure 24. Although simple linear correlation is depicted, the basic idea extends to multiple linear correlation.

Discussion of the models. The results for February are good. The fits (R^2) are notably better than those (usually less than 0.30) obtained in regression studies that estimate the occurrence of thunderstorms [e.g., Zak, 1977]. The author is not aware of

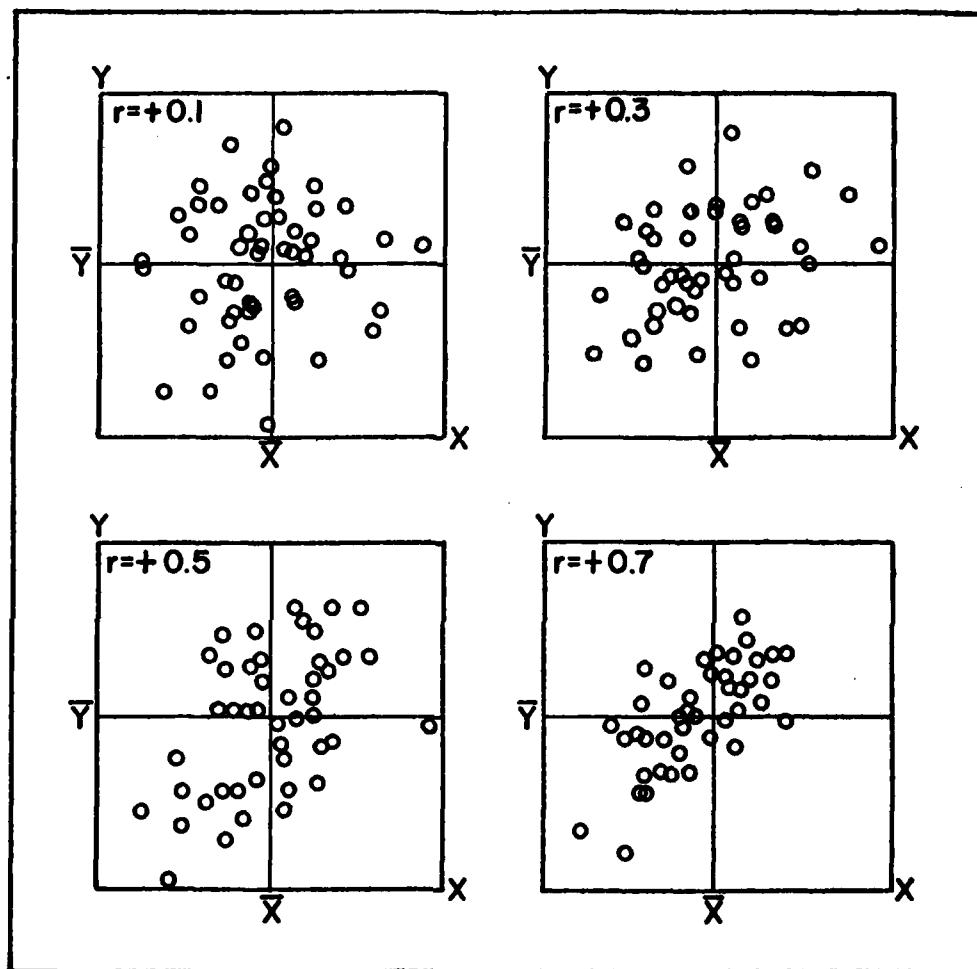


Fig. 24. Scatter diagrams and their associated correlation coefficients, r . The random variables are X and Y . The respective means are \bar{X} and \bar{Y} .

any regression studies that attempt to explain the variability in the occurrence of lightning. The log models were either about the same in fit or slightly better than the commensurate ordinary models. Both additive and multiplicative effects were probably present in the models. No single regressor of importance appeared only in the log models.

The sample size and list of regressors in each model are available in Tables 25 and 26. One would prefer to have a larger sample size relative to the number of regressors, but the data sets used and the results obtained are adequate to allow inferences to be made. The significance of the coefficients that correspond to the selected regressors are given in Table 26. It is noteworthy that among the coefficients included in the models, 45% are significant at the 1% level, 39% at the 5% level, and the remaining 16% at the 10% level.

An interesting relationship between the H-component of the magnetic vector, H, and the average height of the terrain, TH, existed in the 2-box data. In the routine analysis of plots of variables and their correlations, it was noticed that in the 2-box data the correlation between H and TH was -0.99. Both variables were significant in the models. This is an extremely strong indication of negative multicollinearity. TH assumed two values in the two boxes. The values of H varied but were in two general groups that corresponded to the longitudes of the two boxes (25°N and 35°N, see Table 2). The relatively low values of TH (coded in hundreds of

m) and the high values of H (typical value 21,393 γ) balanced each other in the model so that the important variation was the residual in H (departure from the group mean) apart from the TH and H balancing. When the residual in H was used as a regressor in place of both TH and H, the other regressors had almost the same coefficients and the fit (R^2) was very similar. The only change, of course, was a large decrease in the size of the intercept. We may not ascribe physical meaning to the -0.99 correlation between TH and H. The T values are for two specific boxes with center grid points of 35°N, 25°E and 35°N, 35°E. The H values were not available by individual boxes. The values of H used in the 2-box data represent two "10° strips" of longitude with center values of 25°E and 35°E that extend from 20°N to 70°N latitude. The H values were actually measured at 42.5°N and 46.8°N (see Table 2). It is important to understand the relationship between TH and H in the data so that we may realize that the physical effect of importance in the 2-box models is the departure of H from its group mean.

Some specific items of interest prior to a discussion of the physical significance of the models may be listed:

1. The freezing level, Z1, appeared in all the models. The sign of the coefficients always was negative as expected and significant (9% level or less). The parameterization of the height of the freezing level, Z2, was significant in five of eight models.

Also, the sign of the coefficient was positive as expected in all models in which Z2 was significant.

2. The planetary geomagnetic index, a_p , was significant in six of eight models. Both a_p and the H-component of the magnetic vector, H, were significant in all the 2-box models. In fact, H was only significant in models with 2-box data.

3. The best moisture regressor is precipitable water, PW, in the 1000-850 mb layer. This regressor has a negative coefficient for the four full-grid models and a positive coefficient for the single 2-box model in which it is significant. The 2-box models include only data for the Eastern Mediterranean. One would expect a direct relationship in this area between low-level moisture and the occurrence of thunderstorms and lightning within the following 6 h. The inverse relationship for the full-grid models may have reflected the influence of low-level dryness in the arid and northern regions of the study area (see Figure 22). The dew-point depression, DD, at 850 mb was significant in five of eight models and indicated a dry layer at 850 mb in both the full-grid and 2-box models. The significance levels of both moisture regressors in the 2-box models were among the highest in the study (9.8, 8.7, and 8.8%). Perhaps the only consistent result regarding moisture was a dry lower atmosphere within 6 h of the occurrence of thunderstorms and lightning in boxes that did not include the Mediterranean Sea.

4. There was a direct relationship between stability, K, and the occurrence of lightning. K appeared in five of eight models.

5. The terrain height, the wind speed, the standard deviation of the wind speed, and the Zürich sunspot number were not important

regressors in the models.

6. The variables in Table 25 and 26 are listed in descending order of importance if one uses the criteria of frequency of appearance in the models and significance of coefficients.

7. There was a moderate degree of multicollinearity as revealed by simple linear correlations among the regressors.

August Results

The same analysis technique was used for the August data as for February. The results were poor, especially compared to the rather positive results of February. The August results are summarized in Tables 27 and 28. The 2-box data refer to the two most active 10° blocks with center grid points at 45°N, 35°E and 45°N, 45°E. The lack of significant coefficients is dramatic compared to the February results in Tables 25 and 26. The only consistent finding was four rather poor models that included only the standard deviation of the wind speed, W2.

Three models in August with all the variables considered had reasonable fits to the data (R^2 of about 0.5). However, the coefficients were insignificant and the backward selection technique failed to produce reasonable model subsets. Also, there were too few regressors for the sample size in two models.

Physical Significance

It is not possible to prove that the variation in cloud-to-ground discharges is caused by the regressors with the use of statistical analyses. Further, it is possible to produce models

TABLE 27. The August Models with an Asterisk Denoting the Significant Coefficients at the 10% Level for Various Stratifications of the Number of Cloud-to-Ground Discharges, D_G .

Regressor	Full Grid [†]				2-Box Data [§]			
	≥ 5	LOG [¶] ≥ 5	≥ 10	LOG [¶] ≥ 10	≥ 5	LOG [¶] ≥ 5	≥ 10	LOG [¶] ≥ 10
W2			*	*			*	*
DD					*			
K					*			
RH								
Z1								
ap								
Z2								
PW								
H								
TH								
S								
W1								

[†]Full grid refers to the 5 x 5 grid of Figure 22.

[§]2-box data refers to the 10° latitude-longitude blocks of Figure 22 with center grid points of 45°N, 35°E and 45°N, 45°E.

[¶]LOG is Napierian logarithm.

TABLE 28. The August Coefficients (Part A), Level of Significance (Part B), and Other Useful Statistics (Part C) for the Models of Table 27.

Regressor	Part A - Coefficients						
	Full Grid [†]			2-Box Data [§]			
	≥ 5	≥ 5	≥ 10	≥ 5	≥ 5	≥ 10	
W2			0.5	0.03		-3.0	-0.07
DU					1.0		
K					0.4		
RH							
Z1							
ap							
Z2							
PW							
H							
TH							
S							
W1							

TABLE 28. Continued

Regressor	Part B - Significance (%) if $\leq 10\%$					
	Full Grid [†]		2-Box Data [§]			
	≥ 5	≥ 10	≥ 5	≥ 10	≥ 10	≥ 10
W2		0.5	0.8		2.5	5.1
DD				6.2		
K				7.3		
RH						
Z1						
ap						
Z2						
PW						
H						
TH						
S						
W1						

TABLE 28. Continued

		Part C - Other Useful Statistics					
		Full Grid†			2-Box Data‡		
Statistic		LOG [¶] ≥5	≥10	LOG [¶] ≥10	≥5	LOG [¶] ≥5	LOG [¶] ≥10
Intercept			12.7	26	-4.7	57.7	3.75
N			52	52	29	18	18
R ²			0.15	0.13	0.17	0.28	0.22
$\hat{\sigma}_\epsilon$			6.9	0.4	6.7	20.5	0.6

Sample size is N, coefficient of determination is R², and the estimated standard deviation of the error is $\hat{\sigma}_\epsilon$.

†Full grid refers to the 5 x 5 grid of Figure 22.

‡2-box data refers to the 10° latitude-longitude blocks of Figure 22 with center grid points of 45°N, 35°E and 45°N, 45°E.

¶LOG is Napierian logarithm.

with good fits to the data and poor physical associations between the dependent variable and the regressors. This is true even if the regressors are chosen carefully, as in this case, on the basis of plausible physical importance. It is the author's opinion that the February results are real and that the August overall models that fit the data well did not represent meaningful physical association between the dependent variable and the regressors.

Most of the lightning in February occurred in data blocks under the influence of the storm track of the Eastern Mediterranean. The major storm track in August was at high north latitudes (north of 45°N). This makes appealing the explanation that organized frontal thunderstorms in February and the associated lightning was much more closely related to the large-scale meteorological regressors than the non-frontal thunderstorms that were frequent in August.

It is especially interesting that the height of the freezing level was the most important regressor. The major recommendation of the author's M.S. thesis [Freeman, 1974] was that a regression analysis should be undertaken to build evidence in support of the importance of the ice process in cloud electrification. This study has produced support for the conclusion that the number of cloud-to-ground discharges that occur varies indirectly with the height of the freezing level in winter. Both supercooled water and ice are typically present at and above the freezing level. But the concentration of negative charge near the freezing level is probably due to the presence of ice hydrometeors. As mentioned previously, the basic physics of spark breakdown implies that as

the distance between the ground and the negative center of charge decreases, the probability of a cloud-to-ground discharge increases.

The presence of low-level moisture and stability as important regressors is not surprising. These regressors were used to attempt to explain the variability in the data due to the variability in the occurrence of thunderstorms.

It is intriguing that measures of geomagnetic activity appear as important regressors. H is less important than ap under the criteria of frequency of appearance in the models and significance of coefficients. H is significant only for the more frequent occurrences of lightning (2-box data). In view of this result, it is interesting that H varies somewhat geographically (see chapter II) and ap is a global measure. The current state of knowledge in solar-terrestrial work is embryonic and the need to establish a morphology first before solid theories of cause and effect may be formulated is obvious.

Wilcox [1975] pointed out that one of the "common threads" in the literature on solar-terrestrial relationships is that meteorological response to apparent solar influence is dominant in winter. Markson [1978a] suggested that the data be stratified by winter and summer months to search for this common thread. This analysis certainly supports the growing evidence of a winter solar-terrestrial effect. Besides the almost casual observation that the earth is closer to the sun in winter than in summer in the Northern Hemisphere, no detailed

physical argument has appeared in the literature to explain the "winter effect."

Wilcox [1975] reviewed evidence that K_p varies systematically in magnitude and polarity as the interplanetary magnetic field sweeps past the earth. Markson [1971, 1975] provided evidence that there is a relationship between solar sector passages and a thunderstorm index. If the statistical relationship presented here between counts of cloud-to-ground discharges and indices of geomagnetic activity is physically meaningful, one may speculate that this means that both variables are influenced by a common variable of solar origin.

The data used in chapter V are given in Appendix C, which includes the dependent variable (greater than or equal to five cloud-to-ground discharges for the full grid) and all regressors. With the models presented in chapter V and the data, an investigator may reconstruct the results and pursue the research further.

CHAPTER VI

SUMMARY AND CONCLUSIONS

The purpose of this research was to understand better some aspects of the distribution and causes of the lightning discharge. The incidence of lightning discharges was estimated, the relationship of lightning-flash density to thunderstorm days was studied, and the causes of the variability in electrical activity were explored.

The estimates of the incidence of discharge include not only the important areal and global statistics but also monthly values over a regularly-spaced grid that covers a large area of the earth. The following general conclusions relative to the incidence of discharge may be made:

1. In general, the Southern Hemisphere tropics (0° - 20° S) were higher in average incidence of discharge than the Northern Hemisphere tropics (0° - 20° N) due to the contribution of the northern part of the South African focus and that of the tropical Pacific islands.
2. The extratropical zone of the Southern Hemisphere (20° S- 35° S) was clearly dominant in average incidence of discharge relative to other zones. This was due to the force of the southern part of the South African focus and the lesser contribution of thunderstorms in Australia.

3. Lightning occurred much less frequently in high (60°N - 90°N) than in middle (21°N - 59°N) latitudes but the number of discharges per square kilometer per second during stormy periods was similar in magnitude.

The relationship between monthly lightning-flash density and monthly mean thunderstorm days was studied. The months of January, April, August, and November were considered. Both sferics and W.M.O. data were used to estimate thunderstorm days. Since a power-law relationship was expected, a logarithmic transformation was initially used in order to estimate the coefficient and power. To use a logarithmic transformation it was necessary to add an arbitrary constant to values of the dependent variable since zeroes were present in the data. It was shown that the logarithmic models were sensitive to the choice of arbitrary constant. Therefore, the logarithmic models were not used, and a curvilinear regression without transformation was used instead. The analysis provided many useable regressions. The relationship of lightning-flash density to thunderstorm days varied by season.

The results were compared to previous work by Pierce [1968] and Maxwell et al. [1970]. The estimate of lightning flash density of this study agreed remarkably well with that of Maxwell et al. for August, especially over the practical range of five to ten thunderstorm days. The agreement with both Pierce and Maxwell et al. for January and August was close for five thunderstorm days but differed notably in all other cases.

The regressions of this study for "all available data" produced

estimates of lightning-flash density generally of the same order of magnitude as that of previous studies. However, all regressions based on stratifications of the data produced very low estimates of lightning-flash density. It is not known whether the variability in the occurrence of lightning, which is great, necessitated a large sample size (i.e., all the data) for the efficacy of the regressions based on stratifications of the data or whether the low densities are real.

The causes of the variability in cloud-to-ground discharges were studied. Although proof of cause is not possible in general with the use of statistical techniques, plausible explanations of the observed variability were developed. The months of February and August for a selected area (Figure 22) of the Eastern Hemisphere were chosen for study. Multiple linear regression was used to compute both ordinary models and those with a logarithmic transformation of the dependent variable. The regressors were available on the NMC grid and were averaged in various ways to conform to the resolution in 10° -blocks of the estimates of cloud-to-ground discharges. Some variables were thresholded prior to averaging. Stratifications of the data by area and number of cloud-to-ground discharges were used.

The main thrust was to explain the variability in cloud-to-ground discharges when significant lightning had occurred. This is the problem of physical and practical importance. Models with a reasonable fit to the data could not be found for stratifications of the dependent variable with less than five discharges-to-ground.

The number of zeroes (75% in February and 54% in August) and small values served as substantial noise in those regressions.

The models for February were dramatically better than those for August. The February thunderstorms that produced the lightning were associated with fronts more often than those in August. Apparently, the large-scale representation of the regressors efficaciously estimated the conditions required for cloud-to-ground lightning only in the organized systems in February. The only consistent result for August was that the standard deviation of the wind speed was almost always the last regressor to be eliminated in the backward selection technique.

The February models fit the data remarkably well (R^2 of 0.3 to 0.6) for this type of work. Equally as important, the backward selection technique produced model subsets that were very stable. All possible regressions were computed and this analysis confirmed that the proper models and variables had been selected by the backward selection technique. The sign of the coefficients made physical sense. All coefficients in the final regression models were statistically significant at the 10% level, and 84% of the coefficients were significant at the 5% level or less. The significant regressors in order of importance were: the height of the freezing level (agl), the planetary geomagnetic index (K_p linearized to ap), a parameterization of the height of the freezing level, precipitable water in the 1000-850 mb layer, the dew-point depression at 850 mb, the K index of stability, and the departure of the H-component of the magnetic force vector from its mean.

The identification of the height of the freezing level as the most important regressor was interesting since the potential importance of this regressor was pointed out in the recommendations section of the author's M.S. thesis [Freeman, 1974]. This research suggests that the number of cloud-to-ground discharges varies indirectly with the height of the freezing level in winter. A plausible physical reason is due to the view that ice hydrometeors carry negative charge at and above the freezing level. Due to the basic physics of spark breakdown, the probability of occurrence of a cloud-to-ground discharge varies indirectly with the distance between the negative center of charge and the ground.

The presence of precipitable water and the K index of stability in the February models was expected. These variables were chosen to attempt to explain the underlying variability in lightning due to the variability in thunderstorms.

It was intriguing that indices of geomagnetic activity were significant in the February models but not in August. One of the common threads in solar-terrestrial studies that show an apparent direct relationship between solar and meteorological events is a predominant "winter effect." This research adds to the growing morphology that is needed to form the basis for a theory that explains cause and effect. If the statistical results presented here have physical meaning, one may speculate that the results indicate that electrical and geomagnetic events that occur on earth

have a common antecedent on the sun.

The hypothesis of this research was that an estimate of the distribution of lightning discharge may be derived from sferics data and that the variation in these data may be studied both physically and statistically by the use of a model. The hypothesis appears to be supported by the results of this research.

CHAPTER VII

RECOMMENDATIONS

In a data study of this magnitude, one usually makes compromises, due to the availability of funds and time, by stratifying the data. All the data were used in Chapter III, The Incidence of Discharge. One would like to see the results of Chapter IV, The Relationship between Lightning-Flash Density and Thunderstorm Days, and Chapter V, Analysis of the Large-Scale Causes of the Variability of Electrical Activity, extended to include different stratifications of the data. This is especially true of Chapter V in that all months should be considered instead of only February and August.

Besides the general recommendation to extend the amount of data used, the following specific recommendations are made:

1. Other regressors should be used to estimate the variability of cloud-to-ground discharges if data could be found. Potential candidates are antecedent rainfall and the duration of time that data blocks are under the influence of fronts.

2. Independent data should be used to pursue the result that cloud-to-ground discharges vary indirectly with the height of the freezing level. It is not known if the averages of regressors within 10° -data blocks preserved sufficient physics to be meaningful and if this result only is present when one works in averages and

on the large scale.

3. The interesting result that geomagnetic indices were important in the estimation of the occurrence of cloud-to-ground discharges should be pursued further. The first step would be to perform a superposed epoch analysis with solar sector passages as key days.

One could use the raw sferics data for 1972 to pursue other lines of research..

1. The geometry of deep convective clouds vs. their electrification would be a fascinating study. One would probably use visual and IR satellite imagery. This may limit the study to the electrification of cloud clusters in the tropics.

2. One could provide quantitative information on the electrification of typhoons. A useful study would be to concentrate on the four typhoons that occurred in the Bay of Bengal in 1972.

REFERENCES

- Aiya, S. V. C., Lightning and power systems, Electro-Technology, J. Soc. Electronic Engineers, Bangalore, 12, 1-12, 1968.
- Bailey, T. W., Personal communication, 1972.
- Barkalova, K. N., Relation between the number of thunderstorms and the amount of sferics that produce a field strength greater than a given level, AFCRL, Contract No. AF 19(628)-3880, Amer. Meteorol. Soc. Translation, Translated from Trudy Glavnaia Geofizicheskaiia Observatoriia, Leningrad, 157, 85-86, 1964. (available from DDC; AD 653 172).
- Berkofsky, L. and E. A. Bertoni, Mean topographic charts for the entire earth, Bull. Amer. Meteorol. Soc., 7, 350-354, 1955.
- Bosart, L. F., T. J. Chen, and R. E. Orville, A preliminary study of the synoptic conditions associated with lightning flashes over Mt. San Salvatore, Lugano, Switzerland, Tellus, 26, 495-504, 1974.
- Brantley, R. D., J. A. Tiller, and M. A. Uman, Lightning properties in Florida thunderstorms from video tape records, J. Geophys. Res., 80, 3402-3406, 1975.
- Brooks, C. E. P., The Distribution of thunderstorms over the globe, Met. Office Geophys. Mem. and Prof. Notes, No. 24, London, 147-164, 1925.
- Brooks, C. E. P., The variation of the annual frequency of thunderstorms in relation to sunspots, Quart. J. Roy. Meteorol. Soc., 60, 153-165, 1934.
- Byers, H. R., General Meteorology, McGraw-Hill, New York, 641 pp., 1974.
- Chalmers, J. A., Atmospheric Electricity, 2nd ed., New York, Pergamon Press, 515 pp., 1967.
- Cianos, N. and E. T. Pierce, A ground-lightning environment for engineering usage, Tech. Rept. 1 SRI Project No. 1834, Contract No. L.S.-2817-A3, Stanford Research Institute, Menlo Park, Calif., 136 pp., 1972.

- Dolezalek, H., Discussion of the fundamental problem of atmospheric electricity, Pure Appl. Geophys., 100, 8-43, 1972.
- Dolezalek, H., Personal communication, 1978.
- Few, A. A., Lightning channel reconstruction from thunder measurements, J. Geophys. Res., 75, 7517-7523, 1970.
- Fitzgerald, D. R., Personal communication, 1977.
- Freeman, W. B., Jr., The distribution of thunderstorm and lightning parameters over the Eastern Hemisphere for 1972, M.S. Thesis, Texas A&M Univ., College Station, Tex., 102 pp., 1974.
- Frisinger, H. H., The History of Meteorology: to 1800, Science History Publications, New York, 143 pp., 1977.
- George, J. J., Weather Forecasting and Aeronautics, Academic Press, New York, 673 pp., 1960.
- Griffiths, J. F., Climate and the Environment, Westview Press, London, 148 pp., 1976.
- Herman, J. R. and R. A. Goldberg, Initiation of non-tropical thunderstorms by solar activity, J. Atmos. Terrest. Phys., 40, 121-134, 1978.
- Heydt, G. and H. Volland, A new method for locating thunderstorms and counting their lightning discharges from a single observing station, J. Atmos. Terrest. Phys., 26, 85-104, 1964.
- Heydt, G. and J. Frisius, Zur bestimmung der geographischen verteilung der atmospherics-oktivitat, Meteorol. Rundschau, 27, 118-119, 1974.
- Hiser, H. W., Sferics and radar studies of South Florida thunderstorms, J. Appl. Meteorol., 12, 479-483, 1973.
- Horner, F., The relationship between atmospheric radio noise and lightning, J. Atmos. Terrest. Phys., 13, 140-154, 1958.
- Horner, F., Narrow-band atmospherics from two local thunderstorms, J. Atmos. Terrest. Phys., 21, 13-25, 1960.
- Horner, F., Radio noise from thunderstorms, Advances in Radio Research, Vol. 2, New York, The Academic Press, 121-204, 1964.

- Horner, F. and P. A. Bradley, The spectra of atmospheric from near lightning discharges, J. Atmos. Terrest. Phys., 26, 1155-1166, 1964.
- Horner, F., Radio noise in space originating in natural terrestrial sources, Planet. Space Sci., 13, 1137-1150, 1965.
- Huschke, R. E., Ed., Glossary of Meteorology, Amer. Meteorol. Soc., Boston, 638 pp., 1959.
- Huzita, A. and T. Ogawa, Charge distribution in the average thunderstorm cloud, J. Meteorol. Soc. Jap., 54, 285-288, 1976.
- Ishikawa, H., Nature of lightning discharges as origins of atmospheric, Proc. Res. Inst. Atmos., Nagoya University, 8A, 1-274, 1960.
- Kalakowsky, C. B. and E. A. Lewis, VLF sferics of very large virtual source strength, Physical Science Research Papers, No. 261, AFCRL Project No. 4603, Air Force Geophysics Laboratory, Bedford, Massachusetts, 1966.
- King, J. H., Ed., Handbook of Correlative Data, NSSDC No. 71-05, NASA, Greenbelt, Md., 204 pp., 1971.
- Kitagawa, N. and M. Brook, A comparison of intracloud and cloud-to-ground lightning discharges, J. Geophys. Res., 65, 1927-1931, 1960.
- Leushin, N. I., Explanation of the cause of non-correspondences of sferics centers and weather conditions, AFCRL, Contract No. AF 19(628)-3880, Amer. Meteorol. Soc. Translation, Translated from Trudy Glavnaia Geofizicheskaja Observatorija, Leningrad, 157, 76-84, 1964. (available from DDC; AD 653 173).
- Livingston, J. M. and E. P. Krider, Electric fields produced by Florida thunderstorms, J. Geophys. Res., 83, 385-401, 1978.
- MacKerras, D., A comparison of discharge processes in cloud and ground lightning flashes, J. Geophys. Res., 73, 1175-1183, 1968.
- Malan, D. J., Radiation from lightning discharges and its relation to the discharge process, Recent Advances in Atmospheric Electricity, New York, Pergamon Press, 557-563, 1958.

- Markson, R., Considerations regarding solar and lunar modulation of geophysical parameters, atmospheric electricity, and thunderstorms, Pure Appl. Geophys., 84, 161-202, 1971.
- Markson, R., Solar modulation of atmospheric electrification through variation of the conductivity over thunderstorms, in Proceedings of the Symposium on Possible Relationships Between Solar Activity and Meteorological Phenomena, Greenbelt, Md., 1974.
- Markson, R., Solar sector-thunderstorm relationships and proposed mechanism for solar control of atmospheric electrical activity, in Proceedings of the Symposium on High Atmosphere and Space Problems in Atmospheric Electricity, Grenoble, 1975.
- Markson, R., Ionospheric potential variations obtained from aircraft measurements of potential gradient, J. Geophys. Res., 81, 1980-1990, 1976.
- Markson, R., Personal communication, 1978a.
- Markson, R., Solar modulation of atmospheric electrification and possible implications for the sun-weather relationship, Nature, 273, 103-109, 1978b.
- Mason, B. J., The physics of the thunderstorm, Proc. R. Soc. London, Ser. A, 327, 433-466, 1972.
- Mason, B. J., In reply to a critique of precipitation theories of thunderstorm electrification by C. B. Moore, Quart. J. Roy. Meteorol. Soc., 102, 219-225, 1976.
- Martin, J. N., and V. W. Hildebrand, Statistical evaluation of sferics distribution, NOLC Rept. 628 Project No. WR 5-0062, Naval Ordnance Laboratory, Corona, Calif., 95 pp., 1965. (available from DDC; AD 620 459).
- Maxwell, E. L., D. L. Stone, R. D. Crogham, L. Ball, and A. D. Watt, Development of a VLF atmospheric noise prediction model, Final Report WRL 70-1H2-VLFNO-R1, Contract No. N00014-69-C-0150, Westinghouse Georesearch Laboratory, Boulder, Colorado, 213 pp., 1970.
- Miller, R. C., Notes on the analysis and severe storm forecasting procedures of the Air Force Global Weather Central, Air Weather Service Technical Report 200 (Rev.), Scott AFB, Il., 102 pp., 1972.

- Moore, C. B., An assessment of thundercloud electrification mechanisms, Proceedings of the Fifth International Conference on Atmospheric Electricity, Garmisch-Partenkirchen, 840 pp., 1974.
- Moore, C. B., Reply to comments by B. J. Mason, Quart. J. Roy. Meteorol. Soc., 102, 225-240, 1976.
- Moyer, V. E., Personal communication, 1974.
- Nakano, M., Characteristics of lightning channel in thunderclouds determined by thunder, J. Meteorol. Soc. Jap., 54, 441-447, 1976.
- Ney, E. P., Cosmic radiation and the weather, Nature, 183, 451-452, 1959.
- Ogawa, T. and M. Brook, The mechanism of the intracloud discharge, J. Geophys. Res., 69, 5141-5150, 1964.
- Ogawa, T. and M. Brook, Charge distribution in thunderstorm clouds, Quart. J. Roy. Meteorol. Soc., 95, 513-525, 1969.
- Pierce, E. T., Electrostatic field-changes due to lightning discharges, Quart. J. Roy. Meteorol. Soc., 81, 211-228, 1955.
- Pierce, E. T., H. R. Arnold, and A. S. Dennis, Very-low-frequency atmospherics due to lightning flashes, Final Rept. SRI Project No. 3738, Contract No. AF 33(657)-7009, Stanford Research Institute, Menlo Park, Calif., 132 pp., 1962.
- Pierce, E. T., A relationship between thunderstorm days and lightning flash density, EOS Trans. AGU, 49, 686, 1968.
- Pierce, E. T., The thunderstorm as a source of atmospheric noise at frequencies between 1 and 100 kHz, Sp. Tech. Rept. 2 SRI Project No. 7045, Contract No. DASA 01-68-C-0073, Stanford Research Institute, Menlo Park, Calif., 90 pp., 1969.
- Pierce, E. T., Latitudinal variation of lightning parameters, J. Appl. Meteorol., 9, 194-195, 1970.
- Pierce, E. T., Personal communication, 1973.
- Popov, A. S., Apparatus for reception and recording of electrical oscillations, J. Russ. Phys. Chem. Soc., 28, 7-9, 1896.

- Prentice, S. A., and D. MacKerras, The ratio of cloud to cloud-to-ground lightning flashes in thunderstorms, J. Appl. Meteorol., 16, 545-550, 1977.
- Quart. J. Roy. Meteorol. Soc., Unsigned comments that preceded the letters to the editor, 102, 219, 1976.
- Rasmussen, L. A., On the approximation of saturation vapor pressure, J. Appl. Meteorol., 17, 1564-1565, 1978.
- Rossby, S. A., Sferics from lightning within a warm cloud, J. Geophys. Res., 71, 3807-3808, 1966.
- Schonland, B. F. J., The Flight of the Thunderbolts, Clarendon Press, Oxford, 152 pp., 1950.
- Scoggins, J. R. and G. S. Wilson, Atmospheric structure and variability in areas of convective storms determined from 3-h rawinsonde data, Final Report NASA CR-2678, Contract No. NAS8-26751, National Aeronautics and Space Administration, Washington, D. C., 118 pp., 1976.
- Smith, L. G., Intracloud lightning discharges, Quart. J. Roy. Meteorol. Soc., 83, 103-111, 1957.
- Sparrow, J. G. and E. P. Ney, Lightning observations by satellite, Nature, 232, 540-541, 1971.
- Takagi, M., The mechanism of discharges in a thundercloud, Proc. Res. Inst. Atmos., Nagoya University, 8B, 1-105, 1961.
- Takeuti, T., Studies on thunderstorm electricity, Proc. Res. Inst. Atmos., Nagoya University, 12A, 1-70, 1965.
- Takeuti, T., M. Nakano, M. Nagatani, and H. Nakada, On lightning discharges in winter thunderstorms, J. Meteorol. Soc. Jap., 51, 494-496, 1973.
- Takeuti, T., Nakano, M., and M. Nagatani, Lightning discharges in Guam and Philippine Islands, 53, 360-361, 1975.
- Taylor, W. L., A VHF technique for space-time mapping of lightning discharge processes, J. Geophys. Res., 83, 3575-3583, 1978.
- Teer, T. L., Lightning channel structure inside an Arizona thunderstorm, Ph.D. thesis, Rice Univ., Houston, Tex., 107 pp., 1973.

- Teer, T. L. and A. A. Few, Horizontal lightning, J. Geophys. Res., 79, 3436-3441, 1974.
- Thompson, A. H. and P. W. West, Use of satellite cloud pictures to estimate average relative humidity below 500 mb, with application to the Gulf of Mexico area, Mon. Weather Rev., 95, 791-798, 1967.
- Turman, B. N., Detection of lightning superbolts, J. Geophys. Res., 82, 2566-2568, 1977.
- Turman, B. N. and B. C. Edgar, Global lightning distributions at dawn and dusk, paper presented at the Spring Meeting of the American Geophysical Union, Miami, 1978.
- Uman, M. A., W. H. Beasley, J. A. Tiller, Y. T. Lin, E. P. Krider, C. D. Weidmann, P. R. Krebbiel, M. Brook, A. A. Few, Jr., J. L. Bohannon, C. L. Lennon, H. A. Poehler, W. Jafferis, J. R. Gulick, and J. R. Nicholson, An unusual lightning flash at Kennedy Space Center, Science, 201, 9-16, 1978.
- Valley, Shea L., Ed., Handbook of Geophysics, Air Force Geophysics Laboratory, Bedford, Massachusetts, 621 pp., 1960.
- Viemeister, P. E., The Lightning Book, New York, Doubleday & Company, Inc., 316 pp., 1961.
- Vorpahl, J. A., J. G. Sparrow, and E. P. Ney, Satellite observations of lightning, Science, 169, 860-862, 1970.
- Wilcox, J. M., Solar activity and the weather, J. Atmos. Terrest. Phys., 37, 237-256, 1975.
- Workman, E. G., M. Brook, and N. Kitagawa, Lightning and charge storage, J. Geophys. Res., 65, 1513-1517, 1960.
- World Meteorological Organization, World distribution of thunderstorm days - Part 1, W.M.O. Publ. No. 21. TP. 6, 1953.
- World Meteorological Organization, World distribution of thunderstorm days - Part 2, W.M.O. Publ. No. 21. TP. 21, 1956.
- Zak, J. A., Forecasting thunderstorms over a 2- to 5-h period by statistical methods, Ph.D. dissertation, Texas A&M Univ. College Station, Tex., 112 pp., 1977.

APPENDIX A: REMOTE SENSING TECHNIQUE

The purpose of this appendix is to expand the information given in Chapter II on the sferics network as suggested by Fitzgerald [1977]. The network was comprised of signal monitors, which were electronic systems that detected and measured random VLF electromagnetic signals (sferics) produced by lightning discharges. Ten signal monitors were in operation during the period January to July 1972 and six during the remainder of the year. Six sensors were sufficient to monitor and record sferics on a global basis. As mentioned previously, this study was confined to the Eastern Hemisphere because only data from that part of the world were available to the author. The signal monitor equipment and recording methodology, sferics-fix techniques, and the system threshold arrays will be explained. Although available, details of the electronic subsections of the signal monitors were considered outside the scope of this study and were not included.

Signal Monitors

The operation of the signal monitor equipment is depicted in Figure 25. A vertical, non-directional, whip antenna and two directional loop antennae were used to receive the sferic waveform. Although all electromagnetic signals appeared on the antennae, the signal monitors recorded on a selective basis, according to the

criteria of waveform half-cycle characteristics, the relative threshold field intensity of the waveform, and the azimuth of arrival. The signal monitors also had the capability to record signals

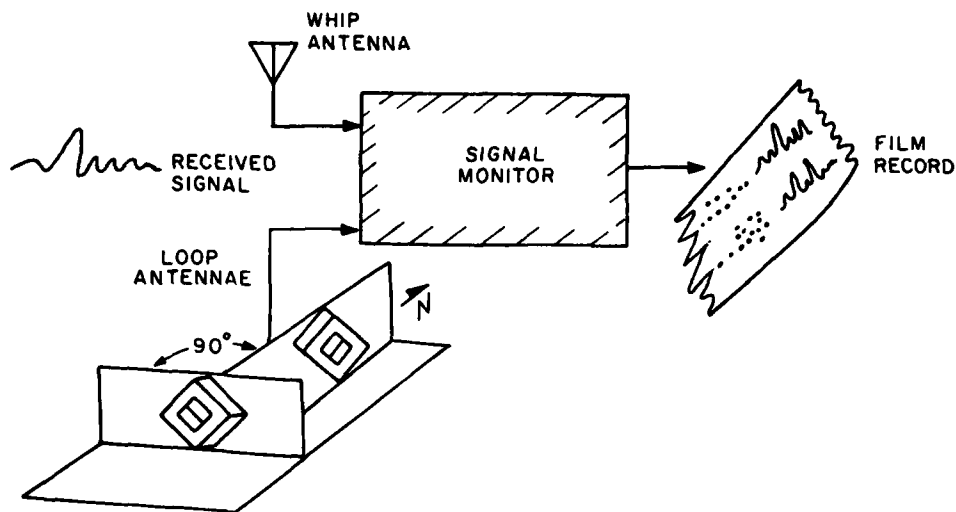


Fig. 25. Signal monitor operation.

selectively based on the energies of the distributed frequencies that composed the waveforms. However, the spectrum analyzer section and the discriminant section which performed this function were not in operation during 1972. The individual waveforms, after analysis by the waveform and azimuth sections, were recorded to an accuracy of 10^{-5} s. The time intervals between return strokes is of the order of milliseconds. For example, Takeuti, Nakano, and Nagatani [1975] observed time intervals of 20-100 ms at five locations in Guam and the Philippine Islands.

A typical recorded waveform is shown in Chapter II (Figure 1). The waveform has the appearance of a sine wave which builds to a peak and then decays to zero in 1000 μ s or less. The half-cycle of maximum amplitude of the recorded waveform occurred within the first 300 μ s of the waveform. The peak energies of all recorded sferics occurred in the frequency range of 250 Hz to 60 kHz.

The whip antenna has a precise electrical length (2 m) for establishing the relative field intensity in volts per meter for each received waveform, irrespective of direction of propagation. Electromagnetic signals that appeared across the antenna produced an output voltage proportional to the electrical height and the received signal intensity. The waveform input circuits received the output of the vertical whip antenna. The pre-recording criteria previously described were determined by the input, threshold control, peak detector and gate selector, and normalizing circuits in conjunction with the loop antennae and azimuth section circuits.

The loop antennae were used to resolve the received signal into two waveforms having an angular separation of 90°. The two waveforms, in turn, produced coordinate voltages that were used to determine the received azimuth of the signal in degrees relative to true north. The azimuth accuracy approximated 1° with a full 360° coverage.

Sferic Fixing Technique

The source location on earth of a sferic was determined by

the use of recording stations. The time of arrival of the spheric at each station was recorded to an accuracy of 10^{-5} s. Then, the difference in time of arrival between stations was converted to distance by the use of the propagation rate at VLF. Although empirical tests were conducted to determine an optimum propagation rate, it was found that the speed of light was acceptable. The speed of light is the speed of propagation of electromagnetic radiation through a perfect vacuum. It is a universal dimensional constant equal to $2.997925 \pm 0.000004 \times 10^{10}$ cm s⁻¹.

Time fixes were obtained by a straightforward application of spherical trigonometry. Consider the case of three stations (I, J, and K) that received a signal as shown in Figure 26.

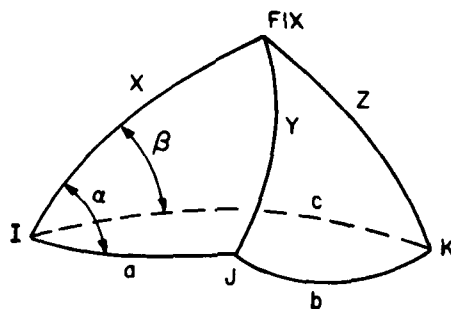


Fig. 26. Fix geometry.

Station I received the signal first. The distances between stations are represented by a , b , and c measured in radians and between the stations and the fix by X , Y , and Z as shown. We will develop formulas to find the angle α and the length of side X .

This will locate the fix on the earth. From the differences of received times converted to distance by use of speed-of-light propagation, we may define:

$$A = X - Y \quad (A1)$$

$$B = X - Z \quad (A2)$$

Thus:

$$Y = X - A \quad (A3)$$

$$Z = X - B \quad (A4)$$

From the law of cosines we know that:

$$\cos Y = \cos a \cos X + \sin a \sin X \cos \alpha \quad (A5)$$

$$\cos Z = \cos c \cos X + \sin c \sin X \cos \beta \quad (A6)$$

Substituting in (A5) and (A6) the values of Y and Z from (A3) and (A4) gives:

$$\cos (X-A) = \cos a \cos X + \sin a \sin X \cos \alpha \quad (A7)$$

$$\cos (X-B) = \cos c \cos X + \sin c \sin X \cos \beta \quad (A8)$$

Expanding the left side of (A7) and (A8) yields:

$$\begin{aligned} \cos X \cos A + \sin X \sin A &= \cos a \cos X + \sin a \\ &\sin X \cos \alpha \end{aligned} \quad (A9)$$

$$\begin{aligned} \cos X \cos B + \sin X \sin B &= \cos c \cos X + \sin c \\ &\sin X \cos \beta \end{aligned} \quad (A10)$$

Simplifying, we obtain:

$$\begin{aligned} \cos X (\cos A - \cos a) + \sin X (\sin A - \sin a \\ \cos \alpha) &= 0 \end{aligned} \quad (A11)$$

$$\begin{aligned} \cos X (\cos B - \cos c) + \sin X (\sin B - \sin c \\ \cos \beta) &= 0 \end{aligned} \quad (A12)$$

That is:

$$\tan X = \frac{\cos a - \cos A}{\sin A - \sin a \cos \alpha} \quad (\text{A13})$$

$$\tan X = \frac{\cos c - \cos B}{\sin B - \sin c \cos \beta} \quad (\text{A14})$$

Clearly

$$\frac{\cos a - \cos A}{\sin A - \sin a \cos \alpha} = \frac{\cos c - \cos B}{\sin B - \sin c \cos \beta} \quad (\text{A15})$$

To simplify, let

$$P = \cos c - \cos B \quad (\text{A16})$$

and

$$R = \cos a - \cos A \quad (\text{A17})$$

Substituting (A16) and (A17) into (A15), we get

$$R (\sin B - \sin c \cos \beta) = P (\sin A - \sin a \cos \alpha) \quad (\text{A18})$$

Also from the figure it can be seen that α and β differ by a constant (CON) that depends on the configuration of stations used. Thus we may write

$$\beta = \alpha - \text{CON} \quad (\text{A19})$$

Thus

$$R [\sin B - \sin c (\cos \alpha \cos (\text{CON}) + \sin \alpha \sin (\text{CON}))] = P \sin A - P \sin a \cos \alpha \quad (\text{A20})$$

and

$$\sin \alpha (R \sin c \sin (\text{CON})) + \cos \alpha (P \sin a - R \sin c \cos (\text{CON})) = (P \sin A - R \sin B) \quad (\text{A21})$$

To simplify further let:

$$S = R \sin c \sin (\text{CON}) \quad (\text{A22})$$

$$T = P \sin a - R \sin c \cos (\text{CON}) \text{ and} \quad (\text{A23})$$

$$Q = P \sin A - R \sin B \quad (\text{A24})$$

We may then write (A21) as

$$S \sin \alpha + T \cos \alpha = Q \quad (\text{A25})$$

Rewriting (A25) in terms of $\cos \alpha$, we have

$$S \sqrt{1 - \cos^2 \alpha} = Q - T \cos \alpha \quad (\text{A26})$$

This is now squared to eliminate the radical

$$S^2 (1 - \cos^2 \alpha) = Q^2 - 2QT \cos \alpha + T^2 \cos^2 \alpha \quad (\text{A27})$$

Collecting terms, we obtain

$$\cos^2 \alpha (T^2 + S^2) - 2QT \cos \alpha + (Q^2 - S^2) = 0 \quad (\text{A28})$$

This is a quadratic equation in $\cos \alpha$. It is solved by using the quadratic formula to give the result

$$\cos \alpha = \frac{2QT \pm \sqrt{4Q^2T^2 - 4(T^2 + S^2)(Q^2 - S^2)}}{2(T^2 + S^2)} \quad (\text{A29})$$

Finally, we substitute the value of $\cos \alpha$ (A29) in (A13) to find X, the distance from station I to the fix.

The system of sensors consistently "fixed" the incoming sferics within the proper geographical area. In fact, frequent tests by Bailey [1972] confirmed that the sferics were consistently fixed within 100 km of their true source location. As described

in the discussion of the data, the datum points (counts of sferics) are valid for a large area bounded by a 10° latitude and 10° longitude block. All that is claimed in this study is that the sferics were fixed within the 10° blocks that have the center points shown in Figure 2.

Threshold Arrays

Definition. The threshold arrays are system intensity values over a regularly spaced grid that represent the minimum field strength, expressed in decibels, below which no signal was located and recorded. Figure 27 shows a portion of a threshold array.

55E	60E	65E	70E	75E	80E	85E	
56.4	55.2	54.1	53.7	53.9	54.7	53.6	40N
55.9	54.6	54.0	54.9	55.4	55.5	54.3	
55.5	54.4	55.3	56.2	56.9	55.8	54.7	30N
61.6	55.7	56.6	57.5	57.3	57.2	55.9	
63.0	61.7	57.9	58.6	58.6	58.1	56.8	20N
57.5	61.9	60.4	58.9	59.9	59.1	57.9	
59.0	60.0	61.1	62.1	61.5	60.2	60.0	10N
60.7	61.7	65.4	64.3	64.3	64.0	64.9	
62.4	67.7	66.5	65.8	65.6	66.6	66.2	EQ
70.1	68.8	67.6	66.4	67.1	68.0	68.9	
71.2	70.0	68.7	67.6	68.5	69.4	70.3	10S
72.3	71.1	69.9	69.1	68.9	70.8	71.8	
73.4	72.2	71.0	70.5	70.2	70.8	75.5	20S
74.5	73.3	72.2	72.0	71.5	73.7	77.0	
76.9	74.4	73.3	73.4	74.2	79.2	78.5	30S
78.0	75.5	76.0	75.0	81.4	80.7	80.0	
85.1	84.7	77.1	83.5	82.9	82.2	81.5	40S

Fig. 27. Example of a threshold array for part of the Eastern Hemisphere. Values are in dB as defined in Chapter III.

The threshold arrays are the results of a model developed by personnel of the U. S. Air Force with the use of an IBM 360-65 computer. Figure 28 illustrates the process used to develop the

arrays. There were two threshold arrays for 1972 that covered the periods January to July and August to December. Two arrays were necessary due to a decrease in the number of sensors in the latter period. The model inputs were information about the sferics source (that is, field strength and location), information about the sensors (that is, location and average, individual sensor thresholds), attenuation tables, and the number of sensors required to determine a fix. The model inputs and the model will be explained in greater detail.

Model inputs. The source information included sferic locations and field-strength intensities. The source locations are regularly-spaced grid points in 5° increments over the Eastern Hemisphere (see Figure 27). The initial field strengths of the sferic source are arbitrarily chosen values. The reason for this will become clear in the explanation of the model.

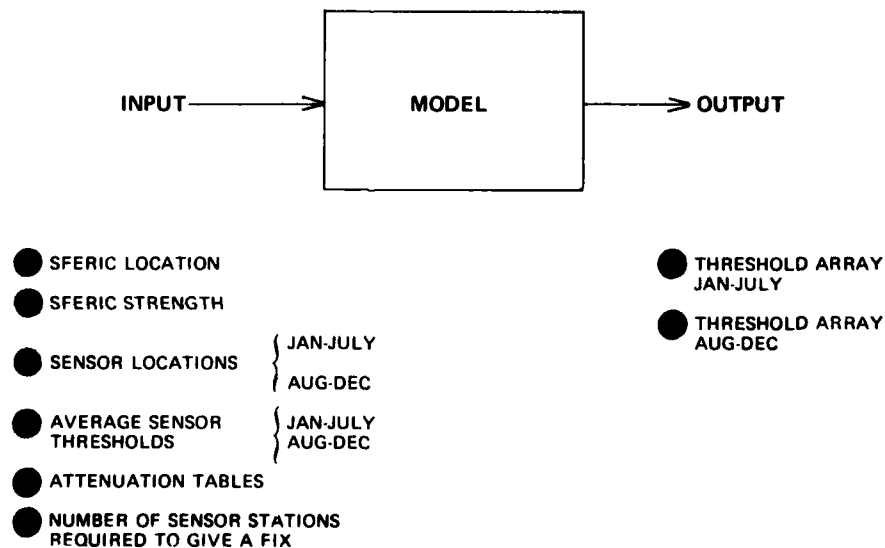


Fig. 28. Illustration of the procedure used to develop the threshold arrays.

The sensor information was straightforward and requires little amplifying discussion. The individual sensor threshold values were determined by adding the operator-set threshold to the basic machine threshold, which was a constant 20 dB above a 1 mV m^{-1} reference. As incident spheric activity increased to a point that the sensor approached saturation, the operator increased his sensor threshold in 1-dB increments so that only the more intense spherics were recorded by his sensor. The resultant threshold values were recorded and averaged for each sensor over the two 6-month periods (Jan to July and Aug to Dec) of 1972.

The signal loss from the source to the sensor due to attenuation was determined by using an empirically-derived table that was based on measurements conducted for the U. S. Air Force by the Denver Research Institute. The actual sensor equipment was used in the measurements. The main factor that affects propagation at VLF is the nature of the boundaries that form the wave guide. These are earth's surface and the D-layer of the ionosphere. Table entries, as depicted in Table 29, were averages of measurements that determined day vs. night and land vs. sea propagation results. The empirical table gave signal loss due to attenuation, expressed in decibels, for each 10^3 -km increment of propagation path. Table values were additive along the propagation path from the source to the sensor. Simple linear interpolation was used when necessary.

TABLE 29. Sample Table for Determining
Signal Loss Due to Attenuation.

Distance (10^3 km)	Incremental Loss (dB)
1	1.5
2	1.8
3	2.3
4	2.1
5	2.4
6	2.0
.	.
.	.
.	.

The final model input was the number of sensor stations required to give a fix. At least three stations were required as a lower bound to determine a fix. Any number of stations may be used, however, up to the total number of stations in the system. A four-station fix was used during the 1972 period.

The model. The threshold arrays represent, on the average, the aggregate sensor or system sensitivity to sferics. As may be seen from Figure 27, each array entry represents the signal sensitivity value for a 5° latitude-longitude block. The method by which a single value is obtained will be explained.

Consider for ease of explanation a hypothetical four sensor system, single source location, and threshold array values as shown in Figure 29. We assume further that a four-station fix

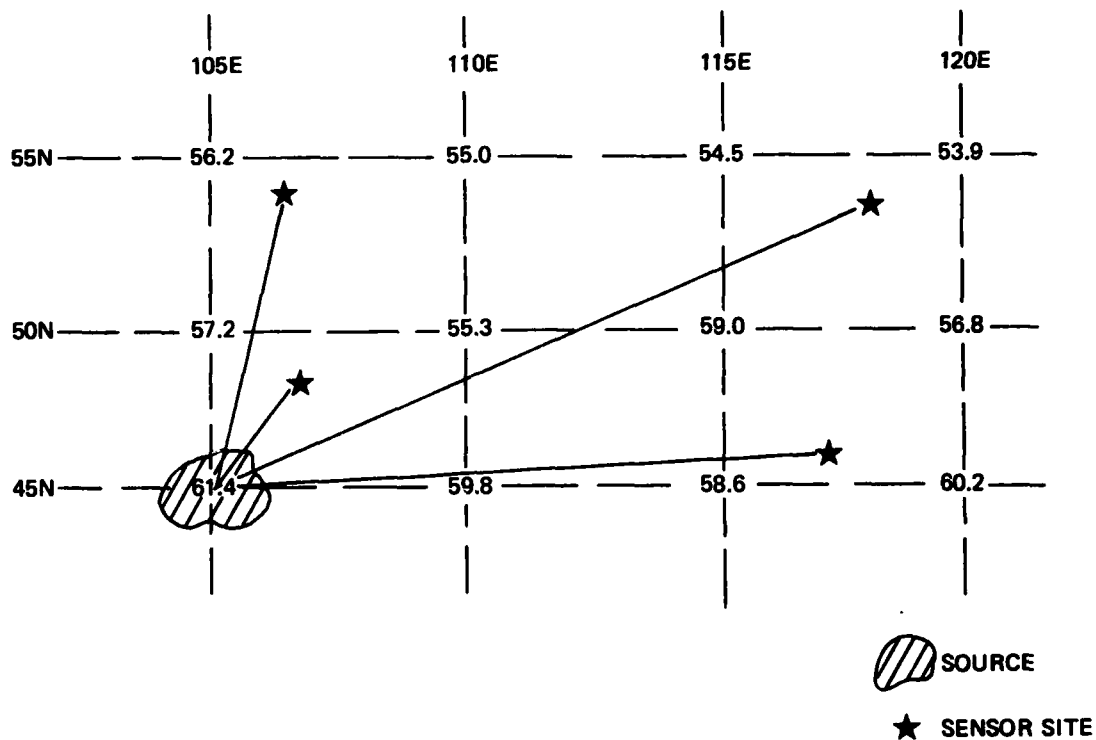


Fig. 29. Illustration of the method used to determine a single threshold-array value (61.4 dB) by the use of a four station fix. Threshold values are in decibels (dB) as defined in Chapter III.

is required to locate and record a spheric. We will discuss the method of obtaining the 61.4 dB value valid for the block centered at 45°N , 105°E . We assume a spherical earth and choose an arbitrary signal field strength, in decibels, and a source location at the center of a given block. The path from the source to each sensor is then determined from spherical trigonometry. The signal loss, in decibels, is then calculated for each path from the attenuation table previously explained (Table 29). The signal loss is subtracted from the source strength to give the strength of the signal upon arrival at each sensor site. This signal strength is compared with the sensor threshold value at each site. Since a "four-station fix" is required, the signal strength upon arrival at each of the four sensor locations must exceed the respective sensor thresholds to be recorded by the system. The source field strength is systematically increased in 0.1 dB increments until an associated, received signal strength is reached at each sensor site that exceeds each sensor threshold. The lowest such value for the 45°N , 105°E grid point in Figure 29 is the 61.4 dB value, which represents the system threshold value. Other grid point values are determined in an identical manner. Figure 30 is a flow-chart depiction of model calculations.

The threshold arrays were used in the normalization of the sferics data. It was necessary to develop meaningful relative values for the counts of sferics over the grid since the sensitivity

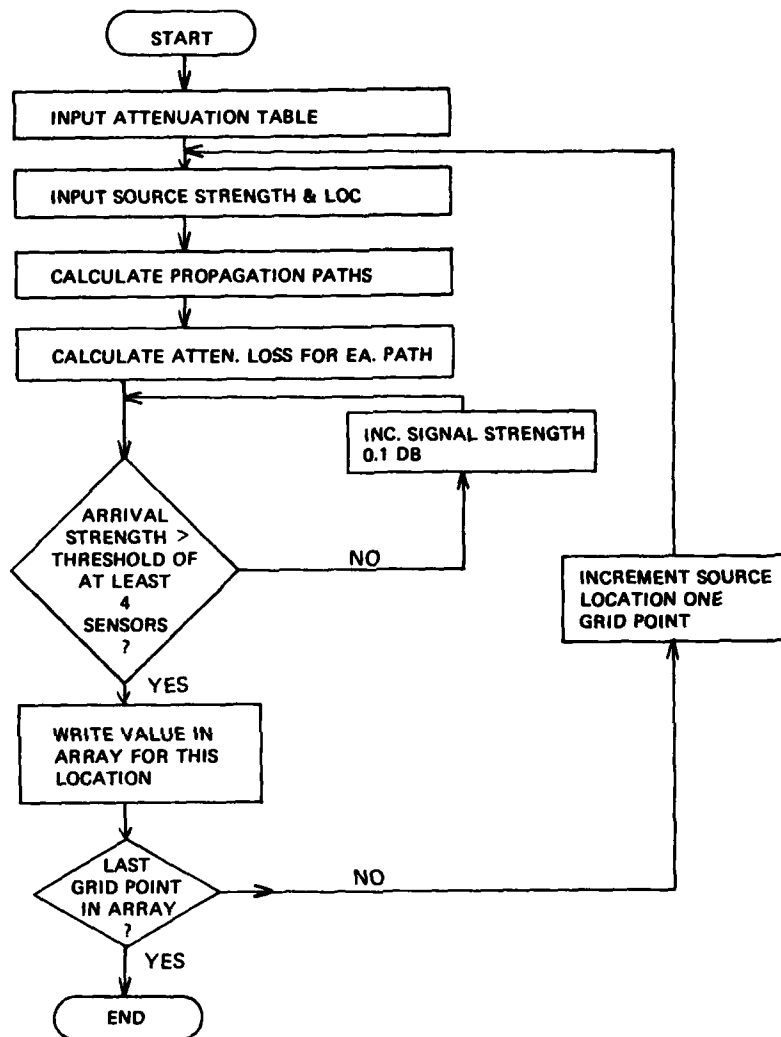


Fig. 30. Flow chart of model calculations used to determine the threshold arrays.

of the system of sensors to the collection of sferics was different for each grid point. The grid-point values of the threshold arrays are lower limits on the log-normal probability distributions used to normalize the counts of received sferics.

APPENDIX B: POSSIBLE SOURCES OF ERROR

It is probable that all the sources of error in this study were not known. Further, a detailed analysis of error is not possible for those sources of error that are known. The error in the counts of sferics is almost certainly much greater than that associated with the other meteorological variables (e.g., wind speed). The error associated with the geophysical variables (i.e., the K_p index and H-component data) and the relative sunspot numbers is not known. However, some qualitative and quantitative statements are possible:

- 1) Instrument errors, for the signal monitors covered in Appendix A, may result from errors in calibration, the setting of gating circuits, etc. Moreover, two signals that are incident at the antenna of a signal monitor at precisely the same instant in time would cause an erroneous distorted waveform to be recorded and counted. However, the resolution in time of a signal monitor for individual, received sferics is 10^{-5} s. It is unlikely that many distorted waveforms were recorded. Further, great care was exercised by the personnel of the Air Force on site in the maintenance and operation of the equipment. The data were considered valid and useful in operation at the Air Force Technical Applications Center (AFTAC) [Bailey, 1972].

2) The sensitivity of the system of sensors was different for each grid point (see Appendix A). The threshold arrays (lower limits on the probability integrals) were used in the normalization of the sferics data to give meaningful relative counts of sferics at grid points. However, the threshold arrays are only mean estimates, dependent to a large degree on propagation laws at VLF. Pierce [1973] stated that propagation at VLF is subject to geographic, geomagnetic, and temporal variability, none of which is known with certainty. It is virtually assured that the method of normalization did not represent that needed to yield accurate relative counts of sferics in all cases.

3) The statistics given in Table 4 are estimates based on empirical or quasi-empirical studies. They may not be close approximations to the state-of-nature at all times. The parameters of the log-normal distribution may change with various effects and the distribution followed by the field-strength intensity due to first return strokes and subsequent return strokes may not be log-normal under all conditions.

Since there is wide agreement that the standard deviation of received sferics ranges from 6 to 8 dB, we may appreciate the effect of varying only this sample statistic. An estimate of the number of lightning discharges for August with standard deviations of 6, 7, and 8 dB is shown in Figure 31. A standard deviation of 7 dB was used in this study as shown in Table 4.

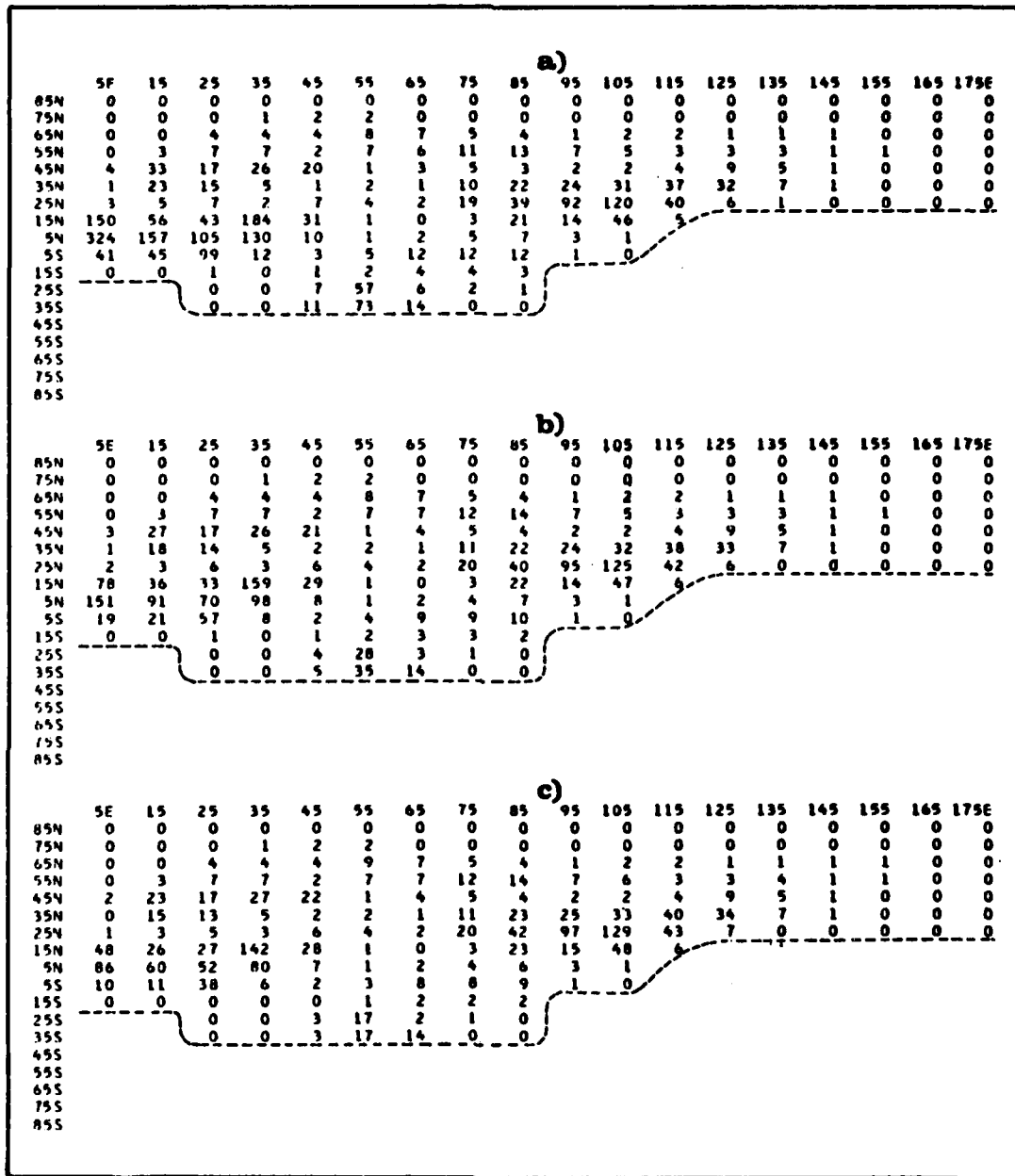


Fig. 31. Comparison of the distributions of lightning discharge for August for standard deviations of received sferics of a) 6 dB, b) 7 dB, and c) 8 dB. Values are in hundreds of discharges for 10° data blocks centered at the points shown. The area of data coverage is north of the broken line.

For a given threshold value at a grid point (i.e., a given lower limit on the probability integrals in (11)), the estimate of lightning discharges increases with increasing standard deviation as shown in Figure 31 (or remains the same due to round-off to the nearest 100 discharges). Since the standard deviation is a measure of dispersion, the probability of occurrence above a given threshold value increases with increasing standard deviation. But the probability integrals that are thus effected enter into (11) in the denominator with the result that the estimates of the number of lightning discharges decreases at a grid point with an increase in standard deviation. In general, there was little change in results caused by varying the standard deviation alone.

4) The analyses of this study depend for efficacy on the rough empirical equations quoted or developed in Chapter III. The only estimate known to the author of the dependence on latitude of the number of subsequent return strokes per cloud-to-ground discharge is that by Pierce [1970] given in (5). Pierce [1970] and Prentice and MacKerras [1977] have offered empirical rules for the variation with latitude of the ratio of cloud, D_C , to cloud-to-ground, D_G , discharges (see Chapters I and III). These respective relationships are given in (9) and (10). We may write (8) by substituting the value of this ratio due to Pierce, M , and the value due to Prentice and MacKerras, M' :

$$D_T = D_G (1 + M) \quad (B1)$$

$$D_T = D_G (1 + M') \quad (B2)$$

Then from (B1)

$$D_G = \frac{D_T}{1 + M} \quad (B3)$$

and from (B2)

$$D_T' = D_T \left(\frac{1 + M'}{1 + M} \right) \quad (B4)$$

where D_T and D_T' are the estimated total number of discharges due to the use of M and M' respectively.

The variation of M , M' , and the ratio, $\frac{1 + M'}{1 + M}$, with latitude is shown in Table 30. The results for August at grid points for (B1) and (B4) are shown in Figure 32. Table 30 and the bottom chart of Figure 32 include values only to 60°N. The estimates of Prentice and MacKerras [1977] extend only to that latitude.

The difference in M and M' were not considered sufficiently significant to merit the use of both estimates in this study. Only the estimate by Pierce of the ratio of cloud to cloud-to-ground discharges was used.

TABLE 30. Variation with Latitude of the Ratio of
Cloud to Cloud-to-Ground Discharges by Pierce
(M) and Prentice and MacKerras (M').

Latitude	M*	M'†	$\frac{1 + M'^{\S}}{1 + M}$
0	9.00	6.32	0.73
5	8.73	6.25	0.75
10	8.00	6.03	0.78
15	7.00	5.69	0.84
20	5.92	5.24	0.90
25	4.90	4.72	0.97
30	4.00	4.16	1.03
35	3.24	3.60	1.08
40	2.60	3.08	1.13
45	2.08	2.63	1.18
50	1.65	2.29	1.24
55	1.29	2.07	1.34
60	1.00	2.00	1.50

$$* M = \frac{9 - (\theta/30)^2}{1 + (\theta/30)^2}, \text{ latitude is } \theta.$$

$$+ M' = 4.16 + 2.16 \cos 3\theta, \text{ latitude is } \theta.$$

§ This ratio is from (B4).

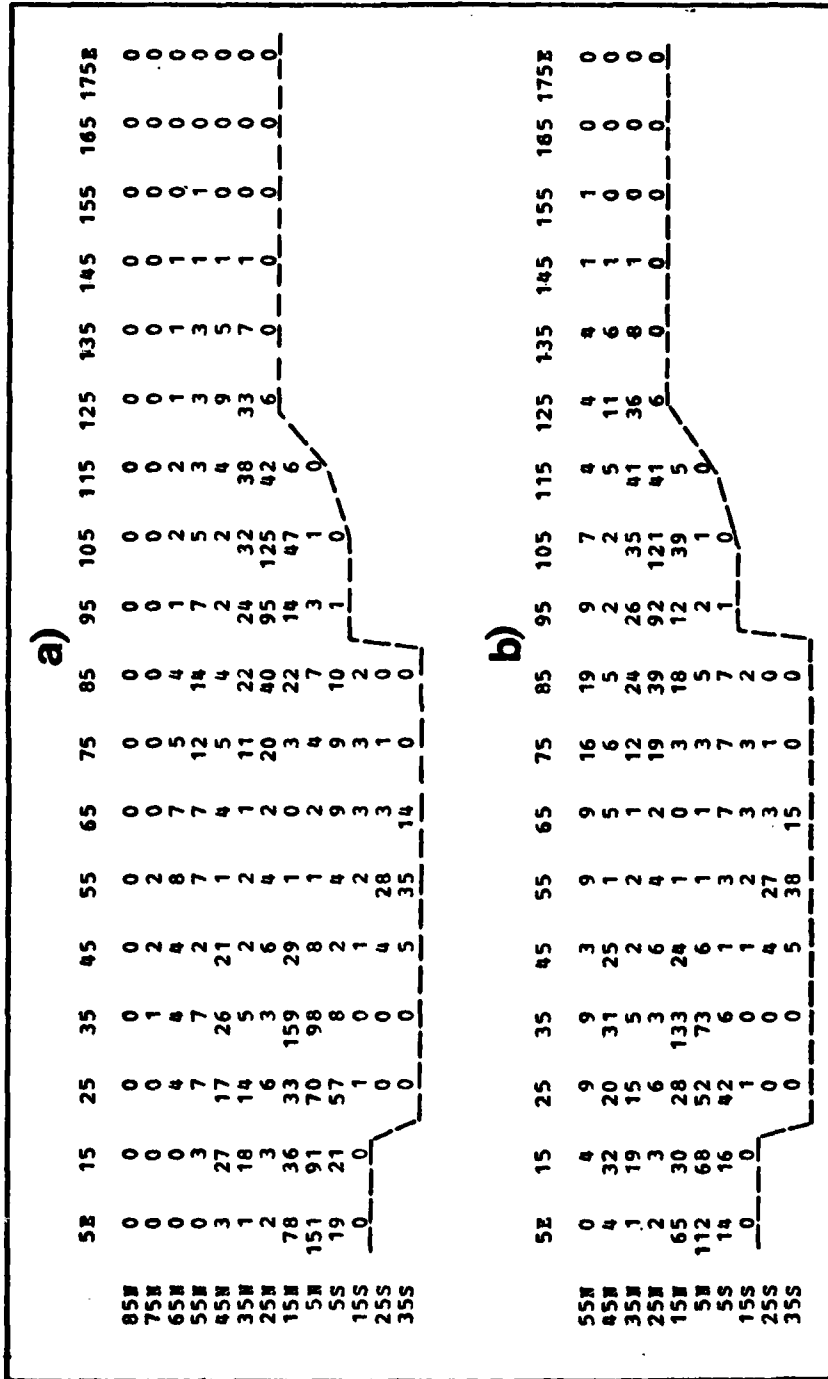


Fig. 32. Comparison of the distribution of lightning discharge for August for estimates of the variation with latitude of the ratio of cloud to cloud-to-ground discharges by a) Pierce and b) Prentice and MacKerras. The standard deviation is 7 dB. The area of data coverage is north of the broken line.

APPENDIX C: DATA ANALYZED IN CHAPTER V

TABLE 31. February Data for Greater Than or Equal to Five Cloud-to-Ground Discharges, D_G.

DAY	HR	LAT	LONG	D _G	DD	PW	K	W1	W2	Z1	Z2	TH	SP	H	S
1	0	45	55	14.8	7.6	0.4	0	31.4	15.5	32.2	150.5	1.3	5.0	33.9	53
1	12	45	55	92.6	10.3	0.6	0	36.2	13.7	35.9	156.0	6.3	2.0	32.3	53
1	0	45	55	162.8	10.5	0.6	27	33.6	14.8	35.6	239.5	3.6	12.0	33.6	53
2	0	45	55	109.4	10.5	0.8	27	30.8	15.4	35.4	582.0	3.1	16.5	33.6	49
2	1	45	55	54.7	10.5	0.8	27	30.8	15.4	35.4	213.4	3.5	16.5	33.6	49
2	2	45	55	54.7	10.5	0.8	27	30.8	15.4	35.4	213.4	3.5	16.5	33.6	49
2	3	45	55	54.7	10.5	0.8	27	30.8	15.4	35.4	213.4	3.5	16.5	33.6	49
2	4	45	55	54.7	10.5	0.8	27	30.8	15.4	35.4	213.4	3.5	16.5	33.6	49
2	5	45	55	54.7	10.5	0.8	27	30.8	15.4	35.4	213.4	3.5	16.5	33.6	49
2	6	45	55	54.7	10.5	0.8	27	30.8	15.4	35.4	213.4	3.5	16.5	33.6	49
2	7	45	55	54.7	10.5	0.8	27	30.8	15.4	35.4	213.4	3.5	16.5	33.6	49
2	8	45	55	54.7	10.5	0.8	27	30.8	15.4	35.4	213.4	3.5	16.5	33.6	49
2	9	45	55	54.7	10.5	0.8	27	30.8	15.4	35.4	213.4	3.5	16.5	33.6	49
2	10	45	55	54.7	10.5	0.8	27	30.8	15.4	35.4	213.4	3.5	16.5	33.6	49
2	11	45	55	54.7	10.5	0.8	27	30.8	15.4	35.4	213.4	3.5	16.5	33.6	49
2	12	45	55	54.7	10.5	0.8	27	30.8	15.4	35.4	213.4	3.5	16.5	33.6	49
3	0	45	55	32.5	7.3	0.2	2	30.4	17.8	32.2	283.8	4.5	9.0	33.0	22
3	1	45	55	137.8	7.3	0.2	2	30.4	17.8	32.2	167.9	4.5	9.0	33.0	22
3	2	45	55	223.9	7.4	0.3	9	33.3	14.6	30.2	122.3	1.5	9.9	33.0	22
3	3	45	55	67.4	6.5	0.3	11	35.5	15.9	32.6	209.9	3.3	9.9	33.0	22
3	4	45	55	99.9	6.5	0.3	11	35.5	15.9	32.6	209.9	3.3	9.9	33.0	22
3	5	45	55	39.3	6.5	0.3	11	35.5	15.9	32.6	209.9	3.3	9.9	33.0	22
3	6	45	55	39.3	6.5	0.3	11	35.5	15.9	32.6	209.9	3.3	9.9	33.0	22
3	7	45	55	39.3	6.5	0.3	11	35.5	15.9	32.6	209.9	3.3	9.9	33.0	22
3	8	45	55	39.3	6.5	0.3	11	35.5	15.9	32.6	209.9	3.3	9.9	33.0	22
3	9	45	55	39.3	6.5	0.3	11	35.5	15.9	32.6	209.9	3.3	9.9	33.0	22
3	10	45	55	39.3	6.5	0.3	11	35.5	15.9	32.6	209.9	3.3	9.9	33.0	22
3	11	45	55	39.3	6.5	0.3	11	35.5	15.9	32.6	209.9	3.3	9.9	33.0	22
3	12	45	55	39.3	6.5	0.3	11	35.5	15.9	32.6	209.9	3.3	9.9	33.0	22
5	0	45	55	36.8	6.9	0.2	1	36.0	13.2	34.8	220.0	3.5	5.0	33.8	44
5	1	45	55	67.3	6.9	0.2	1	36.0	13.2	34.8	220.0	3.5	5.0	33.8	44
5	2	45	55	67.3	6.9	0.2	1	36.0	13.2	34.8	220.0	3.5	5.0	33.8	44
5	3	45	55	67.3	6.9	0.2	1	36.0	13.2	34.8	220.0	3.5	5.0	33.8	44
5	4	45	55	67.3	6.9	0.2	1	36.0	13.2	34.8	220.0	3.5	5.0	33.8	44
5	5	45	55	67.3	6.9	0.2	1	36.0	13.2	34.8	220.0	3.5	5.0	33.8	44
5	6	45	55	67.3	6.9	0.2	1	36.0	13.2	34.8	220.0	3.5	5.0	33.8	44
5	7	45	55	67.3	6.9	0.2	1	36.0	13.2	34.8	220.0	3.5	5.0	33.8	44
5	8	45	55	67.3	6.9	0.2	1	36.0	13.2	34.8	220.0	3.5	5.0	33.8	44
5	9	45	55	67.3	6.9	0.2	1	36.0	13.2	34.8	220.0	3.5	5.0	33.8	44
5	10	45	55	67.3	6.9	0.2	1	36.0	13.2	34.8	220.0	3.5	5.0	33.8	44
5	11	45	55	67.3	6.9	0.2	1	36.0	13.2	34.8	220.0	3.5	5.0	33.8	44
5	12	45	55	67.3	6.9	0.2	1	36.0	13.2	34.8	220.0	3.5	5.0	33.8	44
6	0	45	55	15.2	6.9	0.2	1	38.2	14.7	35.7	158.2	3.4	5.0	33.8	44
6	1	45	55	15.2	6.9	0.2	1	38.2	14.7	35.7	158.2	3.4	5.0	33.8	44
6	2	45	55	15.2	6.9	0.2	1	38.2	14.7	35.7	158.2	3.4	5.0	33.8	44
6	3	45	55	15.2	6.9	0.2	1	38.2	14.7	35.7	158.2	3.4	5.0	33.8	44
6	4	45	55	15.2	6.9	0.2	1	38.2	14.7	35.7	158.2	3.4	5.0	33.8	44
6	5	45	55	15.2	6.9	0.2	1	38.2	14.7	35.7	158.2	3.4	5.0	33.8	44
6	6	45	55	15.2	6.9	0.2	1	38.2	14.7	35.7	158.2	3.4	5.0	33.8	44
6	7	45	55	15.2	6.9	0.2	1	38.2	14.7	35.7	158.2	3.4	5.0	33.8	44
6	8	45	55	15.2	6.9	0.2	1	38.2	14.7	35.7	158.2	3.4	5.0	33.8	44
6	9	45	55	15.2	6.9	0.2	1	38.2	14.7	35.7	158.2	3.4	5.0	33.8	44
6	10	45	55	15.2	6.9	0.2	1	38.2	14.7	35.7	158.2	3.4	5.0	33.8	44
6	11	45	55	15.2	6.9	0.2	1	38.2	14.7	35.7	158.2	3.4	5.0	33.8	44
6	12	45	55	15.2	6.9	0.2	1	38.2	14.7	35.7	158.2	3.4	5.0	33.8	44
7	0	45	55	22.3	12.0	0.0	1	40.0	11.9	39.1	192.0	10.0	5.0	33.3	44
7	1	45	55	22.3	12.0	0.0	1	40.0	11.9	39.1	192.0	10.0	5.0	33.3	44
7	2	45	55	22.3	12.0	0.0	1	40.0	11.9	39.1	192.0	10.0	5.0	33.3	44
7	3	45	55	22.3	12.0	0.0	1	40.0	11.9	39.1	192.0	10.0	5.0	33.3	44
7	4	45	55	22.3	12.0	0.0	1	40.0	11.9	39.1	192.0	10.0	5.0	33.3	44
7	5	45	55	22.3	12.0	0.0	1	40.0	11.9	39.1	192.0	10.0	5.0	33.3	44
7	6	45	55	22.3	12.0	0.0	1	40.0	11.9	39.1	192.0	10.0	5.0	33.3	44
7	7	45	55	22.3	12.0	0.0	1	40.0	11.9	39.1	192.0	10.0	5.0	33.3	44
7	8	45	55	22.3	12.0	0.0	1	40.0	11.9	39.1	192.0	10.0	5.0	33.3	44
7	9	45	55	22.3	12.0	0.0	1	40.0	11.9	39.1	192.0	10.0	5.0	33.3	44
7	10	45	55	22.3	12.0	0.0	1	40.0	11.9	39.1	192.0	10.0	5.0	33.3	44
7	11	45	55	22.3	12.0	0.0	1	40.0	11.9	39.1	192.0	10.0	5.0	33.3	44
7	12	45	55	22.3	12.0	0.0	1	40.0	11.9	39.1	192.0	10.0	5.0	33.3	44
8	0	45	55	80.7	18.9	0.0	1	45.4	13.3	41.8	161.5	16.1	13.0	33.3	44
8	1	45	55	80.7	18.9	0.0	1	45.4	13.3	41.8	161.5	16.1	13.0	33.3	44
8	2	45	55	80.7	18.9	0.0	1	45.4	13.3	41.8	161.5	16.1	13.0	33.3	44
8	3	45	55	80.7	18.9	0.0	1	45.4	13.3	41.8	161.5	16.1	13.0	33.3	44
8	4	45	55	80.7	18.9	0.0	1	45.4	13.3	41.8	161.5	16.1	13.0	33.3	44
8	5	45	55	80.7	18.9	0.0	1	45.4	13.3	41.8	161.5	16.1	13.0	33.3	44
8	6	45	55	80.7	18.9	0.0	1	45.4	13.3	41.8	161.5	16.1	13.0	33.3	44
8	7	45	55	80.7	18.9	0.0	1	45.4	13.3	41.8	161.5	16.1	13.0	33.3	44
8	8	45	55	80.7	18.9	0.0	1	45.4	13.3	41.8	161.5	16.1	13.0	33.3	44
8	9	45	55	80.7	18.9	0.0	1	45.4	13.3	41.8	161.5	16.1	13.0	33.3	44
8	10	45	55	80.7	18.9	0.0	1	45.4	13.3	41.8	161.5	16.1	13.0	33.3	44
8	11	45	55	80.7	18.9	0.0	1	45.4	13.3	41.8	161.5	16.1	13.0	33.3	44
8	12	45	55	80.7	18.9	0.0	1	45.4	13.3	41.8	161.5	16.1	13.0	33.3	44
9	0	45	55	162.6	17.4	0.0	1	47.6	14.6	40.9	146.5	17.8	13.0	33.3	44
9	1	45	55	162.6	17.4	0.0	1	47.6	14.6	40.9	146.5	17.8	13.0	33.3	44
9	2	45	55	162.6	17.4	0.0	1	47.6	14.6	40.9	146.5	17.8	13.0	33.3	44
9	3	45	55	162.6	17.4	0.0	1	47.6	14.6	40.9	146.5	17.8	13.0	33.3	44
9	4	45	55	162.6	17.4	0.0	1	47.6	14.6	40.9	146.5	17.8	13.0	33.3	44
9	5	45	55	162.6	17.4	0.0	1	47.6	14.6	40.9	146.5	17.8	13.0	33.3	44
9	6	45	55	162.6	17.4	0.0	1	47.6	14.6	40.9	146.5	17.8	13.0	33.3	44
9	7	45	55	162.6	17.4	0.0	1	47.6	14.6	40.9	146.5	17.8	13.0	33.3	44
9	8	45	55	162.6	17.4	0.0	1	47.6	14.6	40.9	146.5	17.8	13.0	33.3	44
9	9	45	55	162.6	17.4	0.0	1	47.6	14.6	40.9	146				

TABLE 32. Continued

DAY	HR	LAT	LONG	D _G	RH	DD	PW	K	W1	W2	Z1	Z2	TH	ap	H	S
22	00	55	23	6	57	7	1	0	20	0	308	0	6	0	5	5
22	00	55	23	7	38	2	2	3	19	2	190	19	6	0	4	8
22	00	55	23	8	32	3	2	3	16	1	204	20	1	0	3	8
22	00	55	23	9	43	1	2	3	12	1	230	22	2	0	2	8
22	00	55	23	10	47	3	2	3	8	1	244	22	2	0	3	8
22	00	55	23	11	44	4	2	3	18	1	244	22	2	0	3	8
22	00	55	23	12	53	5	2	3	16	1	227	22	2	0	3	8
22	00	55	23	13	57	4	2	3	11	1	209	22	2	0	3	8
22	00	55	23	14	57	3	2	3	7	1	197	22	2	0	3	8
22	00	55	23	15	50	3	2	3	13	1	186	22	2	0	3	8
22	00	55	23	16	45	3	2	3	18	1	170	22	2	0	3	8
22	00	55	23	17	36	2	2	3	20	1	152	22	2	0	3	8
22	00	55	23	18	25	2	2	3	25	1	124	22	2	0	3	8
22	00	55	23	19	12	2	2	3	30	1	93	22	2	0	3	8
22	00	55	23	20	0	2	2	3	34	1	59	22	2	0	3	8
22	00	55	23	21	0	2	2	3	37	1	24	22	2	0	3	8
22	00	55	23	22	0	2	2	3	39	1	0	22	2	0	3	8
22	00	55	23	23	0	2	2	3	41	1	0	20	2	0	3	8
22	00	55	23	24	0	2	2	3	43	1	0	18	2	0	3	8
22	00	55	23	25	0	2	2	3	45	1	0	16	2	0	3	8
22	00	55	23	26	0	2	2	3	47	1	0	14	2	0	3	8
22	00	55	23	27	0	2	2	3	49	1	0	12	2	0	3	8
22	00	55	23	28	0	2	2	3	51	1	0	10	2	0	3	8
22	00	55	23	29	0	2	2	3	53	1	0	8	2	0	3	8
22	00	55	23	30	0	2	2	3	55	1	0	6	2	0	3	8
22	00	55	23	31	0	2	2	3	57	1	0	4	2	0	3	8
22	00	55	23	32	0	2	2	3	59	1	0	2	2	0	3	8
22	00	55	23	33	0	2	2	3	61	1	0	0	2	0	3	8
22	00	55	23	34	0	2	2	3	63	1	0	0	2	0	3	8
22	00	55	23	35	0	2	2	3	65	1	0	0	2	0	3	8
22	00	55	23	36	0	2	2	3	67	1	0	0	2	0	3	8
22	00	55	23	37	0	2	2	3	69	1	0	0	2	0	3	8
22	00	55	23	38	0	2	2	3	71	1	0	0	2	0	3	8
22	00	55	23	39	0	2	2	3	73	1	0	0	2	0	3	8
22	00	55	23	40	0	2	2	3	75	1	0	0	2	0	3	8
22	00	55	23	41	0	2	2	3	77	1	0	0	2	0	3	8
22	00	55	23	42	0	2	2	3	79	1	0	0	2	0	3	8
22	00	55	23	43	0	2	2	3	81	1	0	0	2	0	3	8
22	00	55	23	44	0	2	2	3	83	1	0	0	2	0	3	8
22	00	55	23	45	0	2	2	3	85	1	0	0	2	0	3	8
22	00	55	23	46	0	2	2	3	87	1	0	0	2	0	3	8
22	00	55	23	47	0	2	2	3	89	1	0	0	2	0	3	8
22	00	55	23	48	0	2	2	3	91	1	0	0	2	0	3	8
22	00	55	23	49	0	2	2	3	93	1	0	0	2	0	3	8
22	00	55	23	50	0	2	2	3	95	1	0	0	2	0	3	8
22	00	55	23	51	0	2	2	3	97	1	0	0	2	0	3	8
22	00	55	23	52	0	2	2	3	99	1	0	0	2	0	3	8
22	00	55	23	53	0	2	2	3	101	1	0	0	2	0	3	8
22	00	55	23	54	0	2	2	3	103	1	0	0	2	0	3	8
22	00	55	23	55	0	2	2	3	105	1	0	0	2	0	3	8
22	00	55	23	56	0	2	2	3	107	1	0	0	2	0	3	8
22	00	55	23	57	0	2	2	3	109	1	0	0	2	0	3	8
22	00	55	23	58	0	2	2	3	111	1	0	0	2	0	3	8
22	00	55	23	59	0	2	2	3	113	1	0	0	2	0	3	8
22	00	55	23	60	0	2	2	3	115	1	0	0	2	0	3	8
22	00	55	23	61	0	2	2	3	117	1	0	0	2	0	3	8
22	00	55	23	62	0	2	2	3	119	1	0	0	2	0	3	8
22	00	55	23	63	0	2	2	3	121	1	0	0	2	0	3	8
22	00	55	23	64	0	2	2	3	123	1	0	0	2	0	3	8
22	00	55	23	65	0	2	2	3	125	1	0	0	2	0	3	8
22	00	55	23	66	0	2	2	3	127	1	0	0	2	0	3	8
22	00	55	23	67	0	2	2	3	129	1	0	0	2	0	3	8
22	00	55	23	68	0	2	2	3	131	1	0	0	2	0	3	8
22	00	55	23	69	0	2	2	3	133	1	0	0	2	0	3	8
22	00	55	23	70	0	2	2	3	135	1	0	0	2	0	3	8
22	00	55	23	71	0	2	2	3	137	1	0	0	2	0	3	8
22	00	55	23	72	0	2	2	3	139	1	0	0	2	0	3	8
22	00	55	23	73	0	2	2	3	141	1	0	0	2	0	3	8
22	00	55	23	74	0	2	2	3	143	1	0	0	2	0	3	8
22	00	55	23	75	0	2	2	3	145	1	0	0	2	0	3	8
22	00	55	23	76	0	2	2	3	147	1	0	0	2	0	3	8
22	00	55	23	77	0	2	2	3	149	1	0	0	2	0	3	8
22	00	55	23	78	0	2	2	3	151	1	0	0	2	0	3	8
22	00	55	23	79	0	2	2	3	153	1	0	0	2	0	3	8
22	00	55	23	80	0	2	2	3	155	1	0	0	2	0	3	8
22	00	55	23	81	0	2	2	3	157	1	0	0	2	0	3	8
22	00	55	23	82	0	2	2	3	159	1	0	0	2	0	3	8
22	00	55	23	83	0	2	2	3	161	1	0	0	2	0	3	8
22	00	55	23	84	0	2	2	3	163	1	0	0	2	0	3	8
22	00	55	23	85	0	2	2	3	165	1	0	0	2	0	3	8
22	00	55	23	86	0	2	2	3	167	1	0	0	2	0	3	8
22	00	55	23	87	0	2	2	3	169	1	0	0	2	0	3	8
22	00	55	23	88	0	2	2	3	171	1	0	0	2	0	3	8
22	00	55	23	89	0	2	2	3	173	1	0	0	2	0	3	8
22	00	55	23	90	0	2	2	3	175	1	0	0	2	0	3	8
22	00	55	23	91	0	2	2	3	177	1	0	0	2	0	3	8
22	00	55	23	92	0	2	2	3	179	1	0	0	2	0	3	8
22	00	55	23	93	0	2	2	3	181	1	0	0	2	0	3	8
22	00	55	23	94	0	2	2	3	183	1	0	0	2	0	3	8
22	00	55	23	95	0	2	2	3	185	1	0	0	2	0	3	8
22	00	55	23	96	0	2	2	3	187	1	0	0	2	0	3	8
22	00	55	23	97	0	2	2	3	189	1	0	0	2	0	3	8
22	00	55	23	98	0	2	2	3	191	1	0	0	2	0	3	8
22	00	55	23	99	0	2	2	3	193	1	0	0	2	0	3	8
22	00	55	23	100	0	2	2	3	195	1	0	0	2	0	3	8

Regressors and units are defined on p. 104 of Chapter V. The treatment of regressors should be reviewed before these data are used. There are 122 observations.

VITA

The author was born on 17 September 1940 in Nashville, Tennessee, to Mr. and Mrs. William B. Freeman. He attended parochial schools in Nashville and graduated from Father Ryan High School in May 1958.

He holds the B.S. in mathematics from Middle Tennessee State College (1965) and completed the basic program in meteorology at Texas A&M University (1969). He earned a masters degree in systems management from The George Washington University (1972) and in meteorology from Texas A&M University (1974). The author also has completed coursework at Vanderbilt University, The College of William and Mary, and Northeastern University.

The author is a career officer in The United States Air Force. He has served in operations as an intercept director (1965-1967) and in various support positions as a meteorologist (1968-present).

He is married to the former Julia Elizabeth Bondurant and they have two sons, Will and Andrew. His permanent mailing address is that of his father at 2808 St. Edwards Drive, Nashville, Tennessee 37211.